Rectifier Transformers: Thermal Modeling and a Predictive Maintenance Application Using Estimated Hotspot Winding Temperatures

TOCHUKWU LOUIS ORANUGO

A Thesis

In the Department

of

Electrical and Computer Engineering

Presented in Partial Fulfilment of the Requirements

for the Degree of Masters of Applied Science

(Electrical and Computer Engineering)

Concordia University

Montreal, Quebec, Canada

November 2014

CONCORDIA UNIVERSITY
SCHOOL OF GRADUATE STUDIES

This is to certify that the thesis prepared

By:　　　　Tochukwu Louis Oranugo

Entitled:　　"Rectifier Transformers: Thermal Modeling and a Predictive Maintenance Application Using Estimated Hotspot Winding Temperatures"

And submitted in partial fulfilment of the requirements for the degree of

Masters of Applied Science

Complies with the regulations of this University and meets the accepted standards with respect to originality and quality

Signed by the final examining committee:

_____ Chair
　　　Dr. M. Z. Kabir

_____ Examiner, External To
　　　Dr. A. Bhomwick (BCEE)　　　　　　　　Program

_____ Examiner
　　　Dr. R. Paknys

_____ Supervisor
　　　Dr. L. A. Lopes

Approved by: _____
　　　　　　　Dr. W. E. Lynch, Chair
　　　Department of Electrical and Computer Engineering

_____20_____　　　　　_____
　　　　　　　　　　　　　　　Dr. Amir Asif, Dean
　　　　　　　　　Faculty of Engineering and Computer
　　　　　　　　　　　　　　　Science

ABSTRACT

Rectifier Transformers: Thermal Modeling and a Predictive Maintenance Application Using Estimated Hotspot Winding Temperatures

Tochukwu Louis Oranugo

Predictive maintenance of rectifier transformers in the aluminum smelting industry has become a major area of interest in planning for a replacement or refurbishment of these assets before a failure event occurs. The end of life of a transformer is linked to the rate of degradation of the winding paper insulation which is mainly due to heating processes. Rectifier transformers are subject to high thermal stress due to harmonic currents flowing through them. The need of monitoring and regulation of the hotspot temperature on the rectifier transformer winding is of great importance to keep the temperatures within safe limits as to preserve its life span. In this thesis, existing thermal models; the IEC model, the improved IEEE model, the G. Swift model and the D. Susa model used for hotspot temperature estimation in regulating power transformers has been adapted to account for increased heating due to harmonic currents flowing in the rectifier transformers. Extrapolation techniques, nonlinear least square optimization and genetic algorithm optimization are used for obtaining the rectifier transformer thermal model parameters using online measurements. The thermal model parameters are obtained in two different cooling fan operation conditions; OFAF mode 1 (one fan operation) and OFAF mode 2 (three fans operation) as the transformers under case study are utilized in these cooling modes. A predictive maintenance technique is implemented using typical loading profiles of the transformers and forecasted ambient temperatures to estimate and regulate future hotspot temperatures within safe temperature limits as derived using an industry accepted end of life equation.

ACKNOWLEDGEMENT

Dedicated to my parents Joseph and Bridget Oranugo

TABLE OF CONTENTS

List of Figures

List of Tables

LIST OF MAJOR SYMBOLS

a – Area

A – Pre-exponential factor in hour^{-1} and has values depending on the amount of water and oxygen dissolved in the insulating oil

β - Oil thermal coefficient

B_m – Maximum flux density

C - Constant associated with oil flow

C_1 – Constant

C_{th-oil} - Oil thermal capacitance

C_{th-wdn} - Winding thermal thermal capacitance

c_p - Specific heat of oil

E_a – Activation energy in KJ/mol with a value of 111

f – Frequency

g - Gravitational constant

g_r - Winding to oil temperature difference at rated load

h – Harmonic order

H – Hotspot factor

I – Fundamental sinusoidal load current

I_h - Load current at harmonic order

I_R - Rated load current

I_{Rec} - The rated rectifier RMS harmonic current

K – Load factor (ratio of load at time t to rated load)

K_{Rec} – Rectifier Transformer Load Factor

K_{11} - Constant

K_{21} - Constant

K_{22} - Constant

k - Oil thermal conductivity

K_h - Hysteresis constant

K_e – Eddy current constant

L - Characteristic dimension, length, width, or diameter

l – Expected lifetime in years

m – An empirically derived exponent to calculate the variation of $\Delta\theta_H$ with changing load

n - An empirically derived exponent used in the calculation of the variation of $\Delta\theta_{TO}$ with load changing load

θ_A - Ambient temperature

θ_H – Hottest spot temperature

$\Delta\theta_{H,i}$ - Initial winding hottest spot rise over top oil temperature at t=0

$\Delta\theta_{H,u}$ - Ultimate hotspot rise over top oil temperature for step load

$\Delta\theta_{H,R}$ – Rated hottest spot temperature rise over top oil temperature

θ_{TO} - Top oil temperature

$\Delta\theta_{TO}$ - Top oil rise over ambient temperature

$\Delta\theta_{TO,i}$ - Initial top oil rise over ambient temperature at t=0

$\Delta\theta_{TO,u}$ – Ultimate top oil rise over ambient temperature for step load

$\Delta\theta_{TO-R}$ - Top oil rise over ambient temperature which can be determined by actual test as specified in the IEEE std c57.12.90-1993 or can be derived from the manufacturers

$\Delta\theta_H$ - Winding hottest spot temperature over top oil temperature

$\Delta\theta_{H.A,R}$ - Hotspot rise over ambient temperature at rated load

$\theta_{H,R}$ - Hotspot temperature at rated load

$P_{1,pu}$ – Load loss dependence on temperature

$P_{a,pu}$- Additional loss(sum of stray and eddy losses) per unit

P_h - Hysteresis Losses

P_e – Core Eddy Current Losses

P_{T-R} - Total Power Losses at rated fundamental current and frequency

P_{NL-R} - No Load Losses at rated fundamental current and frequency

P_{DC-R} - DC winding resistance losses at rated fundamental current and frequency

$P_{DC-R(pu)}$ - DC winding resistance losses per unit value at rated conditions

P_{EC-R} - Winding eddy current losses at rated fundamental current and frequency

$P_{EC-R(pu)}$ - Winding eddy current loss per unit value at rated conditions

P_{OSL-R} - Other stray losses in tank and other metal parts at rated fundamental current and frequency

$P_{OSL-R(pu)}$ - Other stray losses per unit value at rated condition

P_{T-Rec} – Rectifier Transformer total Power Losses

P_{LL-Rec} - Rectifier Transformer total Load Losses

P_{NL-Rec} - Rectifier Transformer no Load Losses

P_{DC-Rec} - Rectifier Transformer DC winding resistance losses

P_{EC-Rec} - Rectifier Transformer winding eddy current losses

$P_{OSL-Rec}$ - Rectifier Transformer other stray losses in tank and other metal parts

$P_{DC-Rec-R}$ − DC winding resistance losses at rated RMS harmonic rectifier current

$P_{EC-Rec-R}$ − Winding eddy current losses at rated RMS harmonic rectifier current

$P_{OSL-Rec-R}$ - Other stray losses in tank and other metal parts at rated RMS harmonic rectifier current

q_{fe} - Heat generated by no-load losses

q_{cu} − Heat generated by load losses

R - Ratio of load loss at rated load to no −load loss on the tap position studied

R_{Rec} − Ratio of load loss at rated rectifier load to no load loss

R_g − Gas constant with a value of 8.314 J/mol/K

R_{th-oil} - Nonlinear thermal resistance of oil which varies based on the oil viscosity with the temperature of the oil.

$R_{th-hs-oil}$ - Nonlinear winding to oil thermal resistance which varies with the viscosity of the oil as temperature changes

T − Thickness of lamination strips

τ_{TO} - Oil time constant of transformer

τ_w - Winding time constant at hotspot location

μ - Oil viscosity

μ_{pu}- Oil viscosity per unit

μ_R- Rated oil viscosity

ρ - Oil density

CHAPTER 1   INTRODUCTION

1.1   Motivation and Objectives

The smelting of aluminum involves the use of high power rectifier transformers which supply electric power to rectifiers for the purpose of converting AC currents to DC currents used in the smelting process. The reliability of the rectifier transformers is of great importance to the aluminum smelting industry as a failure of this asset could lead to loss of revenue due to reduced productivity as well as cost from unplanned replacement or refurbishment. Time based maintenance such as Dissolved Gas Analysis (DGA), periodic monitoring of oil and winding hotspot temperatures, Frequency Response Analysis test (FRA), Partial Discharge Test (PD), as well as other electrical tests are used to assess the health condition of this critical equipment [1]. These techniques have limitations as they only assess the present health condition of the transformer and cannot be used to determine the future state of health. Therefore, the need for a predictive maintenance solution to estimate this failure period has become a major area of interest.

The expected lifetime of a transformer is a minimum of 25 years for a transformer operating with a winding hotspot temperature between 65°C and 95°C [2]. In the industry, a criterion for determining the end of life of a transformer is by assessing the paper insulation around the winding with the degradation of the paper insulation due to factors such as pyrolysis (heating), oxidation and hydrolysis with pyrolysis being the main source of degradation [1,3]. Based on this criterion, transformer loss of life equations have been developed by the IEEE [4], IEC [5] as well as other researchers such as N. Lelekakis, D. Martin, and J, Wijaya [6,7] using the winding hotspot temperature.

Rectifier transformers are subject to more thermal stress when compared to regular power transformers used for power transmission and distribution and this is due to the harmonic currents flowing through them created by the rectifiers [8, 9, 10, 11, 12]. This requires the installation of efficient cooling systems on the transformer as well as good transformer loading management to reduce the heating.

Alcoa is the leading producer of primary and fabricated aluminum in the world and as such utilizes rectifier transformers in their line of production. Presently, the Baie Comeau smelter has six 47.9 MVA Oil Forced Air Forced (OFAF) rectifier transformers in the pot line D which have been in service for 30 years. The OFAF system consists of one oil pump and three fans which are utilized differently between the winter and summer seasons. In the winter, the rectifier transformers operate with one fan (OFAF mode 1) or three fans on (OFAF mode 2) and the pump on while in the summer they operate with all three fans on (OFAF mode 2) and the pump on. It is the desire of the smelter to keep the rectifier transformers for another period of 20 years before it replaces the asset; therefore a predictive maintenance scheme is needed.

This thesis presents a predictive maintenance solution for preserving the life of the rectifier transformers by the control of future estimated winding hotspot temperatures using forecasted transformer loading profiles and forecasted ambient temperatures to keep the winding hotspot temperature within threshold values as determined by N. Lelekakis et al. loss of life equations [7]. This technique also allows for the optimization of the transformer loading and cooling fan usage.

The hotspot temperature of the winding of most transformers is measured by the use of calibrated gauges using measurements from thermocouples installed in the top oil of the transformer and load factor from current transformers installed on the winding with the calibration based on heat tests by the manufacturer. Recently, the use of fiber optics installed at various locations of the winding has presented more reliable winding hotspot temperature measurements but is however limited in use due to high cost of installation for old and new transformer units which is difficult to justify [13].

Alternatively, thermal models proposed by the IEEE [4] and IEC [5] are used to predict the hotspot temperatures as a sum of the ambient temperature, top oil rise above ambient temperature and hotspot rise above top oil temperature. The IEEE model [4] does not fully account for variations in the ambient temperature and was improved by B.C. Lesieutre et al [14] to include this phenomenon. Other thermal models based on thermal-electrical analogy, heat transfer theory and application of lumped capacitance method were proposed by G. Swift [15, 16] which were then modified by A. Elmoudi [13, 17] to include the effect of transformer loss dependence on hotspot temperature and later by D. Susa [18, 19] to include the effect of oil viscosity dependence on top oil temperature. It will be important to note that no model has been universally accepted as the best thermal model as one model may predict hotspot temperatures for a transformer better and may not be the case for another.

In this thesis, the improved IEEE model [14], the IEC model [5], the G. Swift model [15] and the D. Susa model [18] are extended to account for increased thermal stress due to the current harmonics flowing through the rectifier transformers which is generated from the rectifier connected in series to it. A comparison of the thermal models is made to select the

thermal model with the least error of hotspot temperature estimation for a rectifier transformer.

The thermal models proposed are characterized by certain thermal parameters. These parameters are usually obtained by heat run tests which require the isolation of the transformer. In events when the transformers cannot be isolated especially with transformers in service, extrapolation techniques are performed using online measurements such as the transformer load factor and ambient temperature. Extrapolation techniques such as the nonlinear least squared method was used by A. Elmoudi in [20, 21, 22] for distribution transformers and genetic algorithms by V. Galdi et al in [23] and W. H. Tang et al in [24] for power transformers. Both methods yielded good estimations of the thermal model parameters and were validated with heat run test values. The rectifier transformers used in this thesis work are all in service and therefore require the use of extrapolation techniques. In this project, the nonlinear least squared optimization and genetic algorithm optimization are applied as extrapolation techniques and compared to see which technique yields best results. The thermal parameters are also obtained for the different cooling modes of the rectifier transformer.

1.2   Thesis Contribution

The main contributions of the thesis are summarized as follows:

- Extension of existing thermal models to rectifier transformers to account for increased transformer losses due to harmonic currents is made. Also, a comparison of the thermal models is shown to obtain the best model for predicting the rectifier transformer top oil and hotspot temperatures.

4

- Two optimization methods; nonlinear least square and genetic algorithm are utilized and compared to estimate the parameters of the thermal models based on data obtained from actual online field measurements. Furthermore, the derivation of the transformer thermal parameters in different cooling states of an OFAF transformer is presented.

- A predictive maintenance application is presented by the planning of the rectifier transformer utilization. Forecasted future loading profiles and ambient temperatures are used to maintain hotspot temperatures within set threshold temperatures for optimization of threshold useful life.

1.3 Thesis Outline

A brief review of predictive maintenance techniques and existing thermal models is presented in Chapter 2. Chapter 3 focuses on rectifier transformer configuration, losses as well as a brief description of the studied Alcoa rectifier transformers. The extension of the existing thermal models to rectifier transformers is also presented in this chapter. A brief description of nonlinear least square optimization (NLLSQ) as well as the estimation of the thermal model parameters using NLLSQ is presented in Chapter 4. In Chapter 5, a review of genetic algorithm is made and the application of genetic algorithms to the estimation of the thermal model parameters is shown. Chapter 6 presents a predictive maintenance application for the Alcoa rectifier transformers by the regulation of future estimated hotspot temperatures.

CHAPTER 2   OVERVIEW OF PREDICTIVE MAINTENANCE AND THERMAL MODELING

2.1   Introduction

This chapter presents a brief review of transformer predictive maintenance techniques which are used to assess transformer health conditions and predict the useful end of life. An end of life equation is presented which links the life of a transformer to the rate of degradation of the winding paper insulation. The degradation process is by the heating, oxidation and hydrolysis of the paper insulation with heating as the main contributor to the depreciation of the paper insulation. A review of existing thermal models of regulating power transformers is also presented which are used for predicting the winding hotspot temperature and forms part of the transformer end of life equation.

2.2   Transformer Predictive Maintenance

Time-based maintenance of transformers which involves maintenance operation over a fixed time interval has been the major practice in the industry. A major drawback with this technique is the blindness to the state of health of the transformers which could result to a failure before the next scheduled maintenance action. An alternative maintenance scheme, predictive maintenance by the means of condition monitoring has been adopted to prevent unexpected failure events and to predict the remaining useful life of the transformers. The IEEE Guide for Application for Monitoring of Liquid Immersed Transformers and Components [25] suggests various condition monitoring techniques. These techniques include oil and winding temperature monitoring, voltage and current monitoring, dissolved

gas analysis (DGA), partial discharge monitoring, moisture monitoring, vibro-acoustic monitoring, bushing power factor measurements as well as pump/fan operation monitoring.

The techniques mentioned above are used to detect degradation in various parts of the transformer but the most important form of degradation is that of the insulation system. In the industry, the end of life of a transformer has been determined to be the point at which the paper insulation of the winding has lost 50% of its mechanical tensile strength [4]. This form of degradation is mainly as a result of thermal stress (hotspot winding temperature) on the paper insulation as well as the amount of moisture and oxygen content in the insulating oil.

In this thesis, thermal condition monitoring is adopted as a predictive maintenance technique for the prediction of the end of life of Alcoa rectifier transformers based on end of life equations as discussed in Section 2.1.

2.2.1 Transformer Loss of Life Estimation

The life of transformers has been linked to the degree of degradation of the paper insulation of the transformer winding. The paper insulation is made up of a polymer of glucose units connected to one another and can be represented as $[C_5H_{10}O_5]_n$, where n is the degree of polymerization (DP). Brand new insulation paper usually has a DP ranging from 1100 to 1200 while a degraded paper has a DP value of 200 [2].

The degradation of the paper takes place by means of pyrolysis, oxidation and hydrolysis. Attempts have been made by the IEEE and IEC to determine the end of life of transformers using loss of life equations as in [4, 5] but have limitations as the equation solely uses the transformer winding hotspot temperature as the source of paper ageing.

7

A more comprehensive end of life equation was developed by N. Lelekakis et al [6,7] which factors in the ageing of paper by the three factors as shown in equation (2.1)

$$l = \frac{\frac{1}{DP_{end}} - \frac{1}{DP_{start}}}{A \times 24 \times 365} \times e^{\frac{E_a}{R_g \times \theta_H}} \quad (2.1)$$

where

l – Expected lifetime in years

E_a – Activation energy in KJ/mol with a value of 111

A – Pre-exponential factor in hour^{-1} and has values depending on the amount of water and oxygen dissolved in the insulating oil and is shown in table 2.1.

R_g – Gas constant with a value of 8.314 J/mol/K

θ_H – Winding hotspot temperature

Table 2.1 Pre-exponential factor for different levels of water and oxygen concentration

A values at Ea = 111 KJ/mol			
Water Content	Low Oxygen	Medium Oxygen	High Oxygen
0.50%	1.52E+08	6.00E+08	1.00E+09
1.00%	3.42E+08	1.30E+09	1.89E+09
1.50%	6.19E+08	1.90E+09	2.60E+09
2.00%	9.86E+08	2.60E+09	3.45E+09
3.00%	1.99E+09	3.70E+09	5.10E+09
4.00%	3.35E+09	5.30E+09	7.10E+09

In this project, the end of life equation as stated in (2.1) will form the basis of the lifetime evaluation of the Alcoa rectifier transformers.

2.3   Transformer Thermal Modeling

With the need to keep the winding hotspot temperature below the rated thermal capability of the paper insulation, efforts have been made in the industry to provide a solution for monitoring this temperature. The use of thermocouples and fibre optics has been broadly adapted by various transformer manufacturers. One major setback with this technique is the high cost of installation as well as cost of replacement in event of damaged thermocouples [13]; therefore, this setback gave birth to formulation of thermal models. Various thermal models have been proposed by the IEEE [4], IEC [5] and many other researchers in [14, 15, 16, 17, 18, 19] to predict the hotspot temperature and will be discussed below.

2.3.1   IEEE Thermal Model

The IEEE guide [4] in clause 7 presents a hotspot temperature model as a summation of the ambient temperature (θ_A), top oil temperature rise above ambient temperature ($\Delta\theta_{TO}$) and hotspot temperature rise above top oil temperature ($\Delta\theta_H$) as given in equation (2.2)

$$\theta_H = \theta_A + \Delta\theta_{TO} + \Delta\theta_H. \qquad (2.2)$$

This model assumes that the transformer hotspot temperature is located near the top of the transformer winding. The second assumption made with this model is that the ambient temperature is constant while the dynamics of an increase and a decrease in the

temperature of the winding hotspot temperature is solely dependent on the loading of the transformer.

2.3.1.1 IEEE Top Oil Rise Above Ambient Model

The IEEE top oil rise above ambient temperature is expressed by means of a first order exponential equation response from an initial temperature state to a final temperature state which is generally influenced by an increase or decrease in the transformer current magnitude. Therefore the IEEE top oil rise above ambient temperature can be given as

$$\Delta\theta_{TO} = \left(\Delta\theta_{TO,u} - \Delta\theta_{TO,i}\right) \times \left[1 - \exp^{-\frac{t}{\tau_{TO}}}\right] + \Delta\theta_{TO,i} \qquad (2.3)$$

which can be expressed by first order differential equation as

$$\tau_{TO}\frac{d\Delta\theta_{TO}}{dt} = \Delta\theta_{TO,u} - \Delta\theta_{TO} \qquad (2.4)$$

where

$$\Delta\theta_{TO,u} = \Delta\theta_{TO-R}\left[\frac{1+RK^2}{1+R}\right]^n \qquad (2.5)$$

$\Delta\theta_{TO,i}$ - Initial top oil rise over ambient temperature at t=0

$\Delta\theta_{TO,u}$ − Ultimate top oil rise over ambient temperature for step load

$\Delta\theta_{TO-R}$ - Top oil rise over ambient temperature which can be determined by actual test as specified in the IEEE std c57.12.90-1993 or can be derived from the manufacturers

τ_{TO} - Oil time constant of transformer

R - Ratio of load loss at rated load to no –load loss on the tap position studied

K – Load factor (ratio of load at time t to rated load)

n - An exponent used in the calculation of the variation of $\Delta\theta_{TO}$ with load changing load and account for the oil viscosity.

2.3.1.2 IEEE Hotspot Rise Above Top Oil Model

The IEEE hotspot rise above top oil temperature is also expressed by means of a first order exponential equation response from an initial temperature state to a final temperature state which is characterized by changes in the transformer load and is given as

$$\Delta\theta_H = \left(\Delta\theta_{H,u} - \Delta\theta_{H,i}\right)\left[1 - \exp^{-\frac{t}{\tau_w}}\right] + \Delta\theta_{H.i} \quad (2.6)$$

which can be expressed as a first order differential equation as

$$\tau_w \frac{d\Delta\theta_H}{dt} = \Delta\theta_{H,u} - \Delta\theta_H \quad (2.7)$$

where

$$\Delta\theta_{H,u} = \Delta\theta_{H,R}K^{2m} \quad (2.8)$$

$\Delta\theta_{H,i}$ - Initial winding hottest spot rise over top oil temperature at t=0

$\Delta\theta_{H,u}$ - Ultimate hotspot rise over top oil temperature for step load

$\Delta\theta_{H,R}$ – Rated hottest spot temperature rise over top oil temperature

τ_w - Winding time constant at hotspot location

m – An empirically derived exponent to calculate the variation of $\Delta\theta_H$ with changing load and accounts for the oil viscosity

11

The exponential constants n and m are used to define the non-linearity of the temperature rise of the oil and winding hotspot respectively and is also characterized by the type of cooling system installed on the transformer as shown in Table 2.2 below.

Table 2.2   IEEE Model Exponential Constants

Type of Cooling	N	m
ONAN	0.8	0.8
ONAF	0.9	0.8
OFAF	0.9	0.8
ODAF	1.0	1.0

where

ONAN – Oil Natural Air Natural

ONAF – Oil Natural Air Forced

OFAF – Oil Forced Air Forced

ODAF – Oil Directed Air Forced

A major drawback with the IEEE thermal models is that it does not account for variation in the ambient temperature oil which therefore leads to a very conservative estimation of the transformer winding hotspot temperature.

2.3.2   An Improved IEEE Thermal Model

B.C Leisieutre et al [14] proposed a new top oil temperature which is an improvement on the IEEE clause 7 thermal model. The derivation of the hotspot temperature is defined as the summation of the top oil temperature and the hotspot temperature rise above top oil temperature given by

$$\theta_H = \theta_{TO} + \Delta\theta_H \qquad (2.9)$$

The IEEE clause 7 model does not correctly account for the variation in the ambient temperature, therefore B.C. Leisieutre et al proposed a new top oil model which effectively accounts for a variation in the ambient temperature and is expressed as

$$\tau_{TO}\frac{d\theta_{TO}}{dt} = \Delta\theta_{TO,u} - \theta_{TO} + \theta_A \qquad (2.10)$$

where $\Delta\theta_{TO,u}$ is still as defined in as

$$\Delta\theta_{TO,u} = \Delta\theta_{To-R}\left[\frac{1+RK^2}{1+R}\right]^n \qquad (2.11)$$

but re-interpreted as ultimate top oil rise over ambient temperature for changing load and constant ambient temperature.

In this new top oil model, one can see that an increase in the ambient temperature at a specific time will not cause a sudden increase in the oil temperature but will lag behind depending on the length of the oil time constant. This phenomenon is more practical as opposed to the IEEE clause 7 model which shows that a sudden increase in ambient temperature in the case of a varying cycle of ambient temperature will result to a sudden increase in the oil temperature.

The hotspot temperature rise above top oil temperature is modeled as stated in the IEEE clause 7.

The modified IEEE model was validated with a 336 MVA OFAF transformer and proved to yield better predictions than the IEEE clause 7 model.

2.3.3 IEC Thermal Model

The IEC guide [5] presents a different approach in the thermal modeling of the winding hotspot temperature by defining the hotspot temperature as a summation of the top oil temperature (θ_{TO}) and the hotspot rise above top oil temperature ($\Delta\theta_H$) given by equation (2.12)

$$\theta_H = \theta_{TO} + \Delta\theta_H . \qquad (2.12)$$

2.3.3.1 IEC Top Oil Rise Model

The top oil temperature is expressed in the form of a differential equation which is governed by the loading of the transformer and the ambient temperature as given in (2.13)

$$\left[\frac{1+RK^2}{1+R}\right]^n \times (\Delta\theta_{To-R}) = K_{11}\tau_{TO} \times \frac{d\theta_{TO}}{dt} + [\theta_{TO} - \theta_A] \qquad (2.13)$$

where

$\Delta\theta_{TO-R}$ - Top oil rise over ambient temperature which can be determined by actual test as specified in the IEEE std c57.12.90-1993 or can be derived from the manufacturers

τ_{TO} - Oil time constant of transformer

R - Ratio of load loss at rated load to no –load loss on the tap position studied

K – Load factor(ratio of load at time t to rated load)

n - An exponent used in the calculation of the variation of $\Delta\theta_{TO}$ with load changing load and accounts for the oil viscosity

θ_A – Ambient temperature

θ_{TO} – Top oil temperature

K_{11}- Constant that introduces the effect of type of cooling system in the oil time constant.

2.3.3.2 IEC Hotspot Rise Above Top Oil Temperature Model

The hotspot rise above top oil temperature is defined by the difference of two hotspot rise temperatures $\Delta\theta_{H1}$ and $\Delta\theta_{H2}$,

$$\Delta\theta_H = \Delta\theta_{H1} - \Delta\theta_{H2}. \quad (2.14)$$

$\Delta\theta_{H1}$ is the fundamental hotspot rise above top oil temperature before taking into account the varying rate of oil flow through the hotspot region and is defined by a differential equation given as

$$K_{22} \times \tau_w \frac{d\Delta\theta_{H1}}{dt} = K_{21} \times \Delta\theta_{H,R} \times K^{2m} - \Delta\theta_{H1} \quad (2.15)$$

$$\Delta\theta_{H,R} = H \times g_r \quad (2.16)$$

where

$\Delta\theta_{H,R}$ – Rated hottest spot temperature rise over top oil temperature

τ_w - Winding time constant at hotspot location

m – An exponent to calculate the variation of $\Delta\theta_H$ with changing load and accounts for the oil viscosity

K_{22} – Constant depending on cooling system type

K_{21} – Constant depending on cooling system type

H – Hotspot factor

g_r - Winding to oil temperature difference at rated load

$\Delta\theta_{H2}$ is the hotspot temperature rise due to the varying rate of oil flow through the hotspot region and is as well expressed as a differential equation

$$\left(\frac{K_{22}}{\tau_{TO}}\right) \times \frac{d\Delta\theta_{H2}}{dt} = (K_{21} - 1) \times \left(\Delta\theta_{H,R} \times K^{2m}\right) - \Delta\theta_{H2} \quad (2.17)$$

The resultant effect of the two hotspot temperature rise is to take into account the fact that a sudden rise in the transformer load current may cause an unexpected peak rise in the hotspot temperature very soon after the load current change.

The exponential constants n and m as well as the constants K_{11}, K_{21}, K_{22}, have different values depending on the type of cooling and is given in table 2.3

Table 2.3   IEC Model Exponential Constants

Type of Cooling	n	m	K₁₁	K₂₁	K₂₂
ONAN	0.8	0.8	0.5	3.0	2.0
ONAF	0.9	0.8	0.5	3.0	2.0
OFAF	0.9	0.8	1.0	1.3	1.0
ODAF	1.0	1.0	1.0	1.0	1.0

2.3.4   G. Swift Thermal Model

A new approach to transformer hotspot temperature was proposed by G. Swift based on heat transfer theory, thermal-electrical analogy and application of lumped capacitance

method [15, 16] and the relationship between heat transfer mechanism and electrical circuit theory and is summarized in Table 2.4 below.

Table 2.4   Thermal-Electrical Analogous Quantities

	THERMAL	ELECTRICAL
THROUGH VARIABLE	heat transfer rate, q watts	current, i, amps
ACROSS VARIABLE	temperature, θ, degree C	voltage, v, volts
DISSIPATION ELEMENT	thermal-resistance, R_{th}, degC/watt	elect-resistance, R_{el}, ohms
STORAGE ELEMENT	thermal-capacitance, C_{th} joules/degC	elect-capacitance, C_{el} farads

2.3.4.1 G. Swift Top Oil Thermal Model

A top oil model is developed as shown in Figure 2.1 which illustrates that the temperature of the top oil is a function of the heat generated by load and no load losses, the ability of the oil to retain the heat produced and the rate of heat transfer between the oil and ambient air.
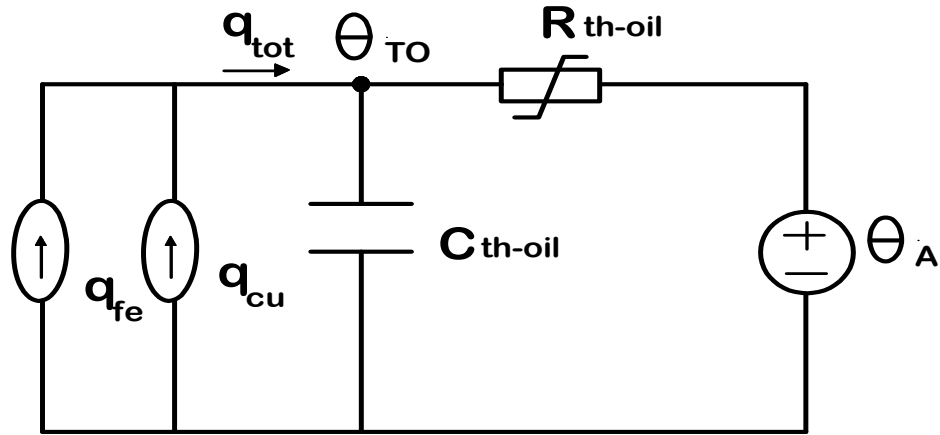
Figure 2.1   G. Swift Top oil Temperature Model.

The amount of heat generated is proportional to the amount of power losses at a given current intensity

$$q_{fe} + q_{cu} \equiv P_{NL} + P_{LL} \quad (2.18)$$

where

q_{fe} - Heat generated by no-load losses

q_{cu} − Heat generated by load losses

P_{NL} − No-load losses

P_{LL} − Load losses

The heat retained by the oil is determined by the specific heat capacity of the oil (C_{th-oil}) as well as the ability of the heat to flow into the ambient air (θ_A) which is affected by the thermal resistivity (R_{th-oil}) of the oil.

18

This model assumes that the transformer tank acts as a perfect conductor and therefore creates no resistance to the flow of heat from the oil to air. Furthermore, the top oil model adds the effect of a nonlinear heat transfer between oil and air due to faster movement of the hotter air at the wall of the transformer tank to the ambient atmosphere with a value of n at 0.8 for air natural cooling and n equals to 1 for forced cooling as given in equation (2.19) which is a solution for the circuit in Figure 2.1

$$q_{fe} + q_{cu} = C_{th-oil} \times \frac{d\theta_{TO}}{dt} + \frac{1}{R_{th-oil}} \times [\theta_{TO} - \theta_A]^{\frac{1}{n}} \qquad (2.19)$$

Defining R as the ratio of q_{cu} to q_{fe} at rated load, the oil time constant (τ_{TO}) as the product of the oil thermal capacity (C_{th-oil}) and the nonlinear thermal resistance (R_{th-oil}) at rated load, the top oil rise above ambient temperature ($\Delta\theta_{TO}$) as the difference between the top oil temperature (θ_{TO}) and the ambient temperature (θ_A), K as load factor(ratio of instantaneous load to rated load) and the total heat generated ($q_{fe} + q_{cu}$) as the product of the top oil rise above ambient temperature ($\Delta\theta_{TO}$) and the nonlinear thermal resistance (R_{th-oil}), the top oil to air model can be defined as

$$\left[\frac{1 + RK^2}{1 + R}\right] \times (\Delta\theta_{To-R})^{\frac{1}{n}} = \tau_{TO} \times \frac{d\theta_{TO}}{dt} + [\theta_{TO} - \theta_A]^{\frac{1}{n}} \qquad (2.20)$$

2.3.4.2 G. Swift Hotspot Thermal Model

A hotspot model is developed to calculate the transformer hotspot temperature as shown in Figure 2.2. The hotspot model is similar to the top oil model with the ambient temperature becoming the top oil temperature and consideration of only load losses as the source of hotspot heating.
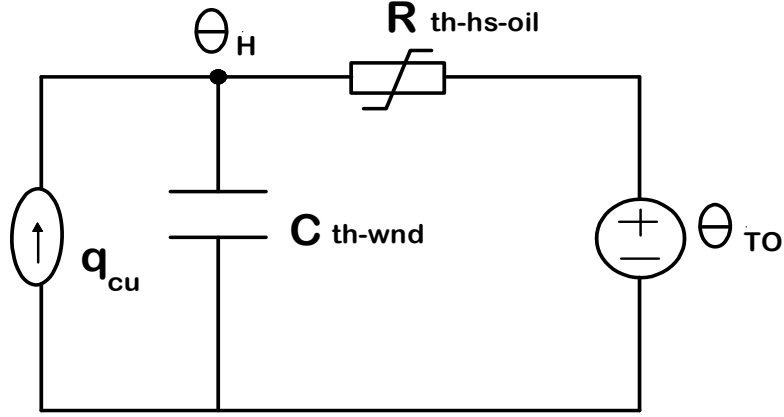
Figure 2.2   G. Swift Hotspot Temperature Model

Solving the circuit in Figure 2.2, the solution presents an equation as given in (2.21)

$$q_{cu} = C_{th-wdn} \times \frac{d\theta_H}{dt} + \frac{1}{R_{th-hs-oil}} \times [\theta_H - \theta_{TO}]^{\frac{1}{m}} \quad (2.21)$$

where

C_{th-wdn} - Winding thermal capacitance

$R_{th-hs-oil}$ - Nonlinear winding to oil thermal resistance which varies with the viscosity of the oil as temperature changes

m – Nonlinear exponential constant

Defining the winding time constant (τ_w) as the product of the winding thermal capacity (C_{th-wdn}) and the nonlinear winding to oil thermal resistance ($R_{th-hs-oil}$) at rated load, the hotspot rise above top oil temperature ($\Delta\theta_H$) as the difference between the hotspot temperature (θ_H) and the top oil temperature (θ_{TO}), K as load factor(ratio of instantaneous load to rated load) and the heat generated (q_{cu}) as the product of the top oil rise above

ambient temperature $(\Delta\theta_H)$ and the nonlinear winding to oil thermal resistance $(R_{th-hs-oil})$, the top oil to air model can be defined as

$$K^2 \times \left(\Delta\theta_{H,R}\right)^{\frac{1}{m}} = \tau_w \times \frac{d\theta_H}{dt} + \left[\theta_H - \theta_{TO}\right]^{\frac{1}{m}} \quad (2.22)$$

2.3.5 A. Elmoudi Thermal Model

A. Elmoudi [13, 17] further advanced the G. Swift hotspot model by including the effect of variance of the winding load losses (winding DC resistance and winding stray eddy current losses excluding the other stray losses in the tank) with the winding hotspot temperature. The winding DC resistance losses increases with winding temperature increase while the winding stray losses decreases with winding temperature increase. The hotspot model is then expressed as

$$K^2 \left[\frac{K_\theta + \dfrac{P_{EC-R(pu)}}{K_\theta}}{1 + P_{EC-R(pu)}}\right] \times \left(\Delta\theta_{H,R}\right)^{\frac{1}{m}} = \tau_w \times \frac{d\theta_H}{dt} + \left[\theta_H - \vartheta_{TO}\right]^{\frac{1}{m}}. \ (2.23)$$

The loss variance with temperature (K_θ) and per unit winding eddy current losses at hotspot location $(P_{EC-R(pu)})$ are defined as

$$K_\theta = \frac{235 + \theta_H}{235 + \theta_{H,R}} \quad (2.24)$$

$$P_{EC-R(pu)} = \frac{P_{EC-H}}{P_{DC-R}} \quad (2.25)$$

where

$\theta_{H,R}$ − rated hotspot temperature

P_{EC-H} - Winding eddy current losses at hotspot location

P_{DC-R} - DC winding resistance losses at rated fundamental current and frequency

The model was validated with a 250 MVA transformer in the field and yielded good results.

2.3.6   D. Susa Thermal Model

D. Susa [18, 19] proposed a similar model to G. Swift model which is an equivalent electrical circuit based on heat transfer principles. The top oil model takes into consideration the effect of varying ambient temperature and total transformer losses in determination of the top oil temperature but redefines the non-linearity of heat flow between the oil and air by a nonlinear oil resistance.

The nonlinear oil resistance is defined by equation (2.26) where the resistance is directly proportional to the oil viscosity. The oil viscosity is a function of the temperature of the oil and the type of cooling system which is defined by the nonlinear exponent n which has a value of 0.2 for ONAN transformers and 0.25 for ONAF, OFAF and ODAF transformers with the assumption that the flow of oil in the transformer is laminar.

$$R_{th-oil} = \frac{1}{C_1 \times a} \times \left(\frac{\mu}{\Delta \theta_{TO}} \right)^n \quad (2.26)$$

where the oil viscosity μ is defined in (2.27) as

$$\mu = 0.0000013573 \times e^{\frac{2797.3}{\theta_{TO} + 273}} \quad (2.27)$$

and the constant C_1 as

$$C_1 = C \times \left[\rho^2 \times g \times \beta \times k^{\frac{1-n}{n}} \times L^{\frac{3n-1}{n}} \times c_p \right]^n \quad (2.28)$$

22

where

k - Oil thermal conductivity

L - Characteristic dimension, length, width, or diameter

g - Gravitational constant

β - Oil thermal coefficient

C - Constant associated with oil flow

a – Area

c_p - Specific heat of oil

ρ - Oil density

The oil viscosity µ and parameters of C_1 are known to be temperature dependent but C_1 parameters remain constant above 40ºC as shown in figure 2.3
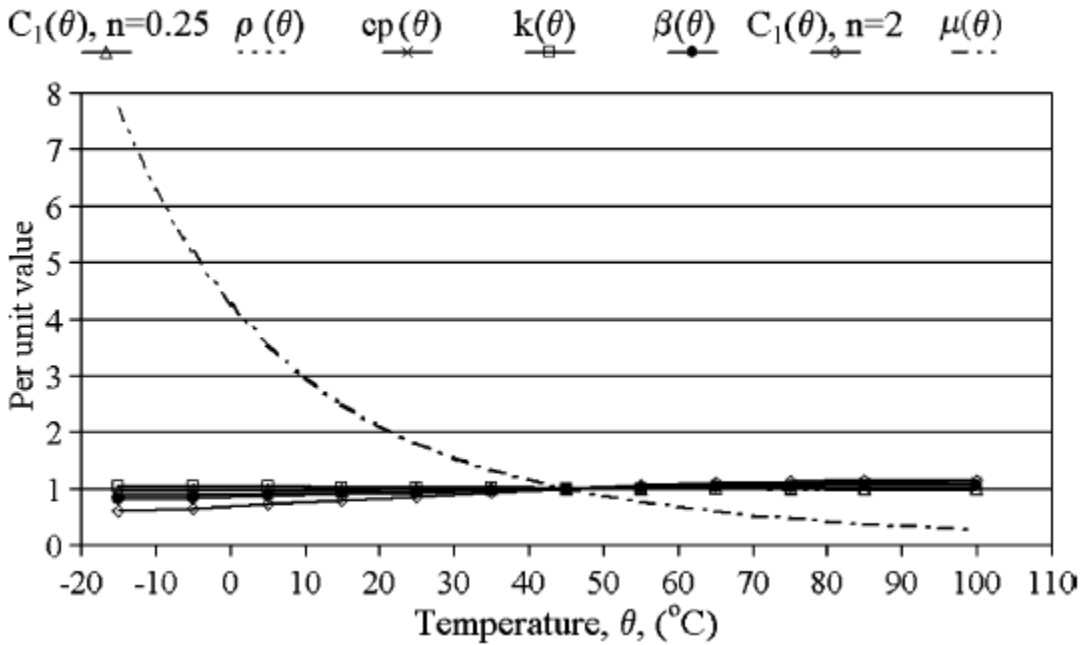
Figure 2.3   Variation of Oil Parameters with Temperature [18]

Defining

- the oil viscosity as

$$\mu = \mu_{pu} \times \mu_R \quad (2.29)$$

- the rated non linear oil to air thermal resistance as

$$R_{th-oil,R} = \frac{1}{C_1 \times a} \times \left(\frac{\mu_R}{\Delta\theta_{To-R}} \right)^n \quad (2.30)$$

- the rated top oil rise above ambient temperature as

$$\Delta\theta_{To-R} = \left(q_{fe} + q_{cu} \right)_R \times R_{th-oil,R} \quad (2.31)$$

- the rated top oil time constant as

$$\tau_{TO} = R_{th-oil,R} \times C_{th-oil} \quad (2.32)$$

- the per unit output load current as

$$K = \frac{I}{I_R} \quad (2.33)$$

- the ratio of load losses to no load losses as

$$R = \frac{q_{cu}}{q_{fe}} \quad (2.34)$$

where

μ_{pu}- Oil viscosity per unit

μ_R- Rated oil viscosity

q_{fe} - Heat generated by no-load losses

q_{cu} – Heat generated by load losses

the top oil model is expressed as

$$\left[\frac{1+RK^2}{1+R}\right] \times \mu_{pu}^n \times \Delta\theta_{To-R} = \mu_{pu}^n \times \tau_{TO} \times \frac{d\theta_{TO}}{dt} + \frac{[\theta_{TO} - \theta_A]^{1+n}}{\Delta\theta_{To-R}^n} \qquad (2.35)$$

D. Susa as well proposed a modified version of his top oil model in [19] by including the variation of the copper losses with winding temperature as shown in (2.36)

$$\left[\frac{1+R \times P_{1,pu} \times K^2}{1+R}\right] \times \mu_{pu}^n \times \Delta\theta_{To-R} = \mu_{pu}^n \times \tau_{TO} \times \frac{d\theta_{TO}}{dt} + \frac{[\theta_{TO} - \theta_A]^{1+n}}{\Delta\theta_{To-R}^n} \qquad (2.36)$$

and

$$P_{1,pu} = K_\theta + \frac{P_{a,pu}}{K_\theta} \qquad (2.37)$$

$$P_{a,pu} = \frac{P_{EC-R} + P_{OSL-R}}{P_{DC-R}} \qquad (2.38)$$

where

$P_{1,pu}$ – Load loss dependence on temperature

$P_{a,pu}$ - Additional loss (sum of stray and eddy losses) per unit

P_{DC-R} - DC winding resistance losses at rated fundamental current and frequency

P_{EC-R} - Winding eddy current losses at rated fundamental current and frequency

P_{OSL-R} - Other stray losses in tank and other metal parts at rated fundamental current and frequency

The hotspot thermal model is also based on the thermal-electrical analogy as the G.Swift model [16] but introduces the effect of load losses with winding temperature as well as the effects of oil viscosity on the nonlinear winding to oil thermal resistance.

25

The nonlinear winding to oil thermal resistance ($R_{th-hs-oil,R}$) is defined in (2.39) and is directly proportional to the oil viscosity and inversely proportional to the hotspot temperature rise over top oil. Also, an exponent m is used to shape the nonlinear behavior of the winding to oil resistance. The exponent m as in [18, 19] is known to vary with cooling system of the transformer and is solely derived empirically through extrapolation techniques.

$$R_{th-hs-oil,R} = \frac{1}{C_1 \times a} \times \left(\frac{\mu_R}{\Delta\theta_{H,R}} \right)^m \qquad (2.39)$$

Defining

- the oil viscosity as

$$\mu = \mu_{pu} \times \mu_R \quad (2.40)$$

- the rated nonlinear winding to oil thermal resistance as

$$R_{th-hs-oil,R} = \frac{1}{C_1 \times a} \times \left(\frac{\mu_R}{\Delta\theta_{H,R}} \right)^n \qquad (2.41)$$

- the rated winding hotspot temperature rise above top oil as

$$\Delta\theta_{H,R} = q_{cu,R} \times R_{th-hs-oil,R} \qquad (2.42)$$

- the rated winding time constant as

$$\tau_w = R_{th-hs-oil,R} \times C_{th-wdn} \qquad (2.43)$$

- the rated transformer winding losses as

$$q_{cuR} \equiv P_{DC-R} + P_{EC-R} \quad (2.44)$$

The hotspot temperature is then expressed as

$$K^2 \left[\frac{k_\theta + \dfrac{P_{EC-R(pu)}}{K_\theta}}{1 + P_{EC-R(pu)}} \right] \times \mu_{pu}^m \times \Delta\theta_{H,R} = \mu_{pu}^m \times \tau_w \frac{d\theta_H}{dt} + \frac{[\theta_H - \theta_{TO}]^{1+m}}{\Delta\theta_{H,R}^m} \quad (2.45)$$

The models were validated with a 250 MVA transformer and showed good results in relation to measured values [19].

2.4 Conclusion

In this chapter, a brief review of predictive maintenance of transformers is given with emphasis on the use of thermal monitoring to estimate the life span of the transformer. Various existing thermal models have been presented while highlighting their different thermal modeling approaches. Based on the review, four of the mentioned thermal models as summarized in Table 2.5 will be considered in this study and will be extended to rectifier transformers to include the effects of increased thermal stress due to harmonic currents and will be presented in the next chapter. The four models include: the improved IEEE model, the IEC model, G. Swift model and D. Susa Model.

Table 2.5   Comparison of Existing Thermal Models for Regulating Transformers

	Improved IEEE Model	IEC Model	G. Swift Model	D. Susa Model
Similarities	Temperature rise is influenced by transformer loading and ambient temperature as well as type of cooling	Temperature rise is influenced by transformer loading and ambient temperature as well as type of cooling	Temperature rise is influenced by transformer loading and ambient temperature as well as type of cooling	Temperature rise is influenced by transformer loading and ambient temperature as well as type of cooling
	Consist of a top oil and hotspot model	Consist of a top oil and hotspot model	Consist of a top oil and hotspot model	Consist of a top oil and hotspot model
Differences	Models the top oil temperature and hotspot temperature as a first order differential equation based on heat transfer principles	Same as the IEEE model but takes into consideration the effect of varying rate of oil flow through the hotspot	Models the top oil and hotspot temperature based on a thermo-electric analogy, lumped capacitance and heat transfer principles	Same as the G. Swift model but includes the effect of varying oil viscosity with top oil temperature

The G. Swift model was considered over the A. Elmoudi model because the A. Elmoudi model contains a parameter, the per unit winding eddy current losses at hotspot location $(P_{EC-R(pu)})$ which is only provided by the transformer manufacturers and are protected by intellectual property rights. The $P_{EC-R(pu)}$ is used to include the effect of variation of the transformer losses with varying hotspot temperature. Therefore, ignoring the effect of this phenomenon, the A. Elmoudi model becomes the G. Swift model.

CHAPTER 3   RECTIFIER TRANSFORMERS THERMAL MODELING

3.1   Introduction

This chapter gives a brief insight into rectifier transformers, its design considerations and winding configurations common in the industry. Also, a focus on the losses that occur in this transformer is presented which forms a basis for the heating in the winding. The effect of harmonics generated from rectifiers connected to these transformers on the losses is presented as well. Furthermore, the selected thermal models are expanded to account for the increased heating due to harmonic currents flowing through the rectifier transformers which will be used for estimating the hotspot temperatures. Lastly, a description of the Alcoa rectifier transformers which is the case study of this thesis is shown.

3.2   Rectifier Transformers

Rectifier transformers are specially designed transformers for rectification applications. They are used for the purpose of voltage regulation and harmonic reduction in rectifying systems. Rectifier transformers are being used in various industrial applications which require very large DC currents such as electrolysis of aluminum, chemical ones for zinc, copper or chlorine. A simplified electrical layout of an aluminum smelter is presented in Figure 3.1 below.
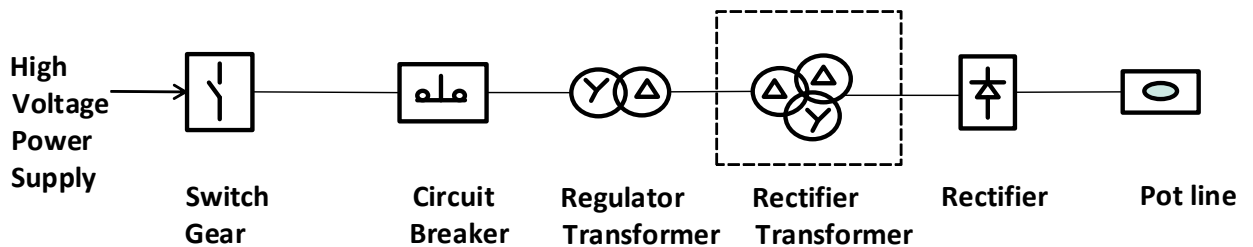
Figure 3.1   Electrical Layout of an Aluminum Smelter

The first rectifier transformers were designed for mercury-arc rectifiers. These transformers were designed to withstand short-circuit failures associated with arc backs from the mercury arc rectifiers and specification of the design can be found in the ANSI/IEEE C57.18-1964 Standard on Pool Cathode Mercury-Arc Rectifier Transformers [8, 26]. These problems brought about the evolution of the semiconductor rectifiers which totally eliminated the issue of arc backs as well as brought about reduction in the weight, size and cost in rectifier transformers. A downside to this new technology is the presence of large harmonic currents which result in undesirable heating of the winding and tap changers.

3.3   Rectifier Transformer Configuration

The design of a rectifier transformer is much more complex when compared to standard distribution and power transformers in terms of winding configuration, bushing arrangement, harmonic cancellation, winding temperature indicators, winding eddy current losses and stray loss heating effect [9, 10, 11, 12].

The winding configuration of a rectifier transformer is of two types; the single way circuit configuration (ANSI circuit #45) which has a delta primary with two wye secondary windings and the bridge type circuit (ANSI circuit #31) which is composed of a wye or delta primary winding with two secondary windings connected in delta and wye [10].

DELTA, TWELVE PHASE, MULTIPLE
DELTA-WYE, DOUBLE-WAY
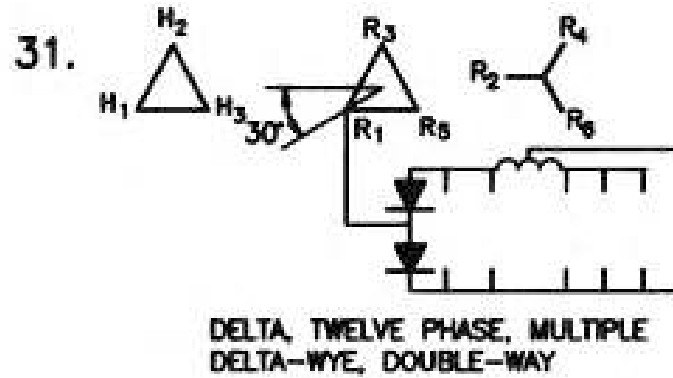
Figure 3.2   ANSI Circuit Number 31 [10]

DELTA, SIX PHASE, DOUBLE WYE
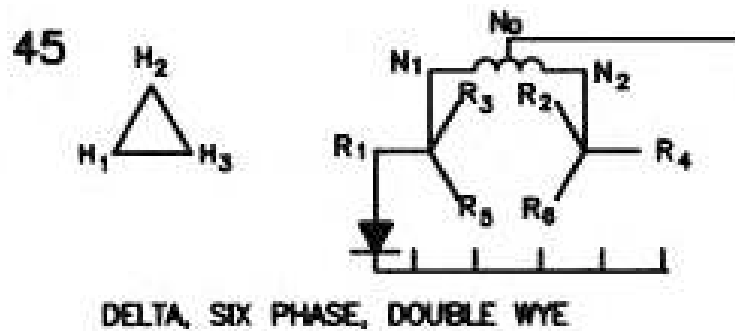
Figure 3.3   ANSI Circuit Number 45 [10]

Rectifier transformers are subject to harmonics from the rectifier connected to them and are usually designed to cancel out these harmonics. The single way circuit rectifier transformers have two three pulse secondary windings. In most cases, the two windings are tightly interleaved which leads to the partial cancellation of their electromagnetic fields resulting in six pulse on both the primary and secondary windings. In the case of the bridge type circuit rectifier transformers, the two six pulse secondary windings may be tightly interleaved which results in a twelve pulse harmonic effect on both primary and secondary windings or may be loosely interleaved resulting in a six pulse harmonic effect on the secondary windings and a twelve pulse effect on the primary winding [8].

The winding temperature indicators used in distribution and power transformers such as bulb type sensors, thermocouples and current transformers are usually affected by harmonics generated from the rectifiers. Fibre optic probes have been found to be impervious to these harmonic currents and are generally recommended for use in these transformers. A major drawback of the fibre optic probes is their fragile nature which makes it impossible to repair or replace if damaged without a rewind of the windings [8].

The bushing arrangement of a rectifier transformer is usually determined by the position of the rectifier and has to be provided by a specifying engineer.

The winding eddy current losses which cause hotspot heating increase due to the presence of harmonic current therefore, a proper impedance balancing, careful winding and reduction in the winding duct will result in a reduction in the effect of the winding stray losses. Also, the use of nonmagnetic materials, conductive shields and magnetic shields in the core clamps and heat minimizes stray losses induced by the harmonic currents [8].

3.4   Rectifier Transformer Losses

The increased temperature rise in the winding of a rectifier transformer due to increased current harmonics by semiconductor rectifiers is a major problem for rectifier manufactures as well as users. This increased heating is due to the increase in transformer losses caused by more harmonics [9, 10]. In rectifier transformer design, a specification of the current harmonics generated by the rectifier is provided by a specifying engineer who has knowledge about the rectifier to enable manufacturers to properly account for the increased losses. In the event where this information is not presented, a $120^o - 60^o$ square current

waveform is assumed which is the ideal case of a current generated by a six pulse rectifier [9].

The losses in a rectifier transformer comprise of no load losses and load losses as in (3.1)

$$P_{T-\text{Rec}} = P_{NL-\text{Rec}} + P_{LL-\text{Rec}} \qquad (3.1)$$

where

P_{T-Rec} − Rectifier Transformer total Power Losses

P_{LL-Rec} - Rectifier Transformer total Load Losses

P_{NL-Rec} - Rectifier Transformer no Load Losses

The no load losses is due to core hysteresis and core eddy current losses [27].

$$P_{NL-\text{Rec}} = P_h + P_e \qquad (3.2)$$

The hysteresis loss is due to resistance of the magnetization and demagnetization of the core caused by the induced alternating magnetic field. The hysteresis loss (P_h) is defined as a function of the maximum flux density and the frequency of the voltage inducing the flux as

$$P_h = K_h \times f \times B_m^{1.6} \qquad (3.3)$$

where

K_h - Hysteresis constant

f – Frequency

B_m – Maximum flux density

The eddy current losses (P_e) are caused by the alternating flux which induces an EMF on the core resulting in circuiting currents in the core. The core is usually laminated with thin sheets of silicon steel to reduce the circulating eddy currents. Therefore the core eddy current losses is a function of the squared of the frequency of the induced flux, the maximum flux density and the thickness of the lamination strip and is given in (3.4) as

$$P_e = K_e \times B_m^2 \times f^2 \times T^2 \qquad (3.4)$$

where

K_e – Eddy current constant

f – Frequency

B_m – Maximum flux density

T – Thickness of lamination strips

In general, the no load losses are constant with a variation in the transformer loading as the losses are affected by the voltage inducing the magnetic flux which remains constant at varying loads.

The load loss on the other hand is composed of three components: the copper winding DC resistance loss (P_{DC-Rec}), the winding eddy current loss (P_{EC-Rec}) and the other stray losses in metallic structures ($P_{OSL-Rec}$) [9, 10, 11, 12].

$$P_{LL-Rec} = P_{DC-Rec} + P_{EC-Rec} + P_{OSL-Rec} \quad (3.5)$$

The winding DC loss is caused by the resistance of the copper winding to currents flowing in the winding and varies with the square of the RMS current as given in (3.6). The winding eddy current loss is caused by curre nt flowing in the winding due to induced voltage by leakage magnetic fields and varies with the square of the frequency of the current as given in (3.7). Stray losses in the tank and other metallic parts are also caused by induced voltages due to leakage magnetic fields and vary with the frequency of the current raised to the power of 0.8 as given in (3.8).

$$P_{DC-\mathrm{Re}c} = P_{DC-R} \sum_{h=1}^{max} \left(\frac{I_h^2}{I_R^2} \right) \quad (3.6)$$

$$P_{EC-\mathrm{Re}c} = P_{EC-R} \sum_{h=1}^{max} \left(\frac{I_h^2}{I_R^2} h^2 \right) \quad (3.7)$$

$$P_{OSL-\mathrm{Re}c} = P_{OSL-R} \sum_{h=1}^{max} \left(\frac{I_h^2}{I_R^2} h^{0.8} \right) \quad (3.8)$$

where

P_{DC-R} - DC winding resistance losses at rated fundamental current and frequency

P_{EC-R} - Winding eddy current losses at rated fundamental current and frequency

P_{OSL-R} - Other stray losses in tank and other metal parts at rated fundamental current and frequency

I_h - Load current at harmonic order

h - Harmonic order

I_R - Rated load current at fundamental current and frequency

P_{DC-R}, P_{EC-R} and P_{OSL-R} are the losses measured using a pure sinusoidal current at the rated fundamental frequency of the rectifier transformer. The measurement using the rated fundamental frequency current complies with industrial standards set in the IEEE std C57.18.10 guide [9] as well as the IEC standard on rectifier transformers [10] and are tagged as guarantee losses for commercial purposes. Most transformer nameplates contain this information as opposed to the rated rectifier transformer losses with harmonic load current. The rated rectifier transformer losses are not guaranteed as they are based on estimates made by a specifying engineer or by the assumption of a 120º - 60º square wave current.

With the assumption of a 120º – 60º square wave current, the rated rectifier transformer losses and current are increased and is summarized in Table 3.1.

Table 3.1   Rectifier Transformer Losses Gain Factor

	Gain Factor	
	6 Pulse	12 Pulse
I_R	1.0274	1.0037
P_{DC-R}	1.0555	1.0075
P_{EC-R}	3.9856	2.0967
P_{OSL-R}	1.2521	1.0545

The RMS current at fundamental frequency is calculated to increase by 1.0274 times for a 6 pulse application and by 1.0037 for a 12 pulse application. The rated winding eddy current loss at fundamental current and frequency is calculated to increase by 3.9856 for a 6 pulse rectifier transformer and by 2.0967 for a 12 pulse rectifier transformer. The rated DC winding resistance loss at fundamental current and frequency is calculated to increase

by a factor of 1.0555 for a 6 pulse rectifier transformer and by 1.0075 for a 12 pulse rectifier transformer. The other stray losses in metallic parts at fundamental current and frequency is calculated to increase by 1.2521 for a 6 pulse rectifier transformer and by 1.0545 for a 12 pulse rectifier transformer [8].

3.5   Thermal Modeling for Rectifier Transformer

Rectifier transformers are subject to harmonic currents generated by the rectifiers which are connected in series to them. These harmonic currents create an increase in the load losses which cause an increase in the heating of the transformer top oil and hotspot temperatures. The thermal models in Chapter 2 do not account for these harmonic losses as they were modeled for power transformers under a sinusoidal load current.

In this thesis project, an adaptation of four of the existing thermal models to rectifier transformers is proposed to incorporate the increase in losses.

The thermal models define the effect of losses in the top oil models of a transformer as

$$\frac{1+RK^2}{1+R} \qquad (3.9)$$

where R is the ratio of load losses to no-load losses at fundamental frequency and K is the load factor or the per unit loading of the transformer and expressed in equation (3.11) as

$$R = \frac{P_{LL-R}}{P_{NL-R}} \quad (3.10) \text{ and } K = \frac{I}{I_R} \quad (3.11)$$

where

P_{LL-R} − Total load losses at rated fundamental current and frequency

P_{NL-R} – No-load losses at rated fundamental current and frequency

I – Fundamental sinusoidal load current

I_R - Rated load current at fundamental current and frequency

The equation (3.9) can be represented as seen in [13] in terms of power losses as a ratio of the total losses at certain load to the rated total losses as given in (3.12) as

$$\frac{1+RK^2}{1+R} = \frac{P_{NL}+P_{LL}}{P_{NL-R}+P_{LL-R}} \qquad (3.12)$$

In order to adapt this equation to rectifier transformers the losses need to be redefined in terms of rectifier transformer losses as

$$\frac{P_{NL-Rec}+P_{LL-Rec}}{P_{NL-Rec}+P_{LL-Rec-R}} = \frac{P_{NL-Rec}+P_{DC-R}\sum\limits_{h=1}^{max}\left(\frac{I_h^2}{I_R^2}\right)+P_{EC-R}\sum\limits_{h=1}^{max}\left(\frac{I_h^2}{I_R^2}h^2\right)+P_{OSL-R}\sum\limits_{h=1}^{max}\left(\frac{I_h^2}{I_R^2}h^{0.8}\right)}{P_{NL-Rec}+P_{DC-Rec-R}+P_{EC-Rec-R}+P_{OSL-Rec-R}}$$

$$(3.13)$$

where

$P_{DC-Rec-R}$ – DC winding resistance losses at rated RMS harmonic rectifier current

$P_{EC-Rec-R}$ – Winding eddy current losses at rated RMS harmonic rectifier current

$P_{OSL-Rec-R}$ - Other stray losses in tank and other metal parts at rated RMS harmonic rectifier current

If we assume that the magnitude of each harmonic current reduces with the same ratio for every variation in the load current flowing through the rectifier transformer as would be

the case in an ideal situation and redefine the load losses to no-load losses in a rectifier transformer as

$$R_{\mathrm{Re}c} = \frac{P_{LL-\mathrm{Re}c}}{P_{NL-\mathrm{Re}c}} \qquad (3.14)$$

and the per unit loading of the rectifier transformer as

$$K_{\mathrm{Re}c} = \frac{\sqrt[2]{\sum_{h=1}^{\max} I_h^2}}{I_{\mathrm{Re}c}} \qquad (3.15)$$

where

I_{Rec} - the rated rectifier RMS harmonic current

the ratio of total losses at certain load to the rated total losses in a rectifier transformer can then be expressed as

$$\frac{P_{NL-\mathrm{Re}c} + P_{LL-\mathrm{Re}c}}{P_{NL-\mathrm{Re}c} + P_{LL-\mathrm{Re}c-R}} = \frac{1 + R_{\mathrm{Re}c}K_{\mathrm{Re}c}^2}{1 + R_{\mathrm{Re}c}} \qquad (3.16)$$

3.5.1 IEC Thermal Model

The adaptation of the IEC thermal models to rectifier transformers to account for the harmonic currents is presented as follows:

The top oil temperature model is expressed as

$$\left[\frac{1 + R_{\mathrm{Re}c}K_{\mathrm{Re}c}^2}{1 + R_{\mathrm{Re}c}}\right]^n \times \left(\Delta\theta_{To-R}\right) = K_{11} \times \tau_{TO} \times \frac{d\theta_{TO}}{dt} + \left[\theta_{TO} - \theta_A\right] \quad (3.17)$$

and the hotspot models as

$$K_{22} \times \tau_w \frac{d\Delta\theta_{H1}}{dt} = K_{21} \times \Delta\theta_{H,R} \times K_{\mathrm{Rec}}^{2m} - \Delta\theta_{H1} \qquad (3.18)$$

$$\left(\frac{k_{22}}{\tau_{TO}}\right) \times \frac{d\Delta\theta_{H2}}{dt} = (K_{21}-1) \times \Delta\theta_{H,R} \times K_{\mathrm{Rec}}^{2m} - \Delta\theta_{H2} \qquad (3.19)$$

3.5.2   Improved IEEE Model

The adaptation of the improved IEEE model to rectifier transformers to account for the harmonic currents is presented as follows:

The top oil temperature model is expressed as

$$\tau_{TO} \frac{d\theta_{TO}}{dt} = \left[\frac{1+R_{\mathrm{Rec}}K_{\mathrm{Rec}}^2}{1+R_{\mathrm{Rec}}}\right]^n \times (\Delta\theta_{To-R}) - \theta_{TO} + \theta_A \qquad (3.20)$$

and the hotspot model as

$$\tau_w \frac{d\Delta\theta_H}{dt} = \Delta\theta_{H,R} \times K_{\mathrm{Rec}}^{2m} - \Delta\theta_H \qquad (3.21)$$

3.5.3   G.Swift Thermal Model

The adaptation of the G.Swift Thermal model to rectifier transformers to account for the harmonic currents is presented as follows:

The top oil temperature model is expressed as

$$\left[\frac{1+R_{\mathrm{Rec}}K_{\mathrm{Rec}}^2}{1+R_{\mathrm{Rec}}}\right] \times (\Delta\theta_{To-R})^{\frac{1}{n}} = \tau_{TO} \times \frac{d\theta_{TO}}{dt} + [\theta_{TO} - \theta_A]^{\frac{1}{n}} \qquad (3.22)$$

and the hotspot model as

$$K_{\mathrm{Rec}}^2 \times (\Delta\theta_{H,R})^{\frac{1}{m}} = \tau_w \times \frac{d\theta_H}{dt} + [\theta_H - \theta_{TO}]^{\frac{1}{m}} \qquad (3.23)$$

3.5.4 D. Susa Thermal Model

The adaptation of the D. Susa thermal model to rectifier transformers to account for the harmonic currents is presented as follows:

The top oil temperature model is expressed as

$$\left[\frac{1+R_{\text{Rec}}K_{\text{Rec}}^2}{1+R_{\text{Rec}}}\right] \times \mu_{pu}^n \times \Delta\theta_{To-R} = \mu_{pu}^n \times \tau_{TO} \times \frac{d\theta_{TO}}{dt} + \frac{[\theta_{TO}-\theta_A]^{1+n}}{\Delta\theta_{To-R}^n} \qquad (3.24)$$

The hotspot model is modified to exclude the effect of varying DC resistance losses and winding stray eddy current losses with the hotspot temperature of the winding. This exclusion was made due to the non-availability of the winding eddy current per unit parameter which is solely known by the transformer manufacturer and is not readily available to customers in transformer datasheets due to intellectual property concerns. Also, from the knowledge that the winding hotspot temperature effect is directly proportional with the DC losses and inversely proportional with the winding stray losses, one can assume that the combined effect of the two losses is very minimal as they counteract each other. The resultant D. Susa hotspot model is shown as

$$K_{\text{Rec}}^2 \times \mu_{pu}^m \times \Delta\theta_{H,R} = \mu_{pu}^m \times \tau_w \times \frac{d\theta_H}{dt} + \frac{[\theta_H-\theta_{TO}]^{1+m}}{\Delta\theta_{H,R}^m} \qquad (3.25)$$

3.6 Case Study: Alcoa Rectifier Transformer

Alcoa is a major producer of primary and fabricated aluminum in the world. Alcoa was instituted in the 1888 by Charles Martin Hall with its headquarters situated in Pittsburg, Pennsylvania, U.S.A. and has spread over the years to over 30 countries.

Alcoa Aluminum Smelters comprise of various high voltage equipment such as Air Insulated Switchgears (AIS), Gas Insulated Switchgears (GIS), Oil and SF_6 Filled Circuit Breakers, Regulator Transformers, Rectifier Transformers, Distribution Transformers and Rectifiers. The reliability of this equipment is very critical to Alcoa as well as to the aluminum smelting industry and various efforts are being made in terms of effective maintenance schemes to optimize the usage of this equipment as well as production output.

The Alcoa Baie Comeau smelter in Canada which is the largest in primary aluminum production when compared to the other two smelters, the Deschambault Smelter and the Becancour Smelter is presently conducting research in predictive maintenance of the high voltage equipment.

The first stage research has been focused on the rectifier transformers as they are very critical in the production chain of aluminum. The rectifier transformers are used in the process of converting ac currents to dc currents which are used for the smelting of the aluminum in the aluminum pots. The research objective is to develop a model which could be used for online monitoring and future estimation of the top oil and hotspot temperatures of the rectifier transformers to enable optimum utilization of these assets as well as to enable scheduling of routine maintenance.

3.6.1 Alcoa Rectifier Transformers

The case study is carried out on the Alcoa Baie Comeau Smelter Potline D rectifier transformers. The Potline D contains six rectifier transformers named TR41-2 to TR46-2. The rectifier transformers are 3-winding transformers and were manufactured by the

General Electric Company of Canada in 1984 and have specifications as shown in Table
3.2

Table 3.2   Rectifier Transformers Specification

Parameters	TR41-2	TR42-2	TR43-2	TR44-2	TR45-2	TR46-2
Power (MVA)	47.9	47.9	47.9	47.9	47.9	47.9
High Voltage (V)	27500	27500	27500	27500	27500	27500
Low Voltage (V)	505.6	505.6	505.6	505.6	505.6	505.6
Output line Current (A)	16330	16330	16330	16330	16330	16330
Type of Cooling	OFAF	OFAF	OFAF	OFAF	OFAF	OFAF
Rated Average Winding Rise above Ambient Temperature (^{o}C)	55	55	55	55	55	55
Mass of Core and Coil (kg)	48000	48000	48000	48000	48000	48000
Mass of Tank (kg)	11000	11000	11000	11000	11000	11000
Mass of oil (kg)	22100	22100	22100	22100	22100	22100
No Load Loss (W)	42800	45800	46300	46300	45000	44800
Load Loss (W)	176000	183600	176200	179000	181500	183800

The windings of the rectifier transformers are designed based on the circuit #31 in the ANSI/IEEE standard guide on rectifier transformers [9] and have a delta primary winding and two secondary windings; one connected in wye and the other in delta.

The rectifier transformers are oil filled with an oil forced air forced (OFAF) cooling system design. The transformers have three fans and one oil pump. The design was made for an operation with two fans at maximum intensity with the other fan as spare and with the oil pump operating continuously at all transformer loading intensity levels.

At the time of installation, the rectifier transformers were subject to 0.75 per unit loading all year round. Presently, the rectifier transformers at the plant run at almost full capacity with 0.95 per unit loading in the winter and 0.88 per unit loading in the summer. During the winter period, the transformer cooling fan is set to operate with one fan on (OFAF mode 1) for oil temperatures above 20°C and with all three fans (OFAF mode 2) for oil temperatures above 55°C while in summer period all three fans are set to operate (OFAF mode 2) for an oil temperature above 20°C.

CHAPTER 4   RECTIFIER TRANSFORMER THERMAL MODEL PARAMETER ESTIMATION USING NONLINEAR LEAST SQUARES

4.1   Introduction

This chapter presents the use of nonlinear least squares optimization as an extrapolation technique for obtaining the rectifier thermal model parameters. The developed thermal models obtained in the previous chapter are characterized by parameters which are obtained through offline heat run tests. Where these tests are not feasible such as the transformers in the case study, extrapolation techniques using online measurements of transformer loading factor, top oil temperature and hotspot temperature are employed. A brief description of the nonlinear least square technique is presented as well as an analysis of the results of this extrapolation technique.

4.2   Introduction to Nonlinear Least Square

The nonlinear least square (NLLSQ) is a data fitting or optimization tool which involves the fitting of x observations to a nonlinear model of y unknown parameters by the linearization of the nonlinear model and the refining of the parameters through iterative processes so as to create a fit with the observations having the least possible error. The least square method was developed by Adrien Marie Legendre in 1805 whose work was used as a standard tool in astronomy and geodesy [28].

The least square technique is currently the most used statistical tool in data fitting and optimization problems as its principles are founded on well-developed mathematical

theories and the solutions are normally distributed around the true or best solutions with the least possible error.

The major advantages of the nonlinear least square method include:

- The ability to fit data to a vast range of functions
- A well-developed mathematical theory which provides a strong confidence in computed results
- Use in problems that have multiple solutions or over-determined systems

Some of the disadvantages of the nonlinear least square method include:

- An iterative process which leads to a slow convergence of results and sometimes to a non-convergence depending on the complexity of the function to be fitted.
- Requires information from a derivation function of the parameters of the function with respect to the error of estimation (residuals). This information might be very difficult to obtain especially for very complex functions.
- The need for an initial guess of the function parameters which must be selected wisely and close to the best or global solution to avoid searching for solutions in a local minimum search space [28].

4.3   Non Linear Least Squares Structure

The structure of a nonlinear least square technique is shown in Figure 4.1
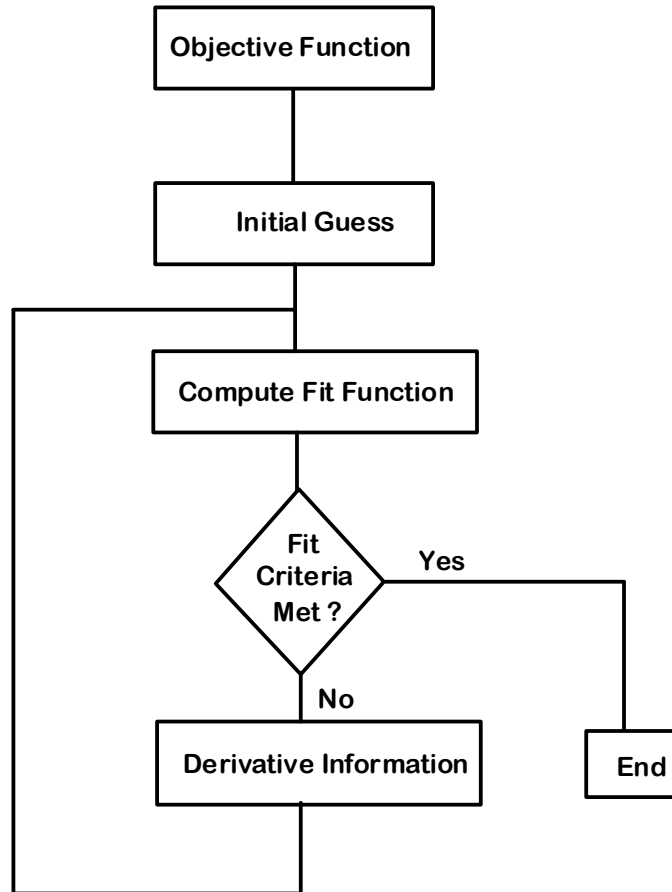
Figure 4.1   Non Linear Least Square Optimization Structure

The objective of the NLLSQ is to minimize the error in fitting a nonlinear function with unknown parameters to a set of given data. Given a nonlinear function in the form $f(x, B_j)$, where x is a known independent variable, B_j is a set of j unknown parameters and a set of measured data points, Y_i, containing i number of observations, the NLLSQ objective function is defined as

$$\min R(x, B_j) = \sum_{K=1}^{i} [Y_i - f_i(x, B_j)]^2 \quad (4.1)$$

where R is the sum of the squared error between the estimated values and the measured values and the main objective is to minimize the error obtained in R to the least possible error.

In order to evaluate the minimize values, it is important to note that the number of observed or measured points, i, should be equal to or greater than the number of unknown parameters, j. In most cases it is better to have a greater number of points as to have more details about the trend of the measured points.

To find the minimum R over the search space of unknown parameters B_j, a computation of the partial derivative of R with respect to each unknown parameter is made and equated to zero as given in equation (4.2)

$$\frac{\partial R}{\partial B_j} = 0 \qquad (4.2)$$

With nonlinear functions, solving this equation may be impossible using normal mathematical techniques and require iterative processes to reach a solution. These iterative processes, require the guessing of initial solutions (parameters) which are then refined based on certain algorithms until the final solution is achieved [28, 29].

The most common algorithms used in NLLSQ are the Newton method, the gradient descent method and the Levenberg Marquardt method.

The newton method [30] is derived from the Taylor series first order expansion of a function expressed as

$$f(x_0 + \delta) \cong f(x_0) + \dot{f}(x_0)\delta \quad (4.3)$$

which is a tangent line to the curve at an initial guess point x_0 and intercepts the x axis at the point $x_0 + \delta$. The goal of the newton method is to find the point x for which $\dot{f}(x)$ is approximately zero. Defining $x_0 + \delta$ as the next guess point, the solution of the next guess point is given as

$$x_0 + \delta = x_0 - \frac{f(x_0)}{\dot{f}(x_0)} \qquad (4.4)$$

The iteration is continued until $\dot{f}(x_0)$ is equal to or approximately zero. The newton method is best used when the guess value is close to the minimum point as to enable a quick convergence.

The gradient descent method [31] is another algorithm used in NLLSQ for the minimization of errors in the data fitting process. It involves changing the direction of an unknown parameter towards the minimum point along the error function slope. Usually it is assumed that the error function is of a convex form and therefore, the aim of the gradient descent algorithm is to slide down the convex function at a rate η until it reaches the minimum point. Given an error function as $f(x_0)$ with an unknown parameter, x_0, the next point on the error function moving in the direction of the function minimum at a descending rate along the gradient is defined as

$$x_0' = x_0 - \eta \dot{f}(x_0) \qquad (4.5)$$

where x_0' is the next point and η is the descending rate. The descending rate in this algorithm approach is a critical component in the convergence towards the minimum point as a large descending rate may result to a very fast sliding along the opposite sides of convex error function making it difficult to hit the minimum and a very small descending

rate will take too long to reach the minimum. Therefore, the determination of a suitable descending rate which is usually done by a trial and error procedure is necessary. It is important to know that the gradient descent method is more suited to problems that have initial guess unknown parameters that are located far off from the minimum on the error function as it may easily skip the minimum when it closes in.

Similar to the newton method, the iteration of the unknown parameter is continued until the function $\dot{f}(x_0)$ is approximately zero which implies that it is at the minimum point.

The levenberg marquardt method [32] is a combination of both the newton method and the gradient descent method. It adopts the gradient descent method at points far from the minimum point and the newton method at point close to the minimum point in the error function of the NLLSQ. This method adopts the strength of both the newton and gradient descent methods are is most often utilized in solving NLLSQ fitting problems when compared to the others.

4.4   Application of Non Linear Least Square Method to Rectifier Transformer Thermal Modeling

The proposed thermal model for the Alcoa Rectifier Transformers consists of two models: the top oil model and the hotspot model. The top oil model is characterized by the rated oil time constant (τ_{TO}), the rated top oil rise above ambient temperature ($\varDelta\theta_{TO-R}$) and the exponential constant (n). The hotspot model on the other hand, is characterized by the rated winding time constant (τ_W), the rated hotspot temperature over top oil temperature ($\varDelta\theta_{H,R}$) and an exponential constant (m).

These parameters which characterize the top oil model and the hotspot model are usually determined by performing heat run tests as specified in the IEEE Std C57.18.10 guide [8] or IEC 600146 guide [9] and require the removal of the transformer from service. Presently at the Alcoa Plant, all the rectifier transformers are in service operating at about full capacity, which makes a heat run test not feasible as this would lead to reduction in output aluminum production. This therefore leads to the need to estimate these parameters.

The nonlinear least square method can be applied to the estimation of these parameters by the fitting of the outputs of the top oil and hotspot models to a set of measured or observed values. The top oil temperature is influenced by two input components: the transformer load factor and the ambient temperature while the hotspot temperature is influenced by the transformer load factor and the top oil temperature. In order to apply the NLLSQ, a set of measured transformer load factor, top oil temperature and hotspot temperature need to be recorded.

If we define Y_{toi} and Y_{hi} as a set of i measured top oil temperature values and hotspot temperature values, $f(x, B_{toj})$ and $f(x, B_{hj})$ as the output of the top oil model and hotspot model respectively due to a set of i measured input components, where B_{toj} represents the parameters that characterize the top oil model, B_{hj} represents the parameters that characterize the hotspot model and x represents the independent variables time (t), load factor (K_{Rec}) and ambient temperature (θ_A) we can estimate B_{toj} by minimizing the error $(R(x, B_{toj}))$, between Y_{toi} and $f(x, B_{toj})$ as defined by

$$\min R(x, B_{toj}) = \sum_{k=1}^{i} \left[Y_{tok} - f_k(x, B_{toj}) \right]^2 \qquad (4.6)$$

In the same manner, we can estimate B_{hj} by the minimizing the error $(R(x, B_{hj}))$, between Y_{hi} and $f(x, B_{hj})$ and is given by

$$\min R(x, B_{hj}) = \sum_{k=1}^{i} \left[Y_{hk} - f_k(x, B_{hj}) \right]^2 \qquad (4.7)$$

4.4.1 Field Measurements

In order to test and validate the proposed thermal model for the rectifier transformer, measurements of the transformer output load factor, ambient temperature, top oil temperature and hotspot temperature are to be taken. The transformer output load is recorded as a function of the output current flowing out of the rectifier as the rectifier transformer is designed to supply maximum current output at rectifier full load. The top oil temperature and hotspot temperature were recorded from the temperature gauges installed on the transformers. The readings of the oil temperature are recorded from a temperature probe placed at the top level of the oil while the hotspot temperature is calculated based on the top oil temperature and the level of current from a current transformer placed on the transformer winding. The calibration of the hotspot temperature gauge was done by the transformer manufacturers based on thermal tests and design experience. The ambient temperature reading was taken from the AccuWeather.com weather network [33] via the internet as no ambient temperature probe is installed at the plant.

The field tests were carried out on two different days to get the readings of the transformers in the two different fan cooling modes OFAF mode 1 and OFAF mode 2 with the OFAF mode 1 measurements on 17 March 2014 and the OFAF mode 2 measurements on 25 March 2014. On both occasions the rectifier transformers were running at almost full

intensity of about 0.96 per unit with all the pumps on. It would have been desirably to vary the rectifier transformer currents to observe the changes in the top oil and hotspot temperatures with varying ambient temperature but due to constraints such as the planned plant aluminum production output, the transformer output was kept constant at about 0.96 per unit with a variance of ±0.01 per unit due to current control by the saturable reactors. The readings for both the OFAF mode 1 and OFAF mode 2 were taken for TR41 to TR45 within a period of 5 hours with an average sampling time of 45 minutes between each measurements as the variation in the ambient temperature was very slow. Measurements for TR46 were not recorded as the gauges were faulty and gave wrong readings. The measurements for taken for the rectifier transformers TR41 to TR45 in the OFAF mode 1 and OFAF mode 2 are shown in Figures 4.2 to 4.11.
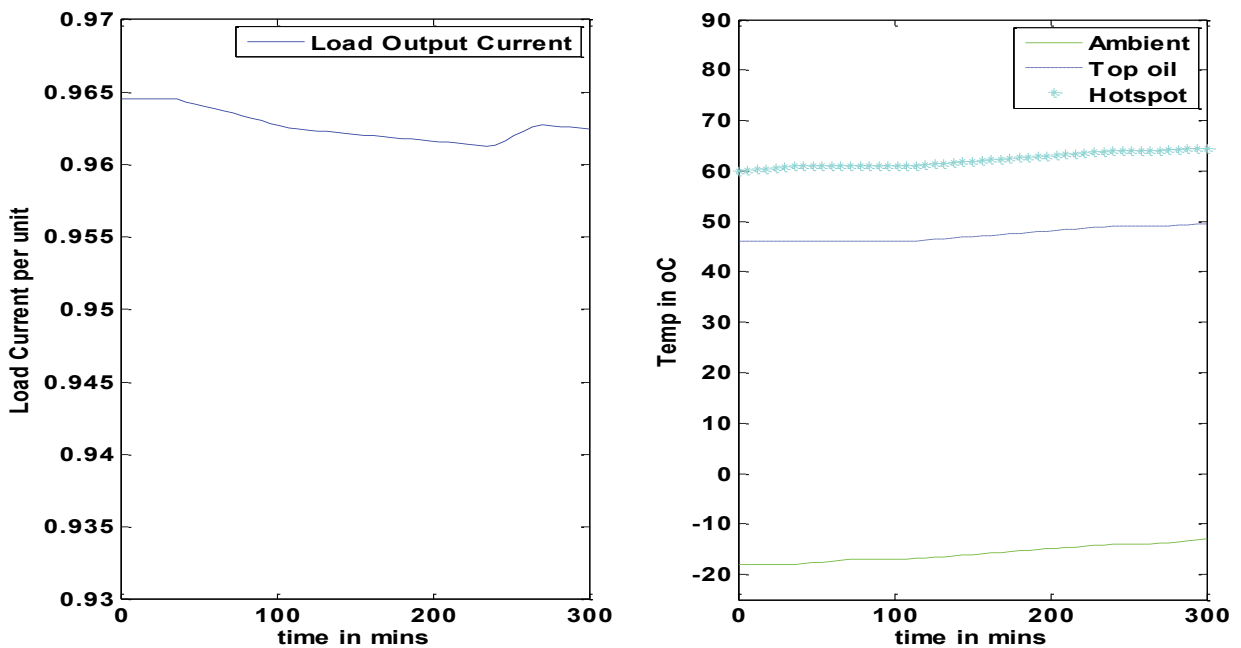
Figure 4.2   Measured TR41 per unit current, Ambient Temperature Top Oil Temperature and Hotspot Temperature during OFAF mode 1 condition
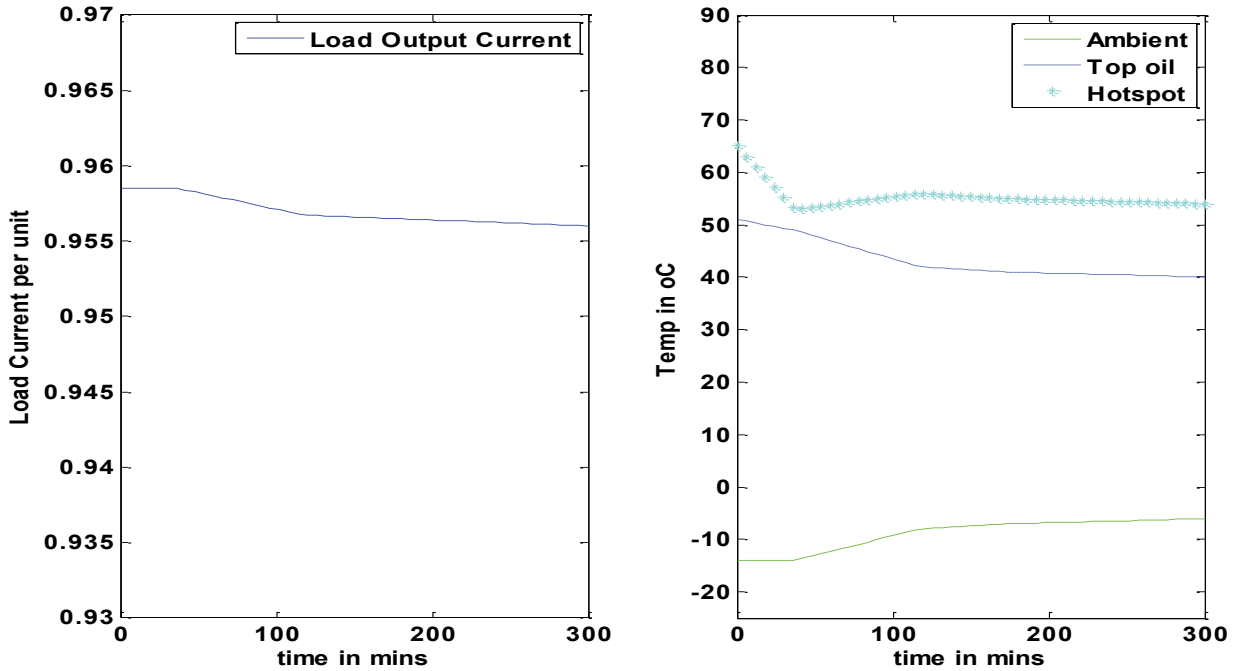
Figure 4.3   Measured TR41 per unit current, Ambient Temperature Top Oil

Temperature and Hotspot Temperature during OFAF mode 2 condition
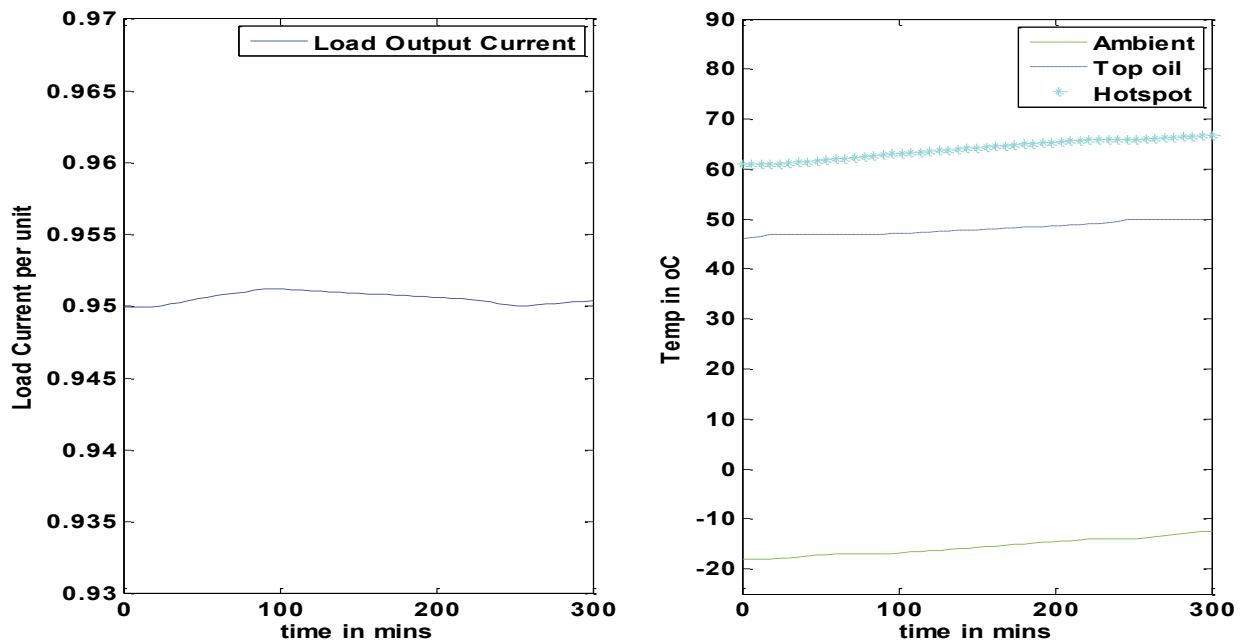
Figure 4.4   Measured TR42 per unit current, Ambient Temperature Top Oil

Temperature and Hotspot Temperature during OFAF mode 1 condition
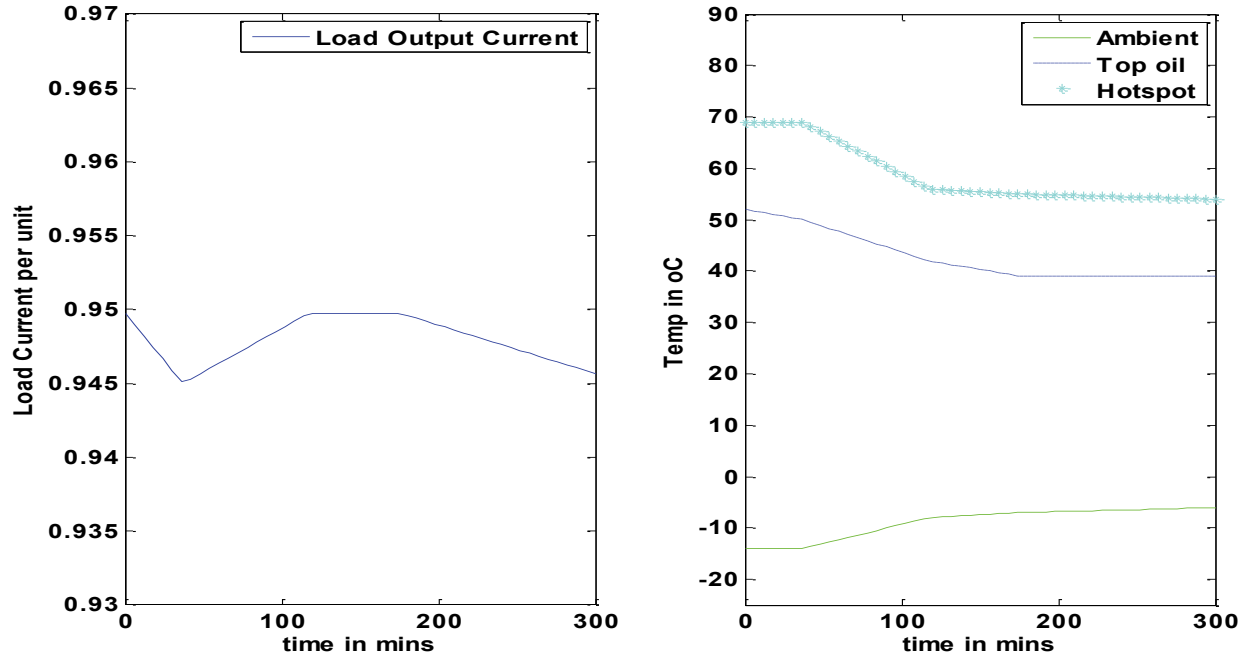
Figure 4.5   Measured TR42 per unit current, Ambient Temperature Top Oil

Temperature and Hotspot Temperature during OFAF mode 2 condition
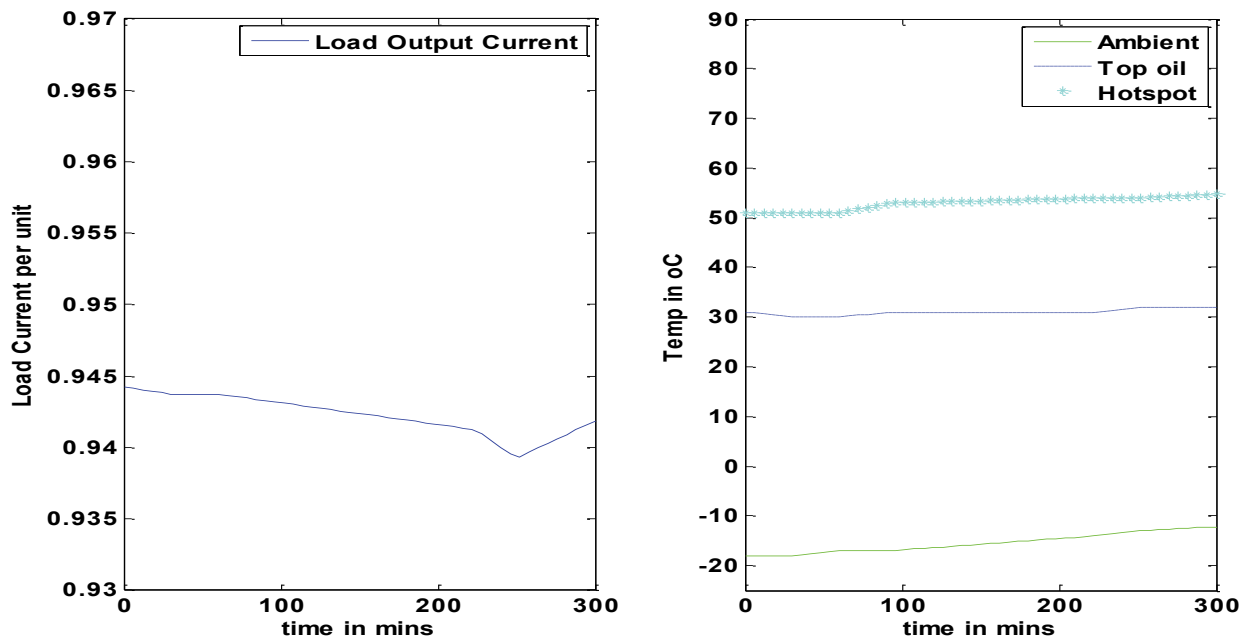
Figure 4.6   Measured TR43 per unit current, Ambient Temperature Top Oil

Temperature and Hotspot Temperature during OFAF mode 1 condition
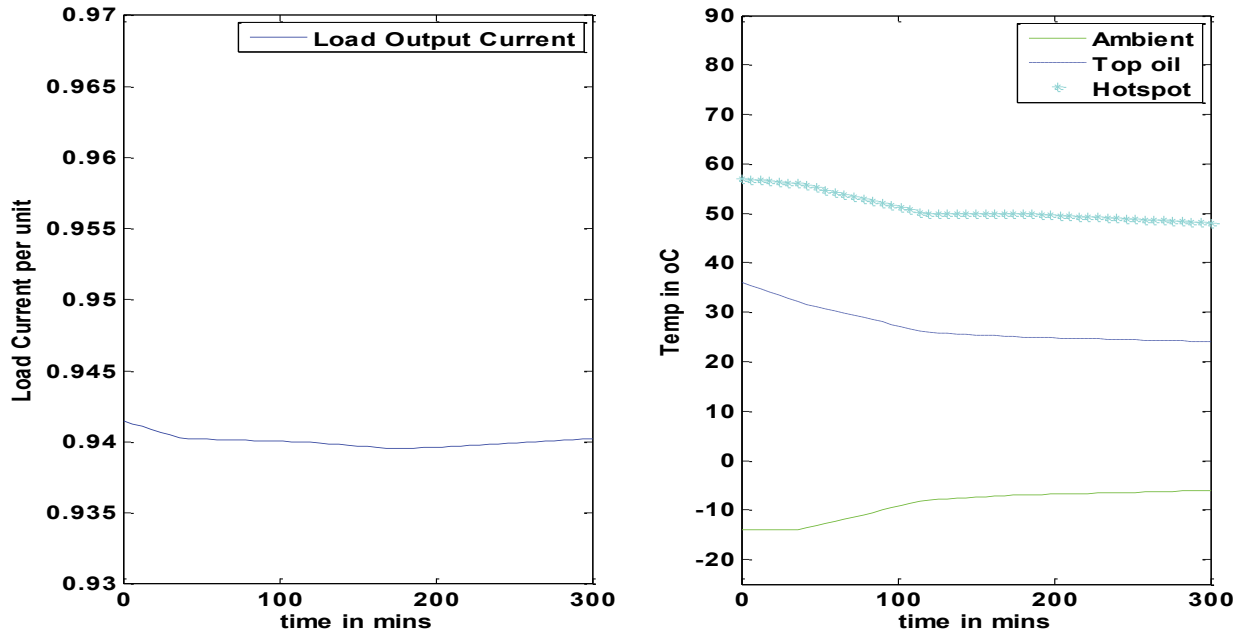
Figure 4.7   Measured TR43 per unit current, Ambient Temperature Top Oil
Temperature and Hotspot Temperature during OFAF mode 2 condition
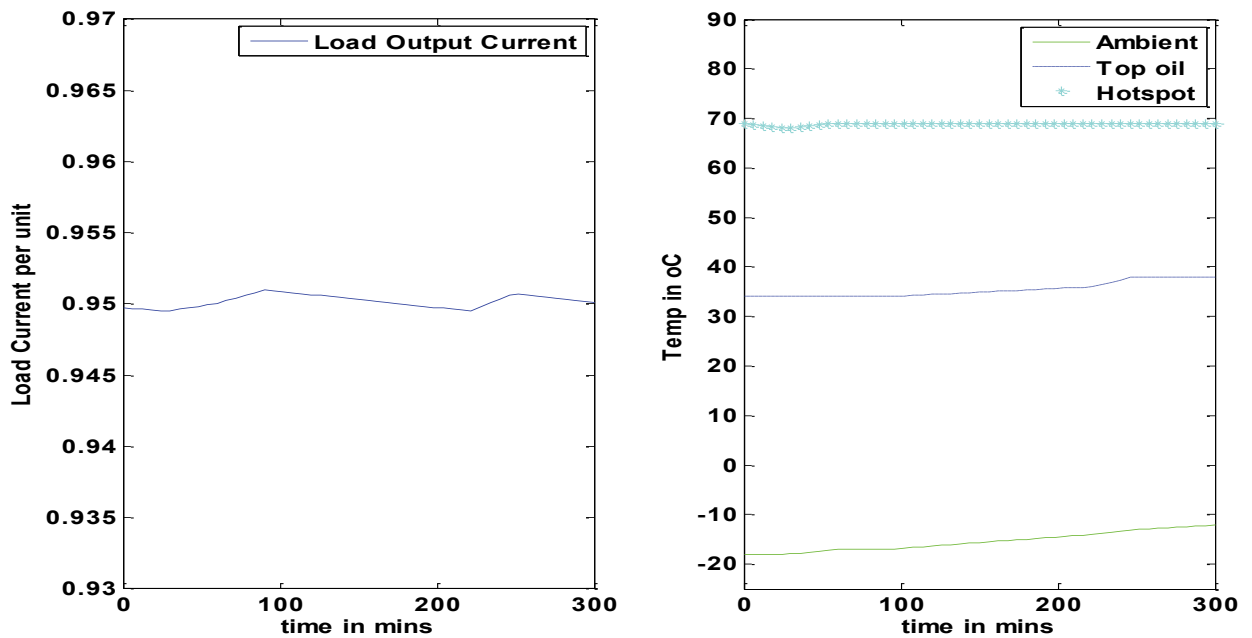
Figure 4.8   Measured TR44 per unit current, Ambient Temperature Top Oil
Temperature and Hotspot Temperature during OFAF mode 1 condition
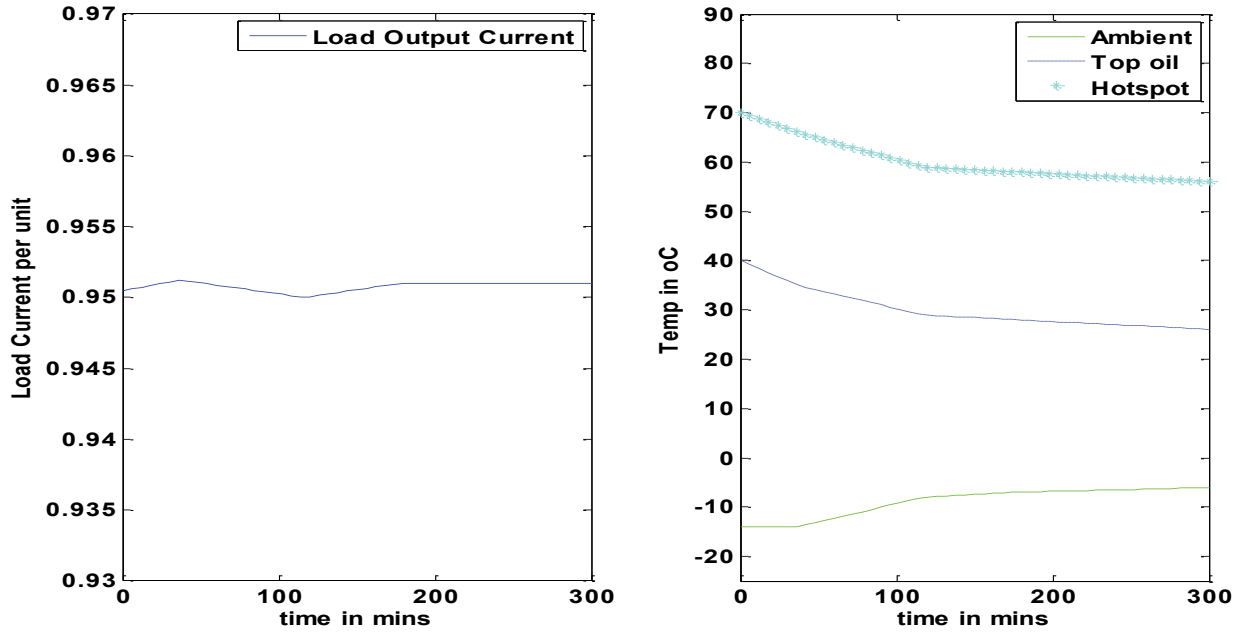
Figure 4.9   Measured   TR44   per   unit   current,   Ambient   Temperature   Top   Oil

Temperature and Hotspot Temperature during OFAF mode 2 condition
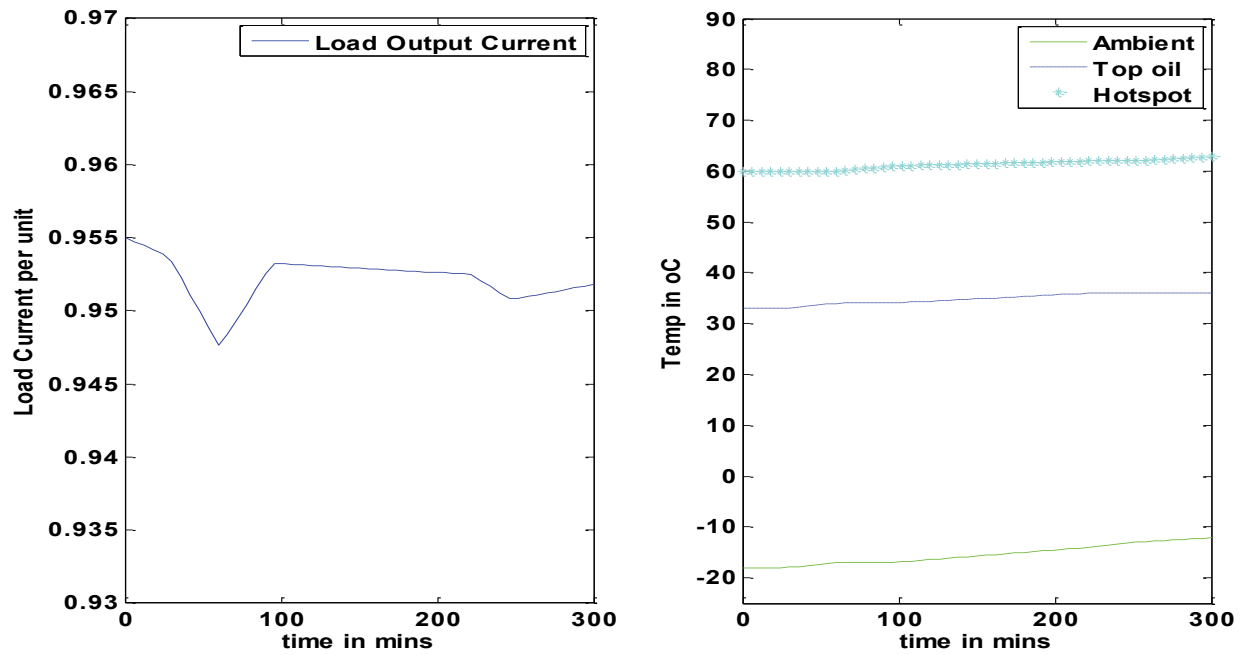
Figure 4.10   Measured   TR45   per   unit   current,   Ambient   Temperature   Top   Oil

Temperature and Hotspot Temperature during OFAF mode 1 condition
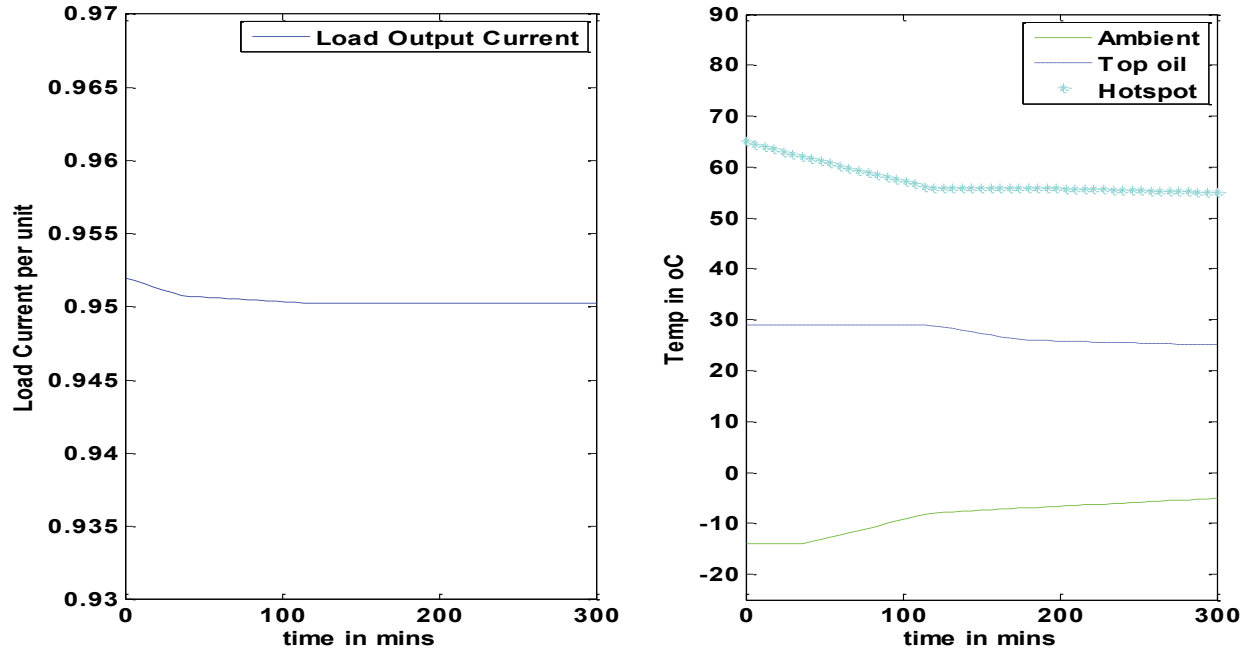
Figure 4.11   Measured TR45 per unit current, Ambient Temperature Top Oil Temperature and Hotspot Temperature during OFAF mode 2 condition

From the measured data, it can be observed that the top oil temperature and hotspot temperature increased as the ambient temperature was increasing with an approximate constant load factor in the OFAF mode 1 condition while the top oil temperature and hotspot temperature decreased for some time and remained constant with increasing ambient temperature with an approximate constant load factor in the OFAF mode 2 condition. The decrease in the top oil and hotspot temperatures is due to the switch in the transformer operating conditions from OFAF mode 1 to OFAF mode 2 while taking the field measurements. Based on these observations, it can be deduced that the influence of the transformer load factor and ambient temperature is less during the OFAF mode 2 conditions when compared to the OFAF mode 1.

Furthermore, it is important to note that the oil temperature profile and hotspot temperature profile of all the transformers are different even though the readings were taken under the same ambient temperature condition and approximately the same load factor on each transformer. Based on this observation, it will be expected that the parameters of the top oil model and hotspot model of each transformer will differ from one another even though the transformers are of the same power, age and manufacturer.

4.4.2   Parameter Estimation Results and Analysis

The parameter estimation is implemented using Matlab Simulink. The developed rectifier transformer thermal models as stated in Chapter 3 are modeled by the use of Matlab Simulink as shown in Figure 4.12 below. A detailed top oil model and hotspot model for each thermal model is given in Appendix 3.
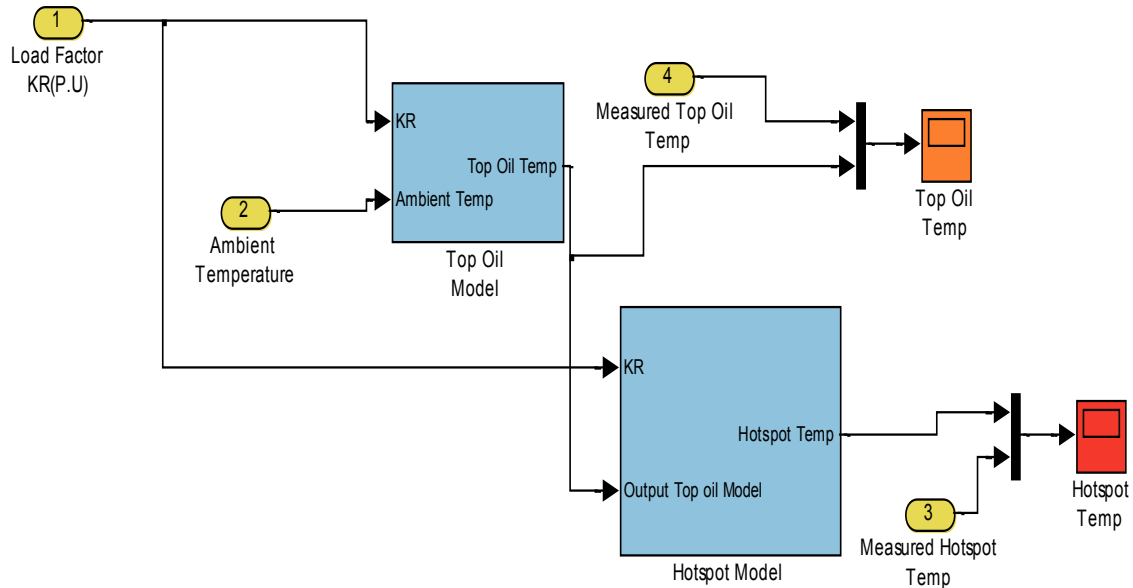
Figure 4.12   Matlab Simulink Implementation for the Rectifier Transformer Thermal Model

The nonlinear least square algorithm used is a custom made optimization toolbox developed by Matlab in the Simulink workspace as presented in figure 4.13 [34] below. The initial guess parameters for the top oil and hotspot models are derived using the guidelines in Appendix 1 which is based on the IEEE guide. The NLLSQ algorithm used in the parameter estimation is the levenberg marquardt method. The number of iterations was set to 100 as to enable the algorithm converge in good time. The mean square error value between the measured and the estimated top oil and hotspot temperatures was set to 0.0001 while the parameter change tolerance was set to 0.0001.
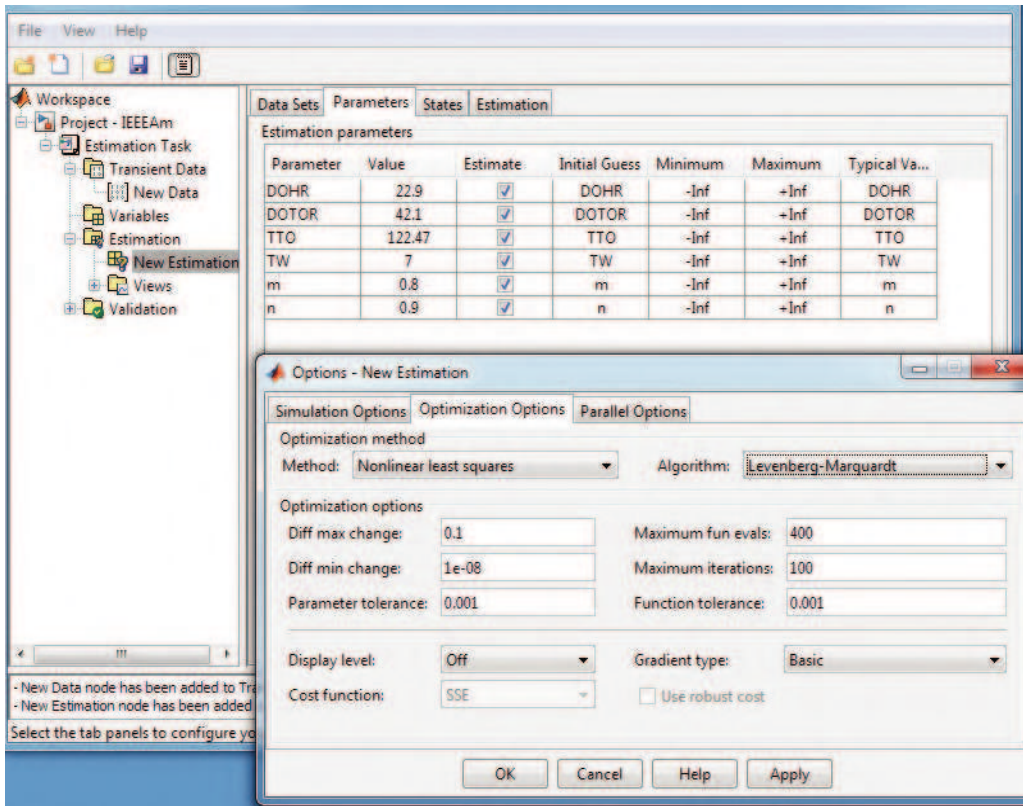
Figure 4.13   Simulink/Matlab Nonlinear Least Squared Optimization Toolbox

The Simulink simulation stop time is set to 300 minutes which is equal to time of the measured data from the field. The initial value for the integrator in the top oil model is set

to be equal to the initial value of the measured oil temperature while the initial value for the hotspot model is set equal to the initial value of the measured hotspot temperature.

The results of the estimated parameters of the thermal models of transformers TR41 to TR45 in the OFAF mode 1 and OFAF mode 2 using the nonlinear least square method are given in Tables 4.1 to 4.4 where

TM1 – Improved IEEE model

TM2 – IEC model

TM3 – G.Swift Model

TM4 – D.Susa Model

Table 4.1   OFAF Mode 1 Top Oil Model Parameter Estimation using Nonlinear Least Squared Method

OFAF MODE 1 PARAMETERS					
		TM1	TM2	TM3	TM4
TR41	$\Delta\theta_{TO\text{-}R}$ (K)	42.1	42.1	42.1	42.1
	τ_{TO}(mins)	122.47	122.47	122.47	118.37
	N	0.9	1.0	1.0	0.25
TR42	$\Delta\theta_{TO\text{-}R}$ (K)	42.1	42.1	42.1	42.1
	τ_{TO}(mins)	116.80	116.80	116.80	118.37
	N	0.9	1.0	1.0	0.25
TR43	$\Delta\theta_{TO\text{-}R}$ (K)	42.1	42.1	42.1	42.1
	τ_{TO}(mins)	120.43	120.43	120.43	175.65
	N	0.9	1.0	1.0	0.25
TR44	$\Delta\theta_{TO\text{-}R}$ (K)	42.1	42.1	42.1	42.1
	τ_{TO}(mins)	118.94	118.94	118.94	160.15
	N	0.9	1.0	1.0	0.25
TR45	$\Delta\theta_{TO\text{-}R}$ (K)	42.1	42.1	42.1	42.1
	τ_{TO}(mins)	118.30	118.30	118.30	165.0
	N	0.9	1.0	1.0	0.25

Table 4.2   OFAF Mode 1 Hotspot Model Parameter Estimation using Nonlinear Least Squared Method

OFAF MODE 1 PARAMETERS					
		TM1	TM2	TM3	TM4
TR41	$\Delta\theta_{(H,R)}$(K)	22.9	22.9	22.9	22.9
	τ_w(mins)	7.0	7.0	7.0	7.0
	M	0.8	0.8	0.8	0.25
TR42	$\Delta\theta_{(H,R)}$(K)	22.9	22.9	22.9	22.9
	τ_w(mins)	7.0	7.0	7.0	7.0
	M	0.8	0.8	0.8	0.25
TR43	$\Delta\theta_{(H,R)}$(K)	22.9	22.9	22.9	22.9
	τ_w(mins)	7.0	7.0	7.0	7.0
	M	0.8	0.8	0.8	0.25
TR44	$\Delta\theta_{(H,R)}$(K)	22.9	22.9	22.9	22.9
	τ_w(mins)	7.0	7.0	7.0	7.0
	M	0.8	0.8	0.8	0.25
TR45	$\Delta\theta_{(H,R)}$(K)	22.9	22.9	22.9	22.9
	τ_w(mins)	7.0	7.0	7.0	7.0
	M	0.8	0.8	0.8	0.25

Table 4.3   OFAF Mode 2 Top Oil Model Parameter Estimation using Nonlinear Least
Squared Method

OFAF MODE 2 PARAMETERS					
		TM1	TM2	TM3	TM4
TR41	$\Delta\theta_{TO-R}$ (K)	42.1	42.1	42.1	42.1
	τ_{TO}(mins)	122.47	122.47	122.47	106.76
	N	0.9	1.0	1.0	0.1
TR42	$\Delta\theta_{TO-R}$ (K)	42.1	42.1	42.1	42.1
	τ_{TO}(mins)	116.80	116.80	116.80	104.71
	N	0.9	1.0	1.0	0.1
TR43	$\Delta\theta_{TO-R}$ (K)	42.1	42.1	42.1	42.1
	τ_{TO}(mins)	120.43	120.43	120.43	151.23
	N	0.9	1.0	1.0	0
TR44	$\Delta\theta_{TO-R}$ (K)	42.1	42.1	42.1	42.1
	τ_{TO}(mins)	118.94	118.94	118.94	136.13
	N	0.9	1.0	1.0	0.1
TR45	$\Delta\theta_{TO-R}$ (K)	42.1	42.1	42.1	42.1
	τ_{TO}(mins)	118.30	118.30	118.30	146.13
	N	0.9	1.0	1.0	0

Table 4.4   OFAF Mode 2 Hotspot Model Parameter Estimation using Nonlinear Least
            Squared Method

OFAF MODE 2 PARAMETERS		TM1	TM2	TM3	TM4
TR41	$\Delta\theta_{(H,R)}$ (K)	22.9	22.9	22.9	22.9
	τ_w(mins)	7.0	7.0	7.0	7.0
	M	0.8	0.8	0.8	0
TR42	$\Delta\theta_{(H,R)}$ (K)	22.9	22.9	22.9	22.9
	τ_w(mins)	7.0	7.0	7.0	7.0
	M	0.8	0.8	0.8	0
TR43	$\Delta\theta_{(H,R)}$ (K)	22.9	22.9	22.9	22.9
	τ_w(mins)	7.0	7.0	7.0	7.0
	M	0.8	0.8	0.8	0
TR44	$\Delta\theta_{(H,R)}$ (K)	22.9	22.9	22.9	22.9
	τ_w(mins)	7.0	7.0	7.0	7.0
	M	0.8	0.8	0.8	0.1
TR45	$\Delta\theta_{(H,R)}$ (K)	22.9	22.9	22.9	22.9
	τ_w(mins)	7.0	7.0	7.0	7.0
	M	0.8	0.8	0.8	0.1

The estimated parameters for the improved IEEE model, the IEC model and the G. Swift
thermal model were the same as the initial guess values for both OFAF modes which
suggest that the heat transfer in a transformer working in the OFAF mode 1 is the same as
in the OFAF mode 2. The D. Susa model presented different values for the time constant
with the other parameters equal to the initial values in the OFAF mode 1. Different values
for the time constant and the exponential constants *n* and *m* were obtained keeping the other
parameters same as the initial guess value in the OFAF mode 2. The oil time constant and
exponential constants in the D.Susa model were observed in the OFAF mode 2 to have
lower values when compared to the OFAF mode 1 condition meaning that the oil takes a
shorter time to heat up with more fans on.

The results of the estimated top oil temperature and hotspot temperature for the transformers in the OFAF mode 1 and OFAF mode 2 for the four different thermal models are shown in Figures 4.14 to 4.33.
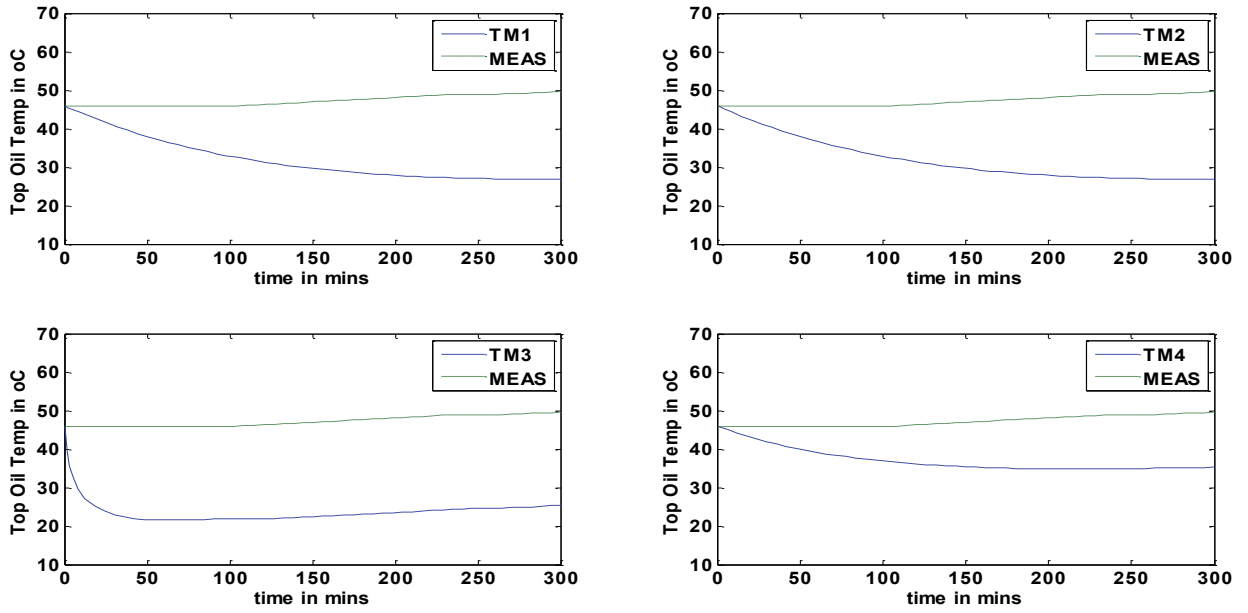
Figure 4.14   TR41 Top Oil Temperature Simulation Results in OFAF mode 1 using nonlinear least squared optimization
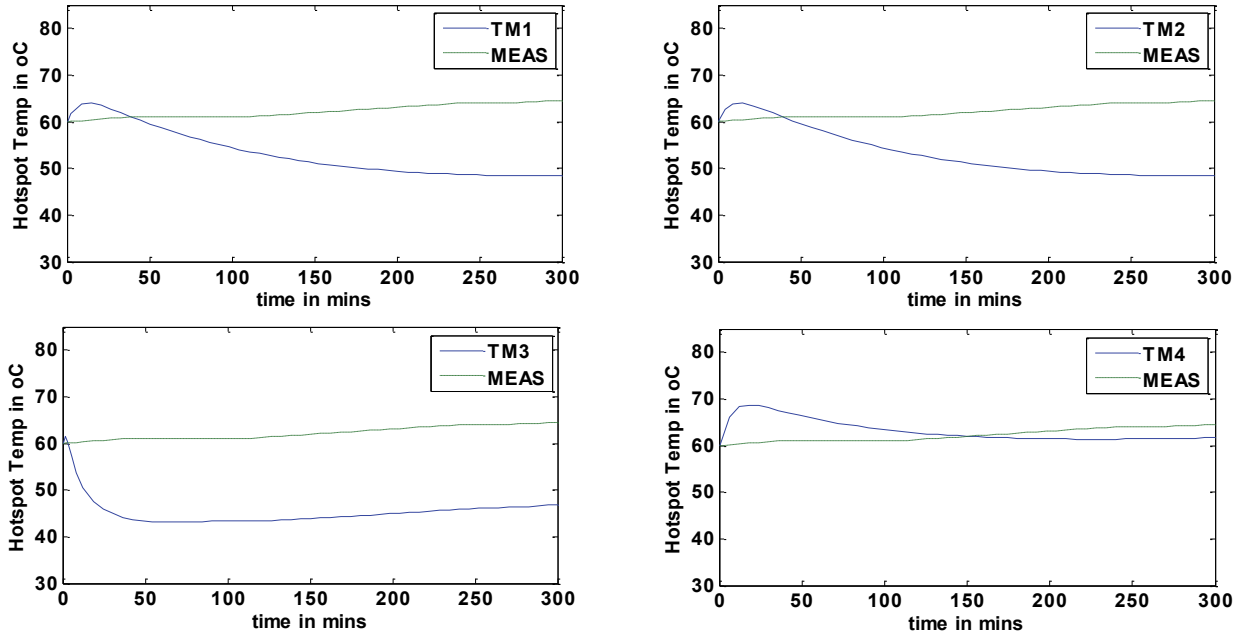
Figure 4.15   TR41 Hotspot Temperature Simulation Results in OFAF mode 1 using nonlinear least squared optimization
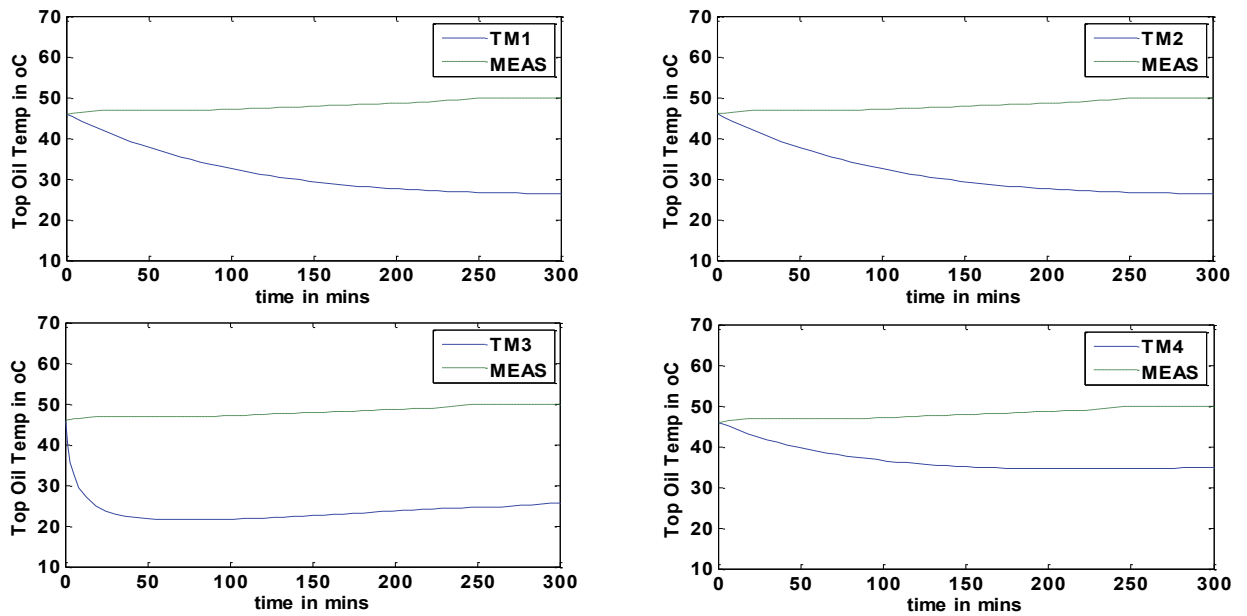
Figure 4.16   TR42 Top Oil Temperature Simulation Results in OFAF mode 1 using nonlinear least squared optimization
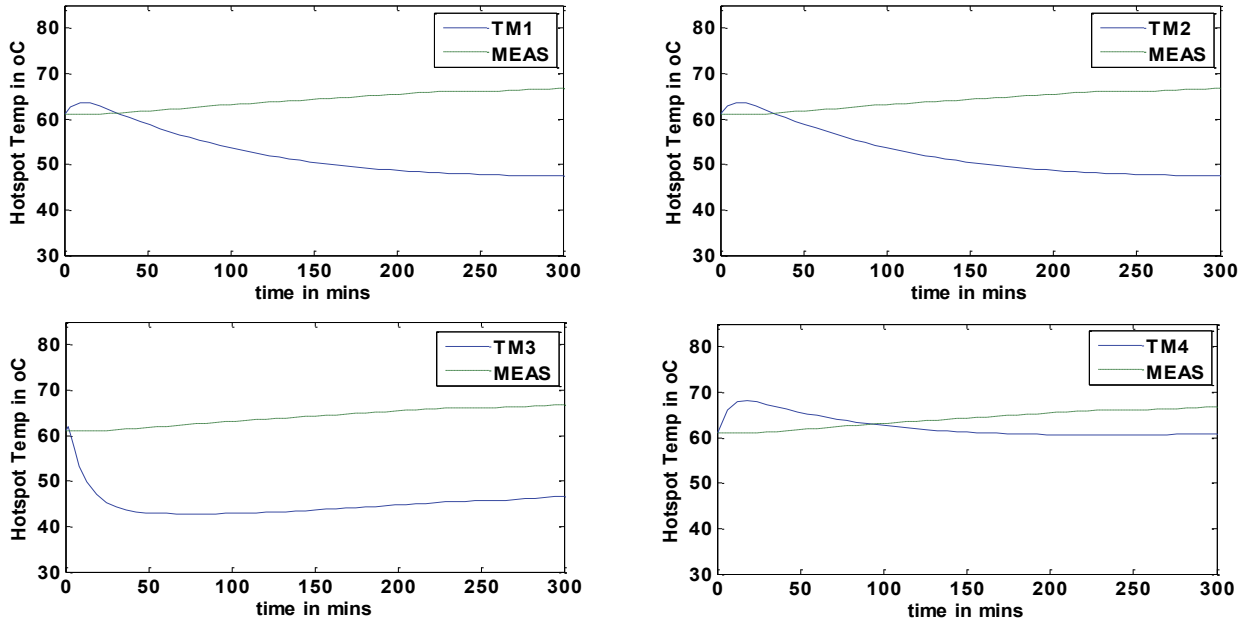
Figure 4.17   TR42 Hotspot Temperature Simulation Results in OFAF mode 1 using
nonlinear least squared optimization
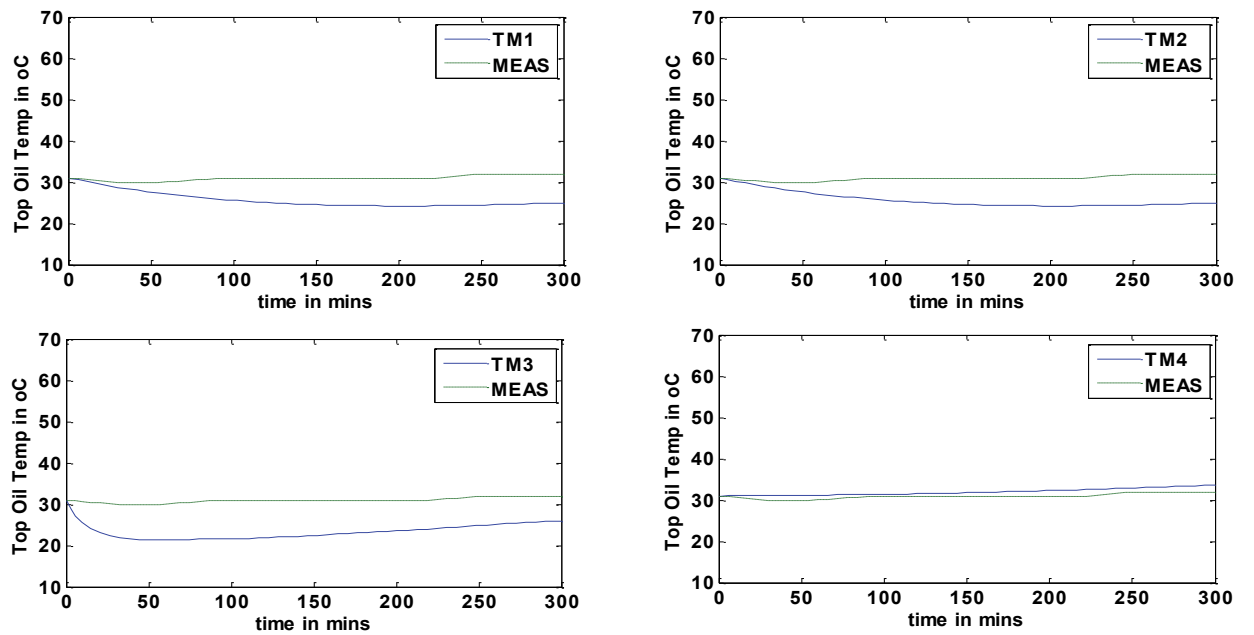
Figure 4.18   TR43 Top Oil Temperature Simulation Results in OFAF mode 1 using
nonlinear least squared optimization
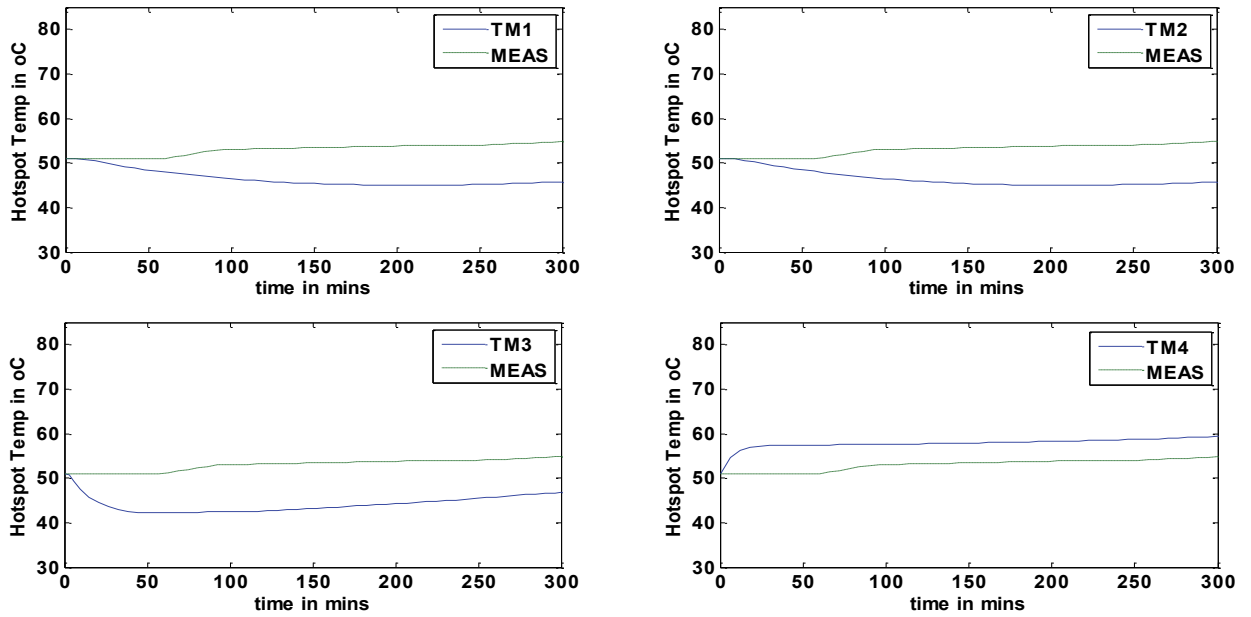
Figure 4.19   TR43 Hotspot Temperature Simulation Results in OFAF mode 1 using nonlinear least squared optimization
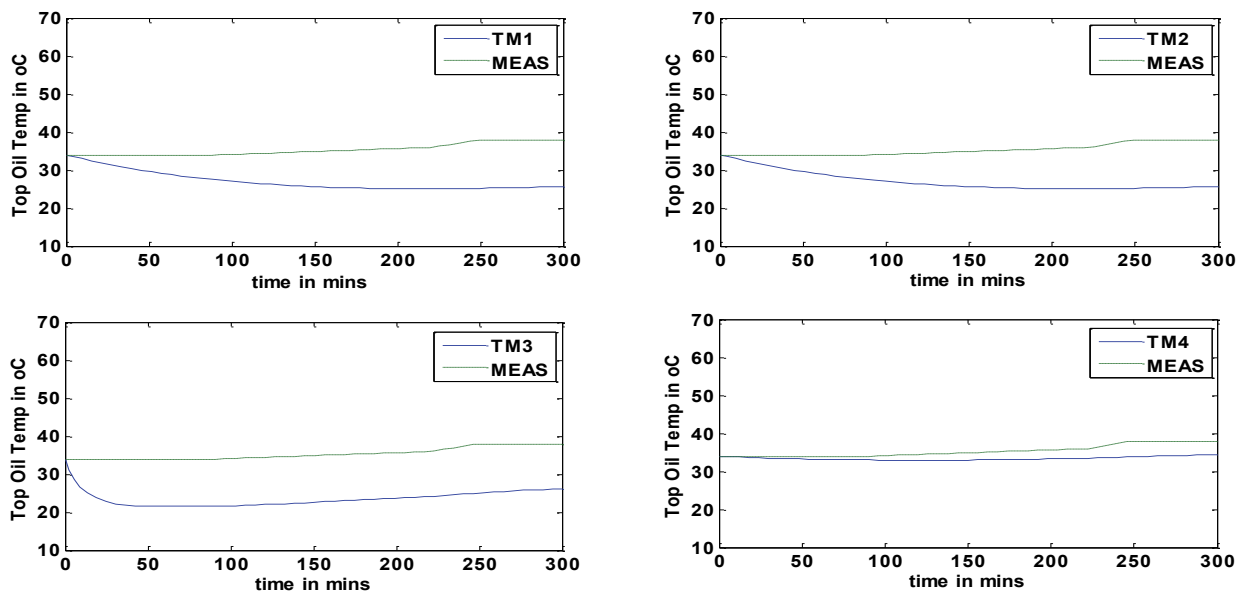
Figure 4.20   TR44 Top Oil Temperature Simulation Results in OFAF mode 1 using nonlinear least squared optimization
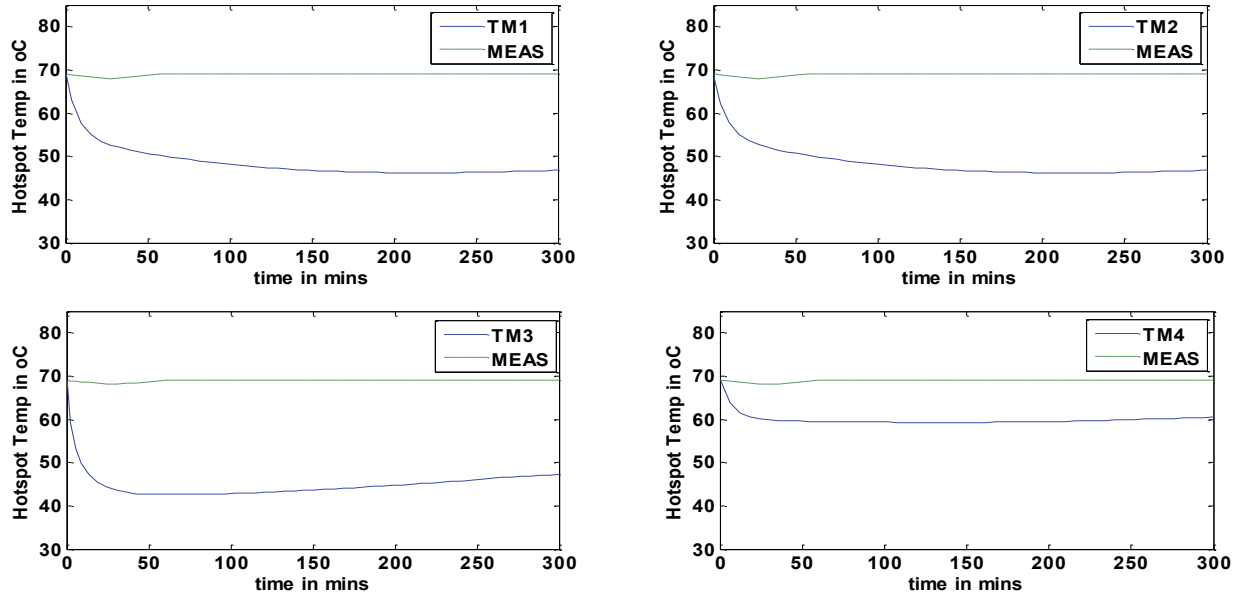
Figure 4.21   TR44 Hotspot Temperature Simulation Results in OFAF mode 1 using nonlinear least squared optimization
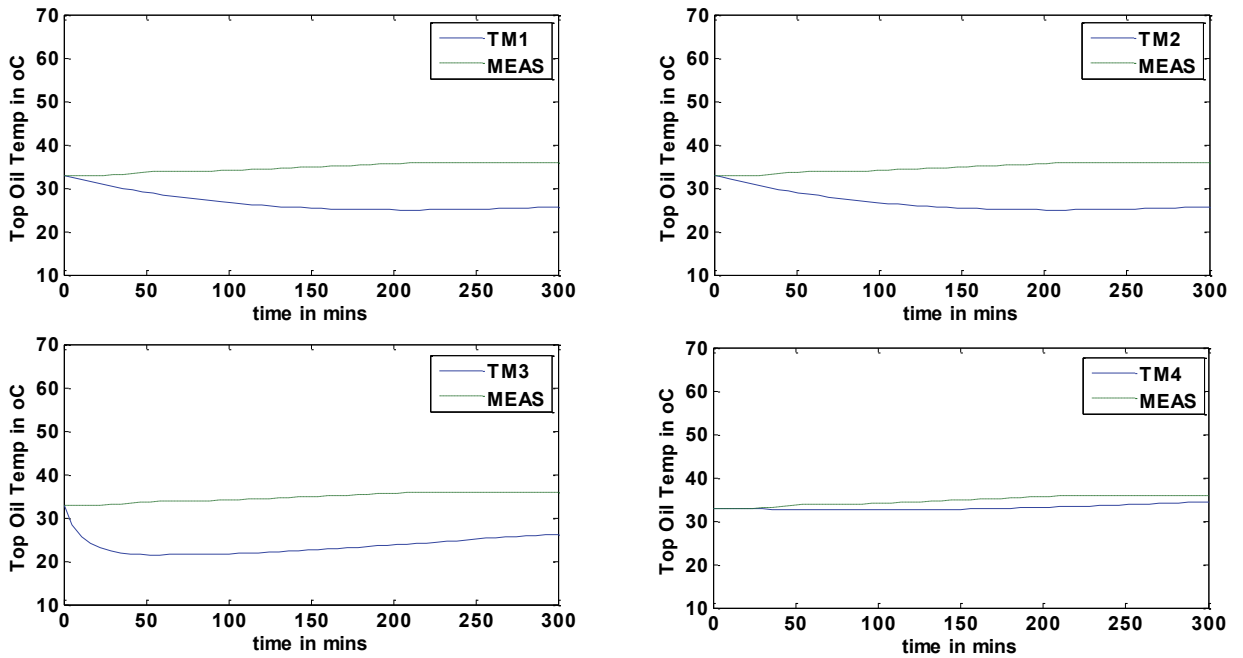
Figure 4.22   TR45 Top Oil Temperature Simulation Results in OFAF mode 1 using nonlinear least squared optimization
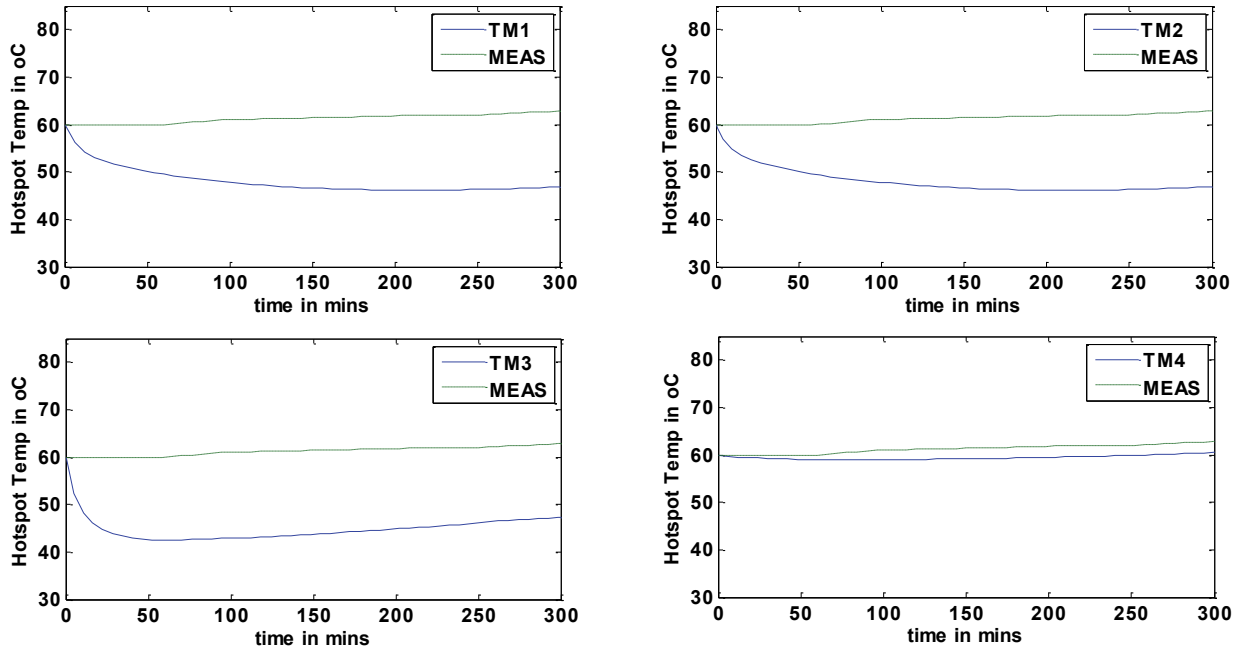
Figure 4.23   TR45 Hotspot Temperature Simulation Results in OFAF mode 1 using
nonlinear least squared optimization
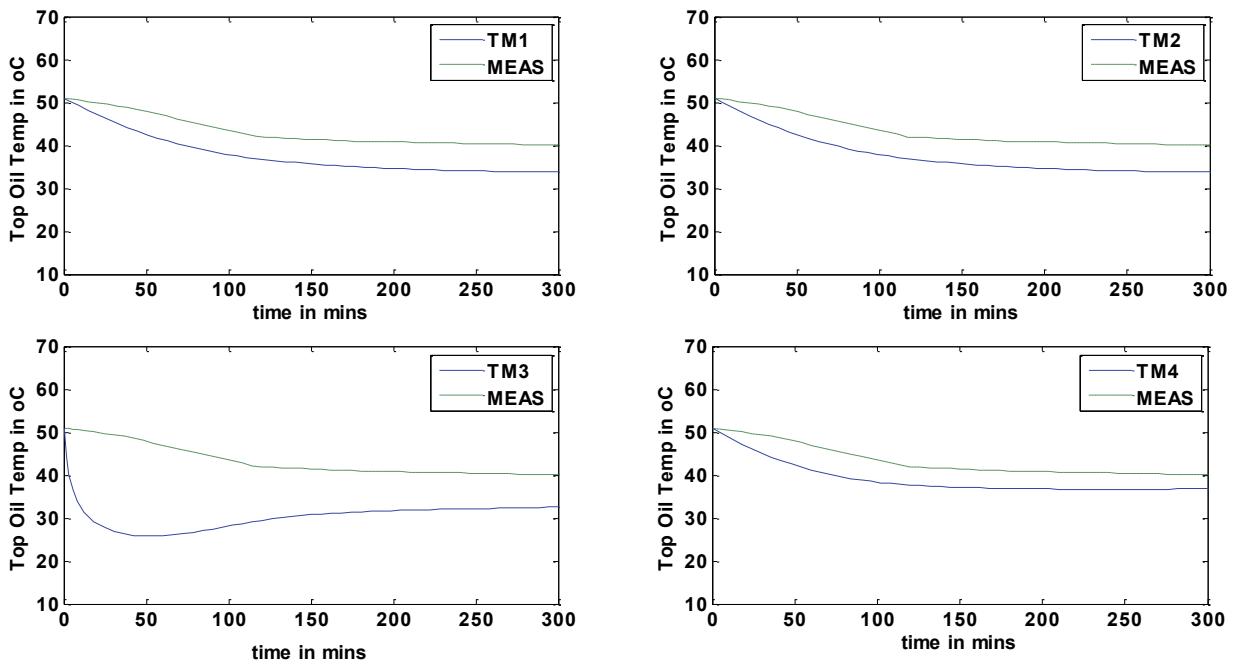
Figure 4.24   TR41 Top Oil Temperature Simulation Results in OFAF mode 2 using
nonlinear least squared optimization
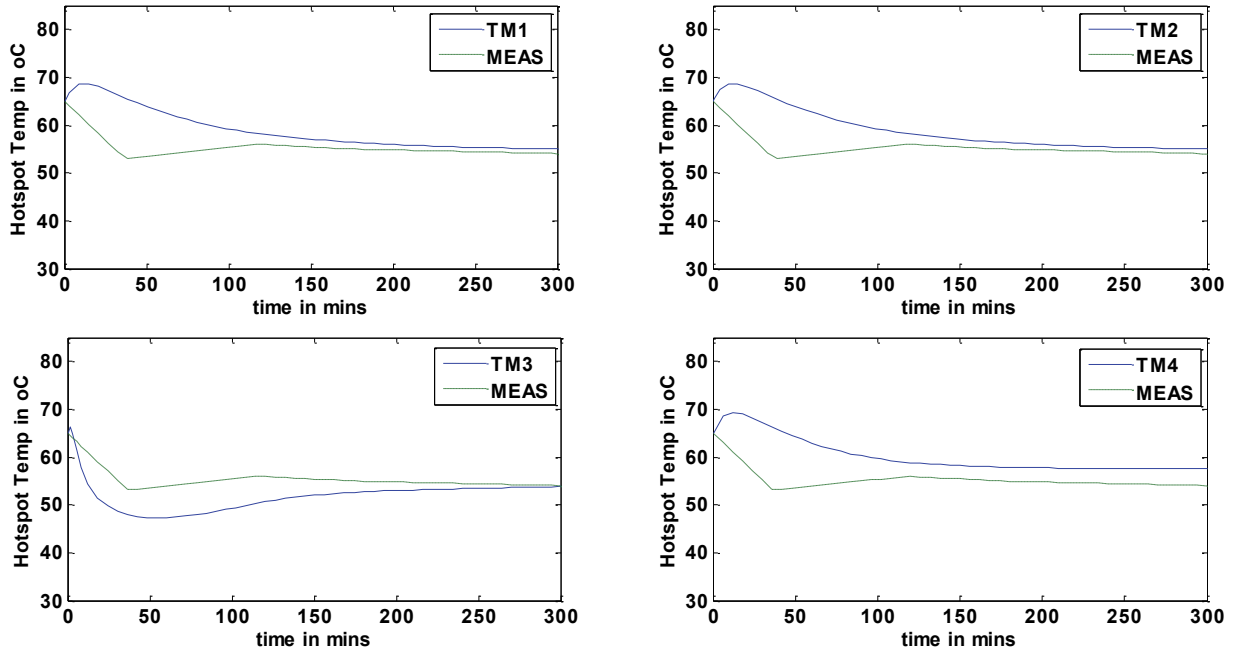
Figure 4.25   TR41 Hotspot Temperature Simulation Results in OFAF mode 2 using nonlinear least squared optimization
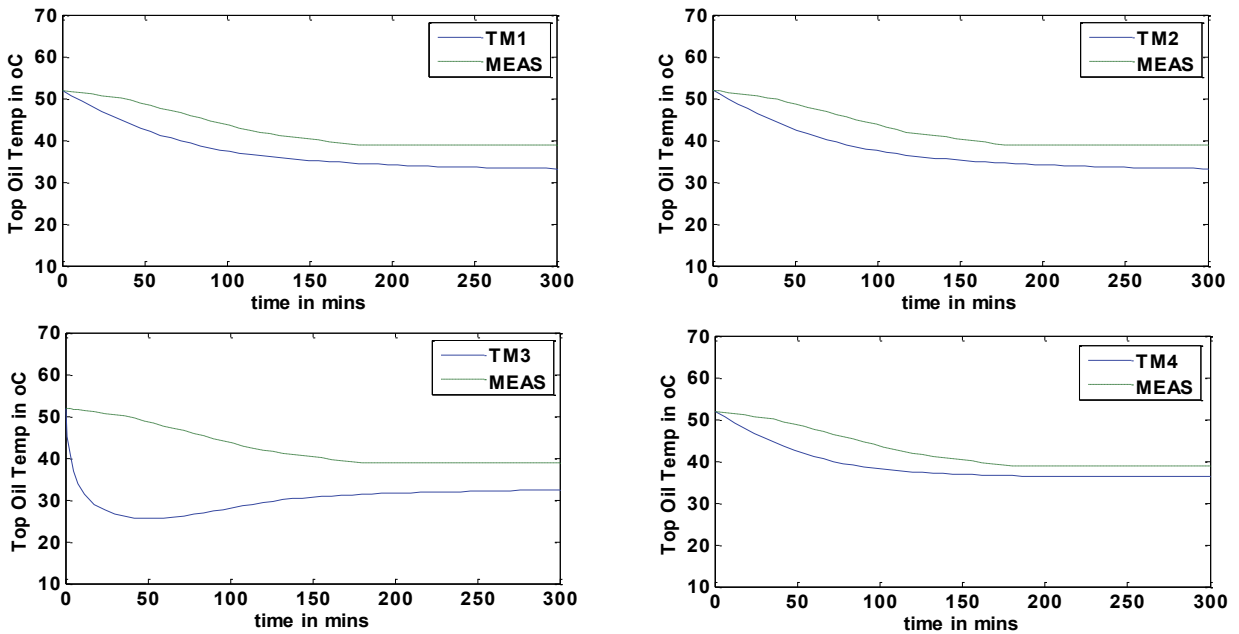
Figure 4.26   TR42 Top Oil Temperature Simulation Results in OFAF mode 2 using nonlinear least squared optimization
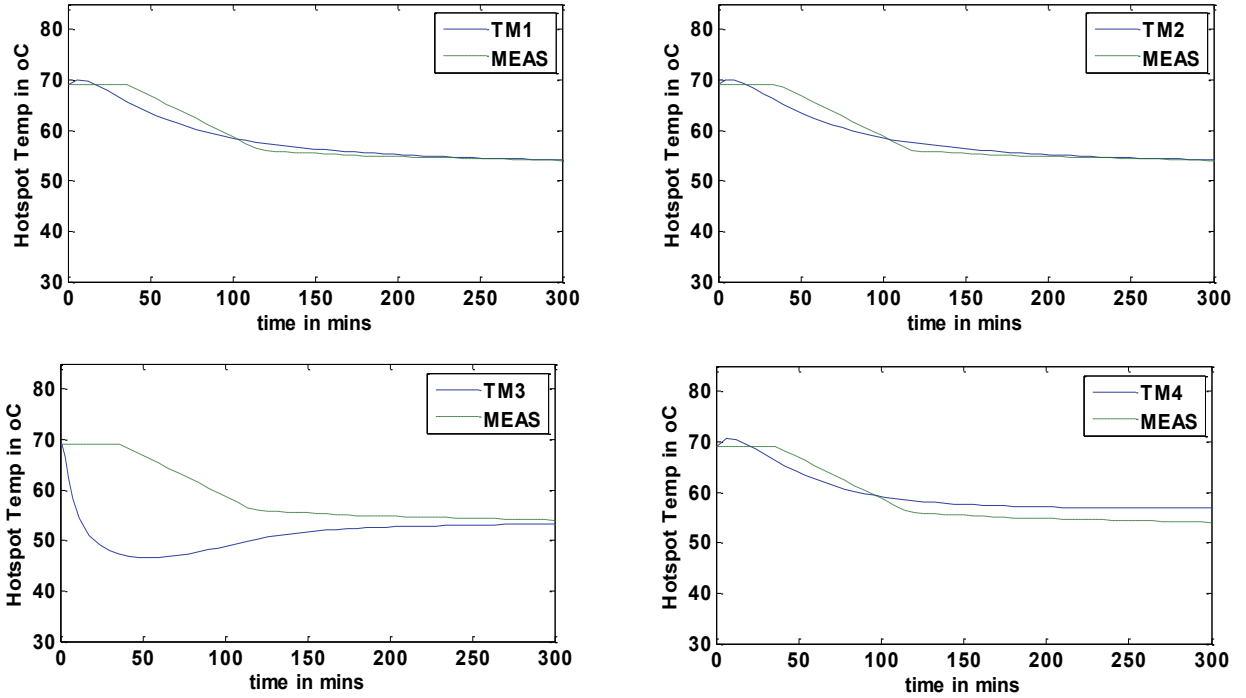
Figure 4.27   TR42 Hotspot Temperature Simulation Results in OFAF mode 2 using nonlinear least squared optimization
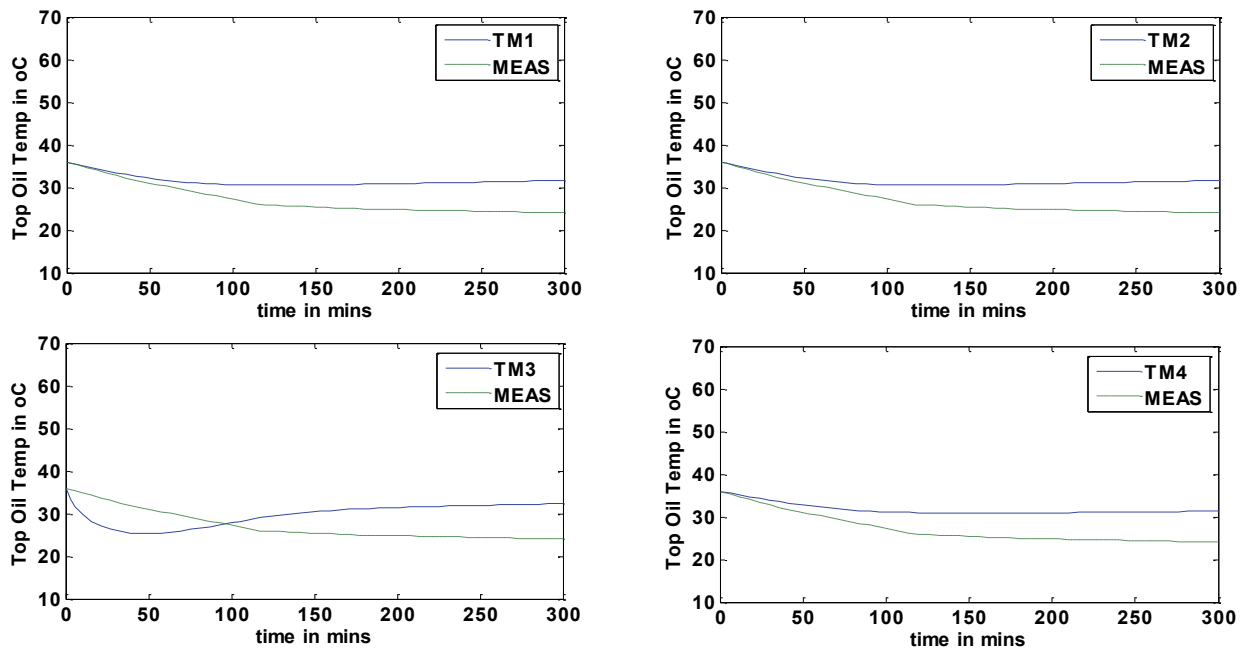
Figure 4.28   TR43 Top Oil Temperature Simulation Results in OFAF mode 2 using nonlinear least squared optimization
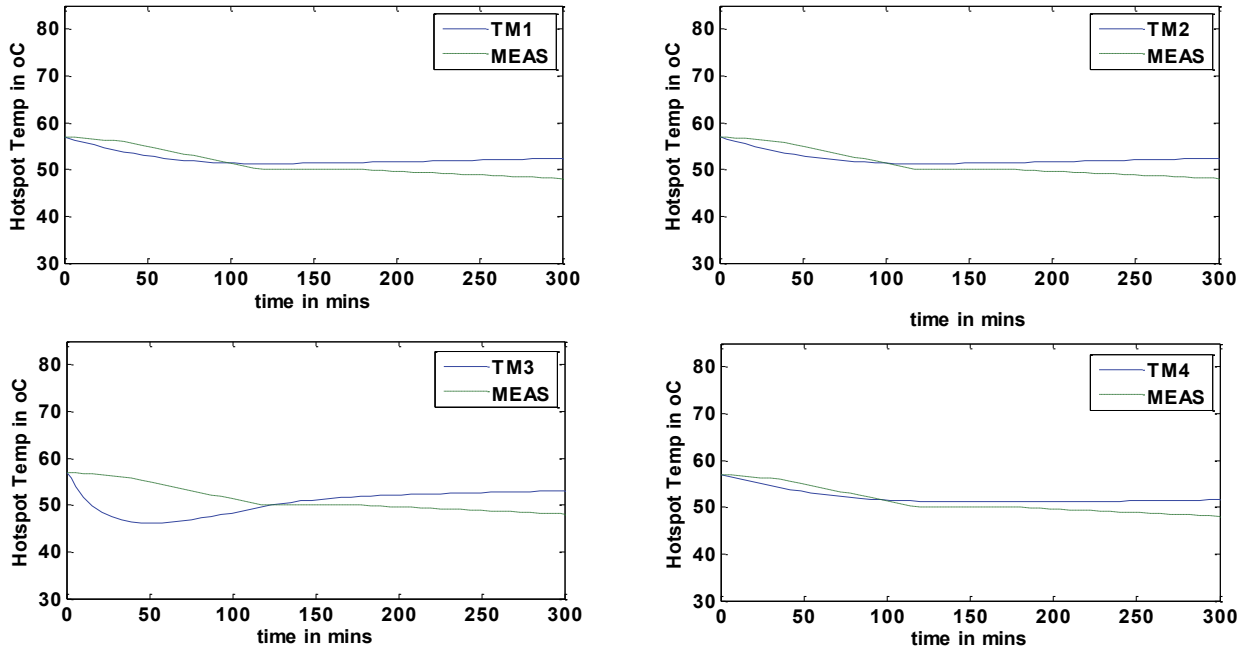
Figure 4.29   TR43 Hotspot Temperature Simulation Results in OFAF mode 2 using
nonlinear least squared optimization
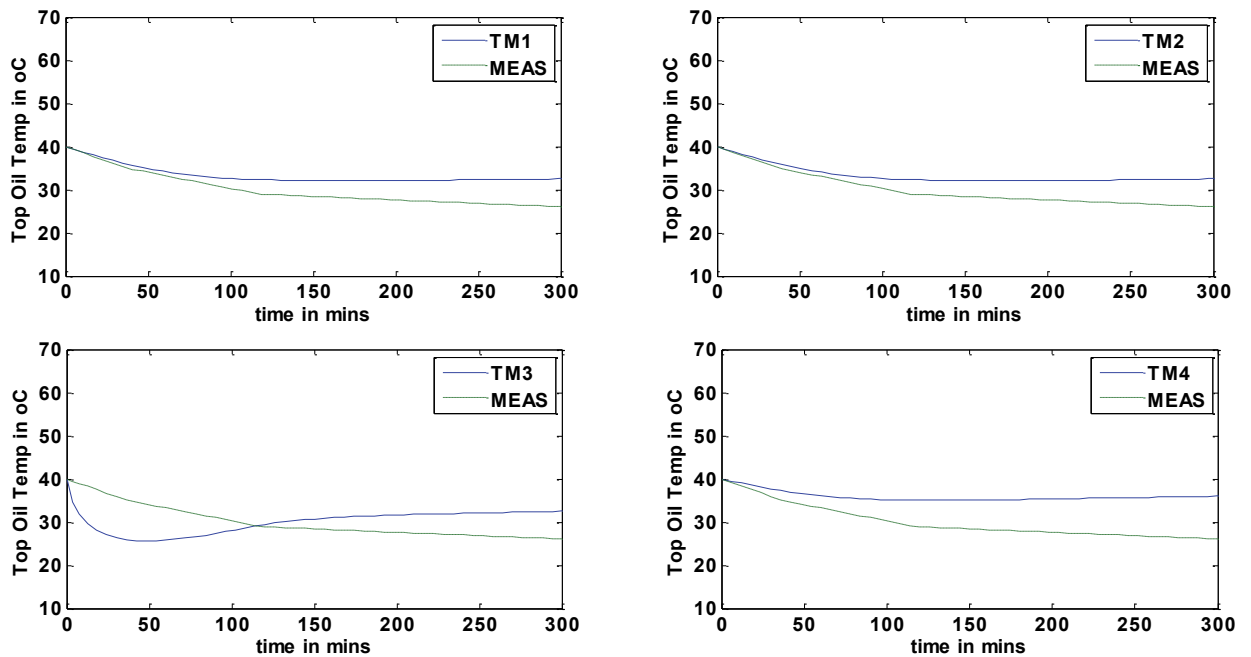
Figure 4.30   TR44 Top Oil Temperature Simulation Results in OFAF mode 2 using
nonlinear least squared optimization
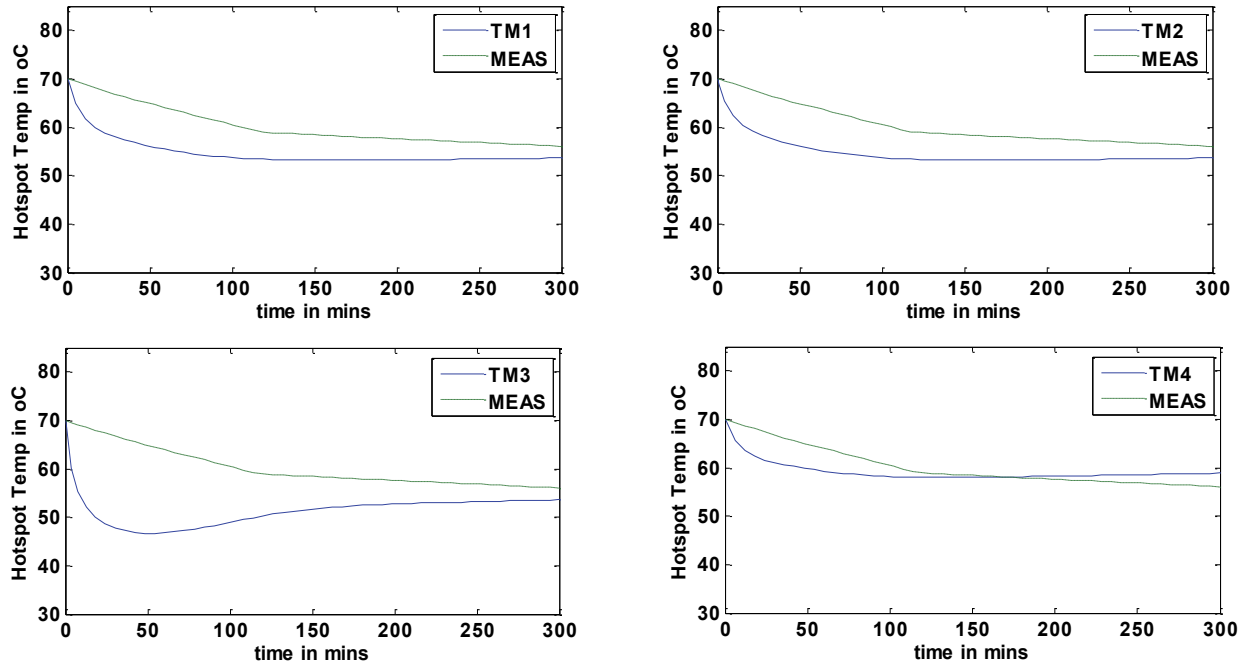
Figure 4.31   TR44 Hotspot Temperature Simulation Results in OFAF mode 2 using nonlinear least squared optimization
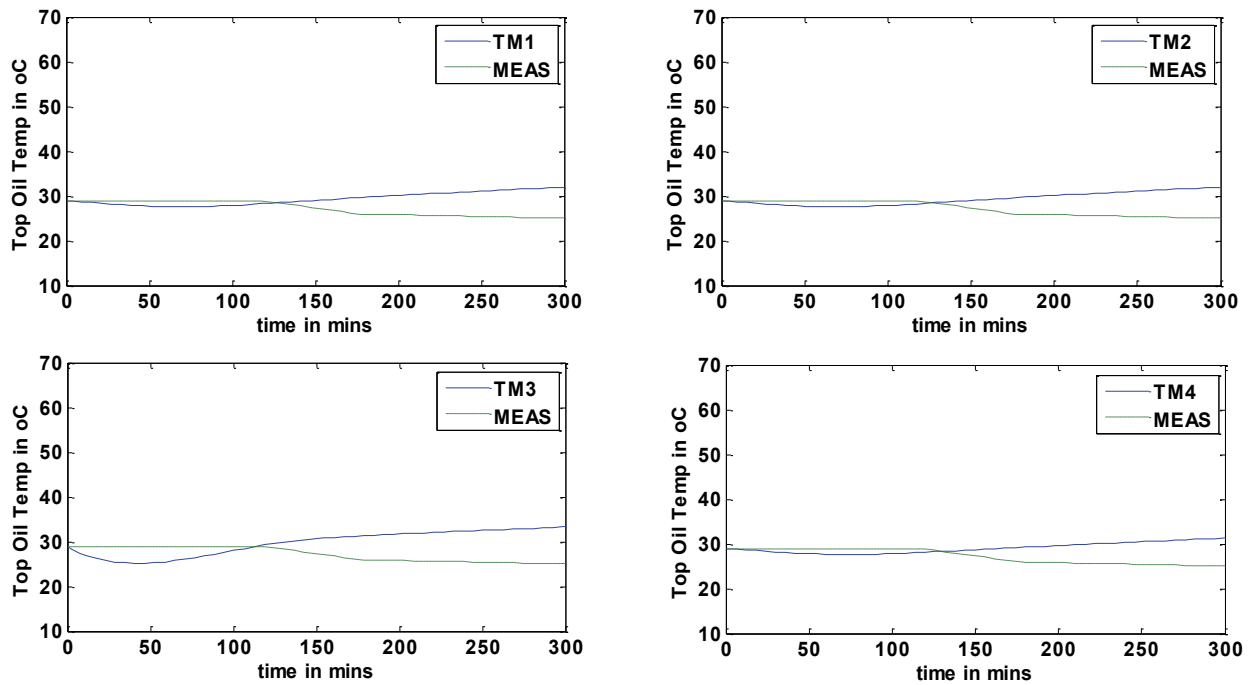
Figure 4.32   TR45 Top Oil Temperature Simulation Results in OFAF mode 2 using nonlinear least squared optimization
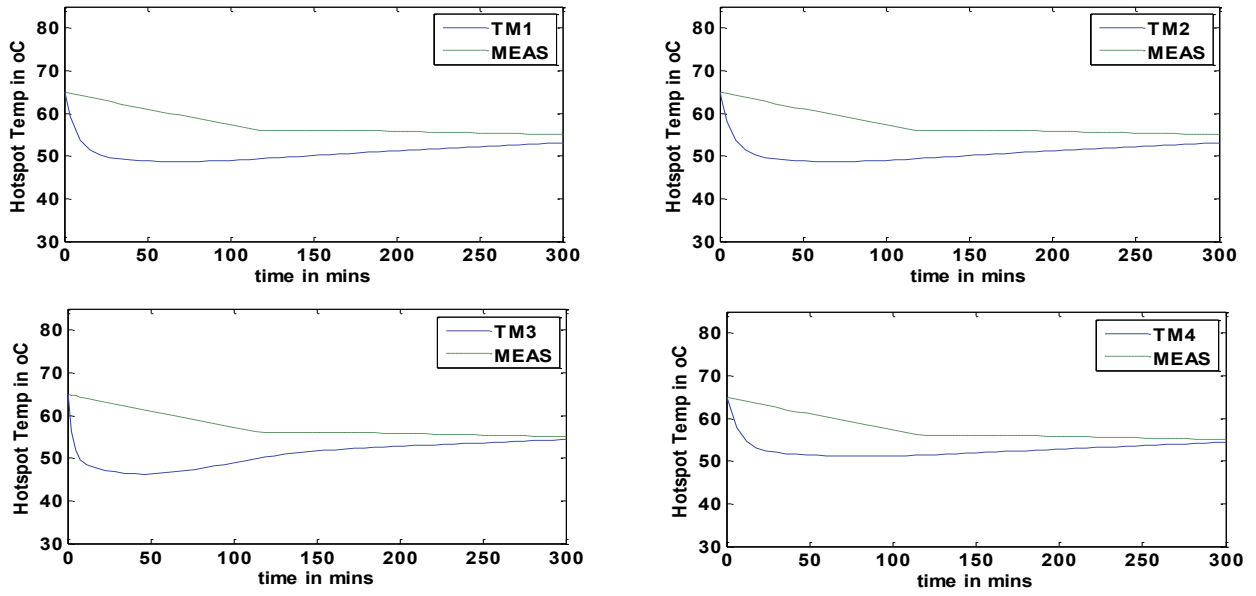
Figure 4.33   TR45 Hotspot Temperature Simulation Results in OFAF mode 2 using nonlinear least squared optimization

A summary of the mean square error in estimated values of the thermal models and measured temperature values of the results obtained from the simulation is shown in Tables 4.5 and 4.6 below.

Table 4.5   Deviation of Nonlinear Least Optimization Results in OFAF Mode 1

Mean Squared Error with Measured Values					
		TM1	TM2	TM3	TM4
TR41	O_{TO} (^{o}C)	16.89	16.01	23.96	10.98
	O_H (^{o}C)	11.15	10.57	16.76	4.19
TR42	O_{TO} (^{o}C)	17.92	16.70	23.99	12.02
	O_H (^{o}C)	13.67	12.96	18.94	6.27
TR43	O_{TO} (^{o}C)	4.92	4.66	7.63	1.02
	O_H (^{o}C)	6.34	6.00	8.88	1.92
TR44	O_{TO} (^{o}C)	8.25	7.81	11.67	2.34
	O_H (^{o}C)	19.70	18.65	23.72	12.18
TR45	O_{TO} (^{o}C)	7.78	7.39	11.19	1.86
	O_H (^{o}C)	12.74	12.04	16.36	5.02

76

Table 4.6   Deviation of Nonlinear Least Optimization Results in OFAF Mode 2

Mean Squared Error with Measured Values		TM1	TM2	TM3	TM4
TR41	O_{TO} (ºC)	5.77	5.47	13.68	3.78
	O_H (ºC)	4.87	4.62	4.23	6.78
TR42	O_{TO} (ºC)	5.94	5.60	13.75	4.00
	O_H (ºC)	1.68	1.59	9.94	2.20
TR43	O_{TO} (ºC)	5.37	5.09	5.68	5.12
	O_H (ºC)	2.34	2.23	4.49	1.77
TR44	O_{TO} (ºC)	4.14	3.98	5.27	3.99
	O_H (ºC)	8.37	5.09	10.28	5.73
TR45	O_{TO} (ºC)	3.49	3.30	5.08	3.38
	O_H (ºC)	7.39	7.02	7.54	6.77

The results show that the D. Susa thermal model temperature estimations have the least errors when compared to the other 3 models; the improved IEEE model, the IEC model and the G. Swift model. The results of the modified D. Susa mode has mean square errors ranging from 1.86ºC to 10.98ºC for the top oil temperature and 1.92ºC to 12.02ºC for the hotspot temperature in the OFAF mode 1 condition and mean square errors 3.38ºC to 5.12ºC for the top oil temperature and 2.20ºC to 6.78ºC for the hotspot temperature in the OFAF mode 2 conditions.

The results obtained show large errors between the estimated and measured temperatures and therefore cannot be used for the purpose of online monitoring and future estimation of the rectifier transformer hotspot temperatures for predictive maintenance purposes.

An alternative method for the estimation of the transformer parameters, genetic algorithm will be investigated for obtaining more accurate estimations and is presented in the next chapter.

CHAPTER 5   RECTIFIER   TRANSFORMER   THERMAL   MODEL PARAMETER   ESTIMATION   USING   GENETIC ALGORITHM

5.1   Introduction

This chapter presents genetic algorithm optimization as an extrapolation technique for obtaining the rectifier transformer thermal model parameters. In Chapter 4, the results obtained using the nonlinear least squares were unsatisfactory, therefore the genetic algorithm is proposed as an alternative to the nonlinear least squares method. A review of genetic algorithm optimization is given in this chapter as well as the application of the genetic algorithm to the rectifier thermal model parameter estimation. A detailed analysis of the results obtained is also presented.

5.2   Introduction to Genetic Algorithm

The Genetic algorithm (GA) [35] is an optimization tool based on the principles of genetics and natural selection. It was developed by John Holland in 1975 and gained a lot of popularity through the works of his student Goldberg who worked on solving the difficult problem of gas pipeline transmission control.

Genetics in biology is known as the trait of an organism. Each organism has a distinct trait stored in its deoxyribonucleic acid (DNA) in the form of genes (a pair of a chromosome). These genes can be transferred to the offspring of the organisms either by mitosis or meiosis. In the case of mitosis where reproduction is by the splitting of organism into multiple organisms, all the genes are transferred to the offspring with exception in the case

of mutation of the genes. In the case of meiosis, it requires the mating of two organisms with different genes to pass on their traits to their offspring. The offspring of the two organisms will contain traits of both parents by the mixture of paternal and maternal genes giving rise to new chromosomes as well as a distinct DNA. In some cases a mutation may occur causing the offspring to have genes absent in the parents.

Natural selection on the other hand involves the dominance of the more fit organisms as well as their offspring in a group of interbreeding organisms. This implies that the more fit organisms remain in the population while the less fit ones are discarded and die off. It is important to note also that the survival of the offspring depends on their fitness and on the genes inherited from the parents.

The Genetic algorithm works by a generation of a random population comprising of individuals known as chromosomes which are evolved under a certain selection rules (natural selection) to a state of minimizing its objective or cost function

The Genetic algorithm is a global minimum seeking tool which has become one of the preferred optimization tools when compared to others such as exhaustive search optimization, analytical optimization, simplex method and newton's method as they are all local minimum seeking tools which require derivative functions.

The GA has many advantages when compared to other optimization tools such as

-       ability to optimize continuous and discrete variables, operates without derivative information,

-       searches a wide sample space on a cost surface at the same time,

- provides a list of optimum solutions,

- encode variables to allow for optimization using encoded variables,

- adaptability for parallel computing, deals with a large pool of variables,

- works with experimental data, numerically generated data and analytical functions.

One major disadvantage of the GA is the computational time it takes to find the minimum cost as it searches a large space on the cost surface.

5.3   Genetic Algorithm Structure

The structure of a GA is presented in the flow chart shown below.
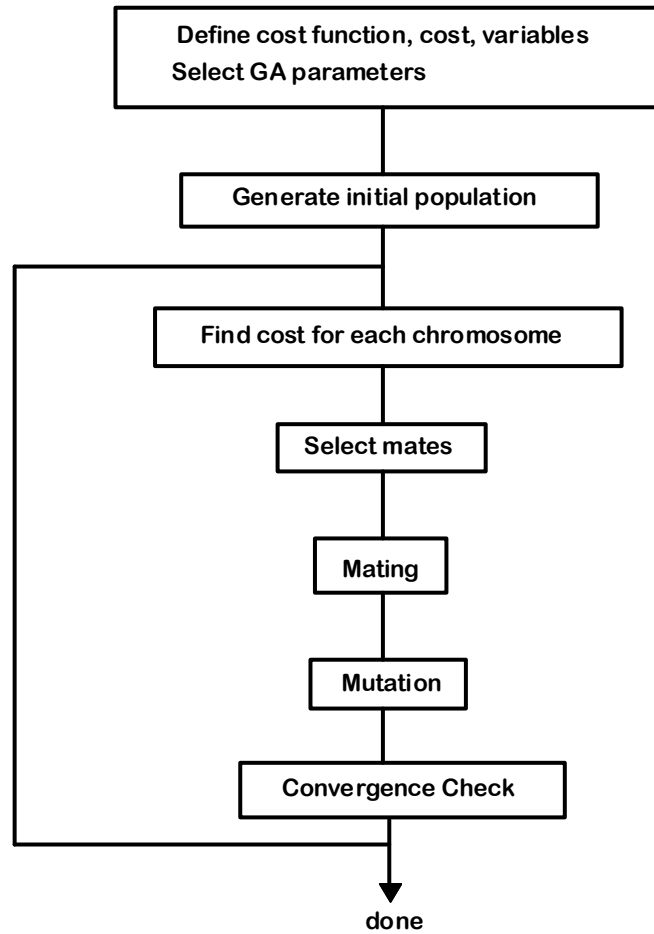
Figure 5.1   Genetic Algorithm Structure [35].

The first stage in the genetic algorithm requires the definition of the variables (chromosome) and cost function, objective function or fitness function to be optimized. This chromosome is an array of n variables and is expressed as

$$chromosomes = [V_1, V_2, \ldots \ldots V_n] \qquad (5.1)$$

The Cost function is defined as a function of the chromosomes as given in (5.2)

$$Cost = f(V_1, V_2, \ldots \ldots V_n) \quad (5.2)$$

The objective of a genetic algorithm is to find a combination of the variables which will yield the minimum cost. The set of variables is generated randomly and may sometimes be set within constraints as to enable the GA search within its global minimum search space to avoid being trapped within a local minimum. The setting of these constraints requires a good knowledge of the system to be optimized.

The generation of the initial population is the next process in the GA optimization technique. A population means a set of m chromosomes, therefore the initial population results in an m by n matrix of variables with each variable bounded within its constraint.

This initial set of population is passed to the cost function to evaluate the cost of each chromosome in the population. Ranking is passed on each chromosome after the evaluation and a rank of 1 is apportioned to the chromosome with the least cost and rank m to the chromosome with highest cost

$$rank\_1 = \min(Cost) = \min\{f(V_1, V_2, \ldots \ldots V_n)\} \quad (5.3)$$

$$rank\_m = \max(Cost) = \max\{f(V_1, V_2, \ldots \ldots V_n)\} \quad (5.4)$$

The next phase of the genetic algorithm process is the selection of mates which involves the selection of chromosomes for mating (Natural selection) and the division of the chromosomes into paternal chromosomes and maternal chromosomes (Pairing). The natural selection process is done by keeping the chromosomes with a low cost and discarding the chromosomes with a high cost. The number of chromosomes discarded will determine the number of offspring to be produced by the kept chromosomes. The process of pairing is a random process where any chromosome is picked to be a paternal

chromosome and any other a maternal chromosome. The division of the kept chromosomes is done in such a way that half the number of kept chromosomes become paternal chromosomes and the remaining half maternal chromosomes. Also, the number of pairs formed will have to be half of the number of chromosomes discarded as to enable the generation of offspring from the parents to fill up the population size.

Mating is the next process whereby the paternal and maternal chromosomes crossbreed to generate two new offspring having the traits (genetics) of both parents. It involves some combination of both parents. A simple process of mating involves choosing randomly one or more points in the parent chromosomes for crossbreeding. For example, given a pair of parents to be

$$Paternal_1 = \begin{bmatrix} V_{p1}, V_{p2}, V_{p3}, V_{p4}, V_{p5}, \ldots \ldots \ldots V_{pn} \end{bmatrix} \quad (5.5)$$

$$Maternal_1 = \begin{bmatrix} V_{m1}, V_{m2}, V_{m3}, V_{m4}, V_{m5}, \ldots \ldots \ldots V_{mn} \end{bmatrix} \quad (5.6)$$

a two point cross breeding of the maternal and paternal offspring will yield two offspring with parent pair exchanging variables (genes) in between the cross points as

$$Offspring_1 = \begin{bmatrix} V_{p1}, V_{p2}, | V_{m3}, V_{m4}, | V_{p5}, \ldots \ldots \ldots V_{pn} \end{bmatrix} \quad (5.7)$$

$$Offspring_2 = \begin{bmatrix} V_{m1}, V_{m2}, | V_{p3}, V_{p4}, | V_{m5}, \ldots \ldots \ldots V_{mn} \end{bmatrix} \quad (5.8)$$

After the mating of the parent chromosomes, the next step in the GA process is the mutation of the genes of a random set of the offspring and parents with the exception of the parent chromosome with rank 1. A mutation is done to allow the GA to explore a broader search space as the population may contain chromosomes in the same search space which may be

a local minima cost area as opposed to a global minimum. A mutation rate (M_R) can be defined to determine the number of individuals to be mutated as

$$Number\ of\ mutations = M_R \times m \times n \qquad (5.9)$$

where m is the population size and n is the number of variables

With a new population set being formed after the mutation, a convergence check is conducted on each chromosome in the population by assessing its costs. If a chromosome with a minimized cost is found the GA is said to have optimized the variables. On the other hand if the minimized cost is not found the GA repeats the same process from a new mating with the more fit chromosomes until the cost function is minimized.

5.4 **Application of General Algorithm Optimization to Rectifier Transformer Thermal Modeling**

As stated in Chapter 4, the developed thermal models consist of two thermal models, the top oil model and the hotspot model which are characterized by parameters that require offline transformer heat run tests. An alternative approach which involves estimation of these parameters from online measured values with the use of optimization technique, genetic algorithm is adopted in this thesis project to avoid turn down times for the transformers.

Applying the genetic algorithm to the top oil model, the chromosomes of the GA are defined as a vector of the unknown top oil model parameters as given in equation (5.10)

$$chromosomes = \left[\Delta\theta_{To-R}, \tau_{TO}, n\right] \qquad (5.10)$$

The cost of the GA for top oil model is defined as the squared error between the estimated top oil temperature and the measured top oil temperature and is expressed as

$$Cost = \sum_{k=1}^{i} [Y_{tok} - f_k(x, \Delta\theta_{To-R}, \tau_{TO}, n)]^2 \quad (5.11)$$

where Y_{to} is the measured top oil temperature and $f_k(x, \Delta\theta_{TO-R}, \tau_{TO}, n)$ is the estimated top model which is a function of the unknown parameters and independent variables, x, consisting of the time, load factor and ambient temperature.

In the same vein, applying GA to the hotspot model, the chromosomes of the GA are defined as a vector of the unknown hotspot model parameters as

$$chromosomes = [\Delta\theta_{H,R}, \tau_w, m] \quad (5.12)$$

The cost of the GA for top oil model is defined as the squared error between the estimated hotspot temperature and the measured hotspot temperature and is expressed as

$$Cost = \sum_{k=1}^{i} [Y_{hk} - f_k(x, \Delta\theta_{H,R}, \tau_w, m)]^2 \quad (5.13)$$

where Y_{hk} is the measured hotspot temperature and $f_k(x, \Delta\theta_{H,R}, \tau_w, m)$ is the estimated hotspot model which is a function of the unknown parameters and independent variables.

5.4.1 Parameter Estimation Results and Analysis

The GA algorithm is implemented using a developed Matlab m-file algorithm with details of the algorithm in Appendix 2. The GA population size was set to 50 and has a maximum number of 35 iterations for the algorithm convergence. A mutation rate of 0.001 is used.

The parameters are bounded to avoid convergence within a local minimum and the bounds are obtained using information from appendix 1 with $\Delta\theta_{TO-R}$ ranging from 20 to 80, $\Delta\theta_{H,R}$ ranging from 10 to 40, ,τ_{TO} ranging from 1 to 300, ,τ_w ranging from 1 to 30, n ranging from 0 to 1 and m ranging from 0 to 1.

The thermal models were modeled with Simulink with simulation stop time set to 300 minutes which is equal to time of the measured data from the field. The initial value for the integrator in the top oil model is set equal to the initial value of the measured oil temperature while the initial value for the hotspot model is set equal to the initial value of the measured hotspot temperature.

The results of the estimated parameters of the thermal models of transformers TR41 to TR45 in the OFAF mode 1 and OFAF mode 2 using genetic algorithm are given in Tables 5.1 to 5.4.

Table 5.1   OFAF Mode 1 Top Oil Model Parameter Estimation using Genetic Algorithm

OFAF MODE 1 PARAMETERS		TM1	TM2	TM3	TM4
		TM1	TM2	TM3	TM4
TR41	$\Delta\theta_{TO\text{-}R}$ (K)	67.7	68.4	69.8	59.7
	τ_{TO}(mins)	112	118	159	164
	n	0.79	0.95	0.93	0.24
TR42	$\Delta\theta_{TO\text{-}R}$ (K)	71.4	71.1253	54.6	65.2
	τ_{TO}(mins)	180	181	237	137
	n	0.93	0.87	0.93	0.13
TR43	$\Delta\theta_{TO\text{-}R}$ (K)	51.4	51.2	50.4	43.9708
	τ_{TO}(mins)	187	188	221	164
	n	0.87	0.84	0.93	0.15
TR44	$\Delta\theta_{TO\text{-}R}$ (K)	56.4	57.7	47.4	51.8
	τ_{TO}(mins)	125	174	178	112
	n	0.88	1.0	0.92	0.14
TR45	$\Delta\theta_{TO\text{-}R}$ (K)	55.7	56.8	35.8	42.9
	τ_{TO}(mins)	171	190	201	239
	n	0.79	0.95	0.93	0.35

Table 5.2   OFAF Mode 2 Top Oil Model Parameter Estimation using Genetic Algorithm

OFAF MODE 2 PARAMETERS					
		TM1	TM2	TM3	TM4
TR41	$\Delta\theta_{TO-R}$ (K)	48.7	48.0	11.9	45.3
	τ_{TO}(mins)	181	187	167	205
	n	0.98	0.91	0.94	0.06
TR42	$\Delta\theta_{TO-R}$ (K)	46.6	42.3	23.9	41.7
	τ_{TO}(mins)	185	254	313	211
	n	0.97	0.93	0.93	0.12
TR43	$\Delta\theta_{TO-R}$ (K)	31.9	32.0	18.8	30.0
	τ_{TO}(mins)	170	161	233	155
	n	0.99	0.90	0.91	0.07
TR44	$\Delta\theta_{TO-R}$ (K)	33.9	33.1	11.9	27.6
	τ_{TO}(mins)	158	181	220	179
	n	0.90	1.0	0.92	0.17
TR45	$\Delta\theta_{TO-R}$ (K)	36.0	35.5	29.3	27.3
	τ_{TO}(mins)	258	298	202	236
	n	0.91	0.93	0.90	0.27

Table 5.3   OFAF Mode 1 Hotspot Model Parameter Estimation using Genetic Algorithm

OFAF MODE 1 PARAMETERS					
		TM1	TM2	TM3	TM4
TR41	$\Delta\theta_{(H,R)}$ (K)	16.1	15.9	16.1	15.8
	τ_w(mins)	10	10	15	9
	M	0.81	0.85	0.83	0.03
TR42	$\Delta\theta_{(H,R)}$ (K)	17.7	17.4	17.7	17.2
	τ_w(mins)	9	10	12	10
	M	0.85	0.80	0.84	0.06
TR43	$\Delta\theta_{(H,R)}$ (K)	24.7	24.3	24.3	23.3
	τ_w(mins)	12	12	9	15
	m	0.82	0.80	0.83	0.05
TR44	$\Delta\theta_{(H,R)}$ (K)	36.0	32.1	36.3	28.5
	τ_w(mins)	11	11	10	11
	m	0.80	0.80	0.80	0.30
TR45	$\Delta\theta_{(H,R)}$ (K)	29.1	28.8	29.2	22.8
	τ_w(mins)	8	9	10	6
	m	0.81	0.84	0.82	0.28

Table 5.4   OFAF Mode 2 Hotspot Model Parameter Estimation using Genetic
              Algorithm

OFAF MODE 2 PARAMETERS					
		TM1	TM2	TM3	TM4
TR41	$\Delta\theta_{(H,R)}(K)$	13.1	13.1	13.6	10.5
	$\tau_w(mins)$	9	6	8	7
	m	0.85	0.79	0.81	0.39
TR42	$\Delta\theta_{(H,R)}(K)$	17.6	17.4	17.5	16.1
	$\tau_w(mins)$	10	11	10	11
	m	0.86	0.86	0.82	0.07
TR43	$\Delta\theta_{(H,R)}(K)$	27.2	27.2	26.4	21.6
	$\tau_w(mins)$	11	13	10	12
	m	0.81	0.82	0.84	0.19
TR44	$\Delta\theta_{(H,R)}(K)$	32.9	31.7	31.8	30.4
	$\tau_w(mins)$	8	12	9	10
	m	0.86	0.80	0.80	0.06
TR45	$\Delta\theta_{(H,R)}(K)$	33.2	32.1	33.1	25.6
	$\tau_w(mins)$	11	11	10	12
	m	0.84	0.75	0.87	0.24

The estimated parameters in each of the four models for all the transformers yielded

different results in both OFAF modes. The oil time constant in all models was observed to

have longer periods in the OFAF mode 2 than in the OFAF mode 1 which indicates that

the oil takes a longer time to cool with three fans on. The rated top oil rise above ambient

was observed to have higher values in the OFAF mode 1 condition when compared to the

OFAF mode 2 case in all models indicating that the oil heats up to higher temperatures in

the OFAF mode 1 condition. The winding time constant and the rated hotspot rise above

top oil temperature in both OFAF modes were approximately about the same values with

little variance. A validation for these results would be that the cooling fans are involved

with extracting heat from the oil to the ambient temperature and have minimal effect on

the winding cooling characteristics. The nonlinear exponent n in the improved IEEE model, the IEC model and the G. Swift model yielded smaller values in the OFAF mode 1 when compared to the OFAF mode 2. The values obtained in mode 2 are approximately equal to the values of an Air Forced cooled transformer as stated in chapter two for the three models while the values obtained in mode 1 are approximately that of an Air Naturally cooled transformer. These results imply that the transformer is better cooled with the three fans on than with one fan on which is expected. The nonlinear exponent m in the three models as stated earlier, present an approximately same value in both OFAF modes and is in line with the value as stated in chapter 2 for OFAF transformers. The nonlinear exponents, n and m obtained in the D.Susa model, show an irregular pattern with an increase and decrease in values between both OFAF modes. The results obtained are expected as the values differ from one transformer to another and vary around the value 0.2 as stated by D.Susa for OFAF transformers in [18, 19].

Also, the parameters in each model differ among the five rectifier transformers as is expected as the measured temperatures for the transformers are not same with the transformers having the same power rating and working under the same load factor and ambient weather conditions.

The results of the estimated top oil temperature and hotspot temperature for the transformers in the OFAF mode 1 and OFAF mode 2 for the four different thermal models are shown in Figures 5.2 to 5.21.
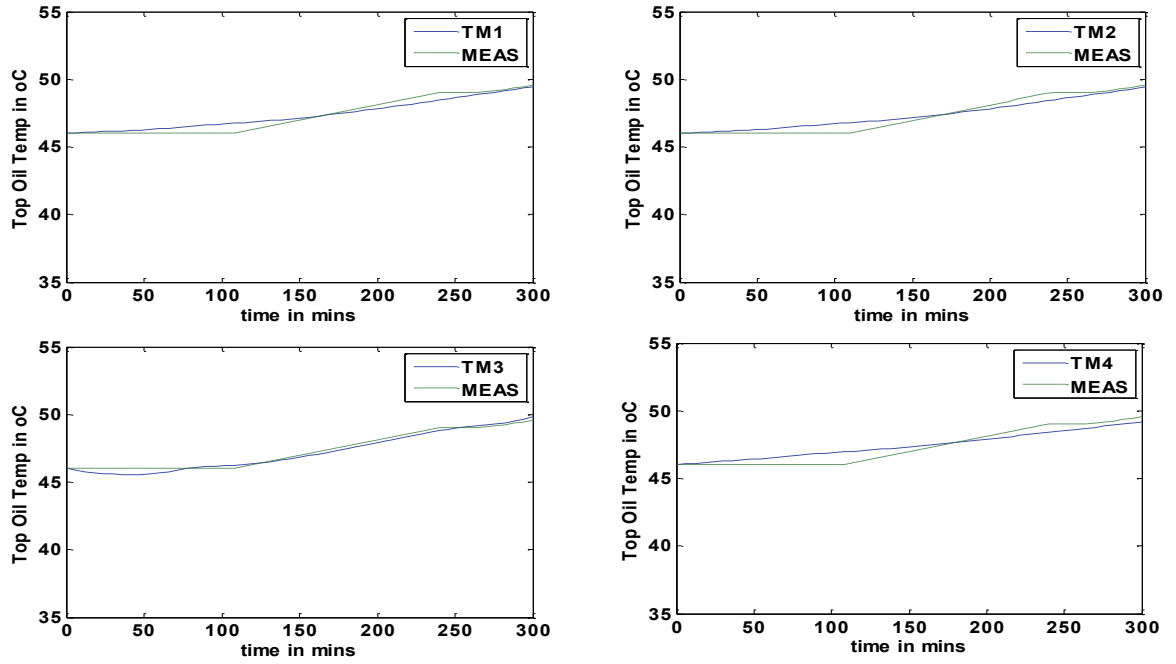
Figure 5.2   TR41 Top Oil Temperature Simulation Results in OFAF mode 1 using
genetic algorithm optimization
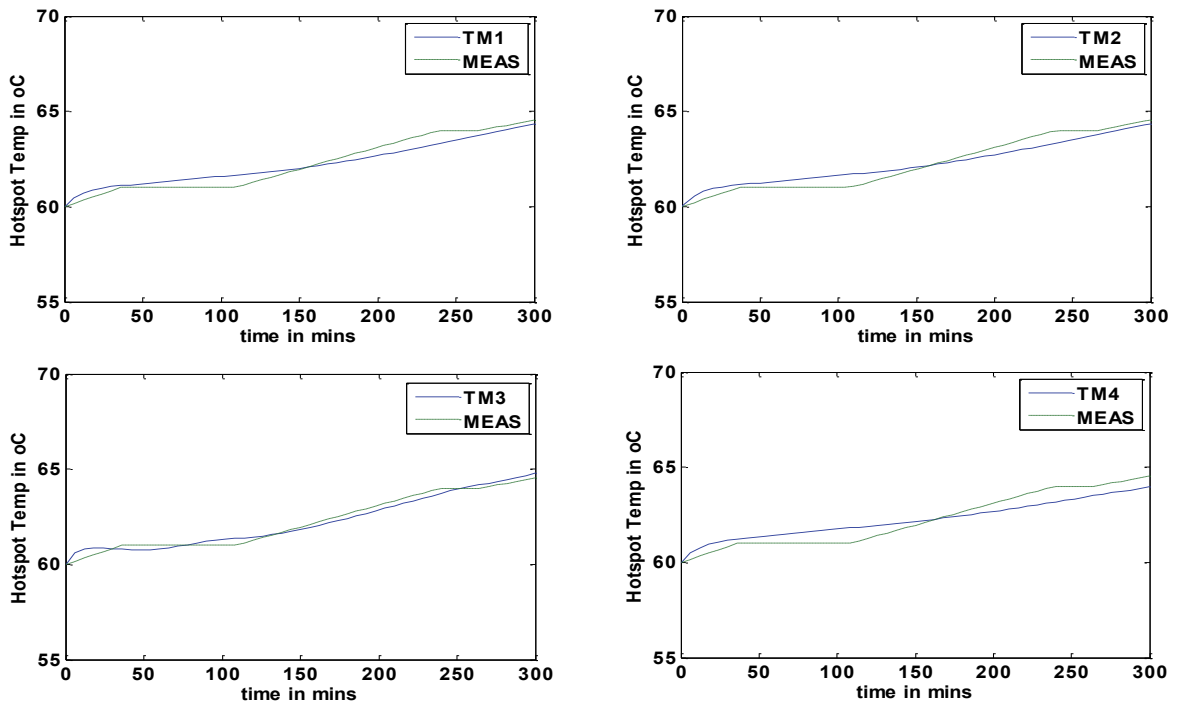
Figure 5.3   TR41 Hotspot Temperature Simulation Results in OFAF mode 1 using
genetic algorithm optimization
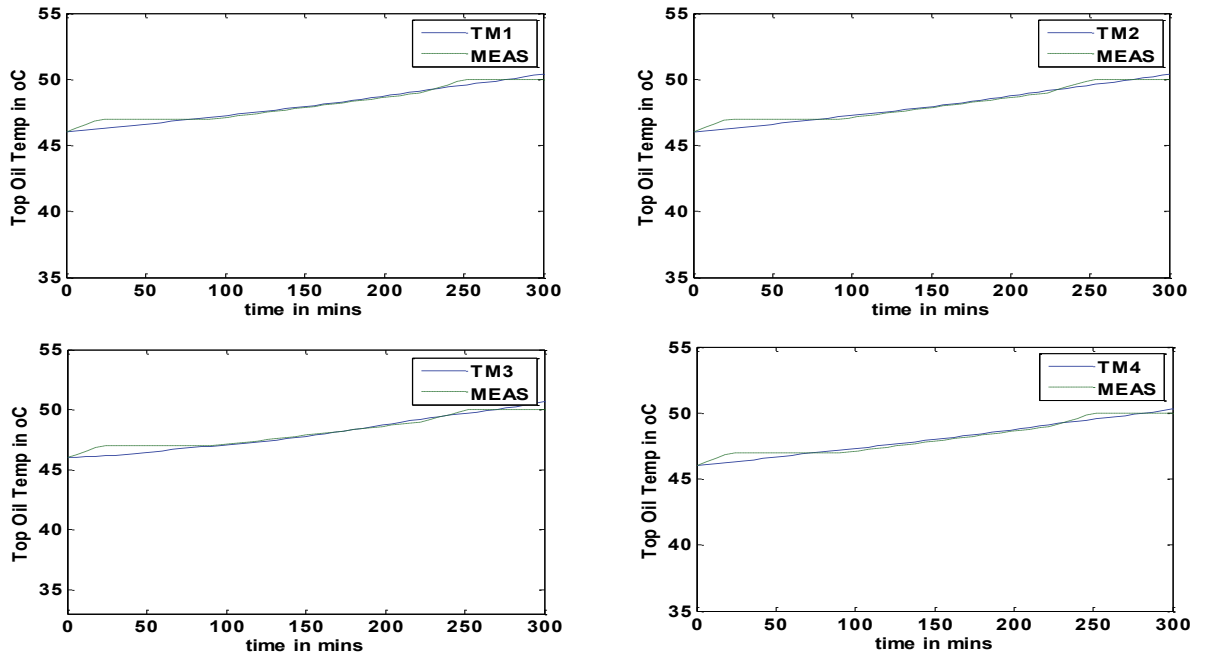
Figure 5.4   TR42 Top Oil Temperature Simulation Results in OFAF mode 1 using
genetic algorithm optimization
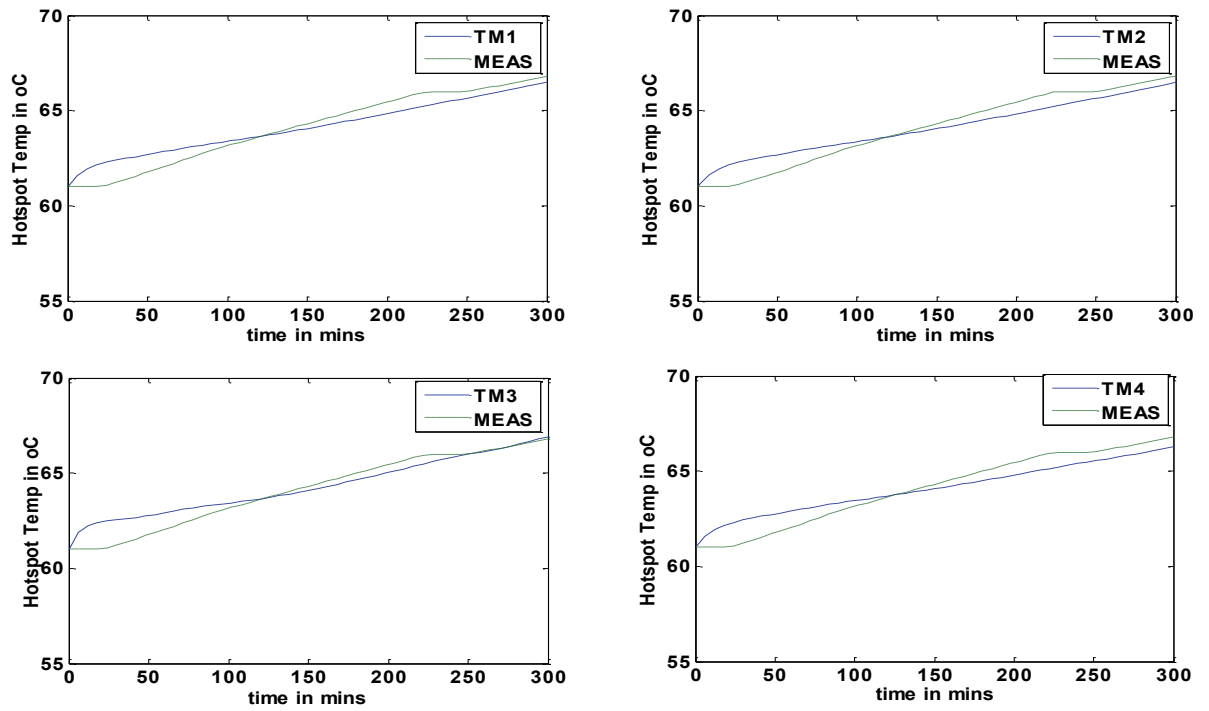
Figure 5.5   TR42 Hotspot Temperature Simulation Results in OFAF mode 1 using
genetic algorithm optimization
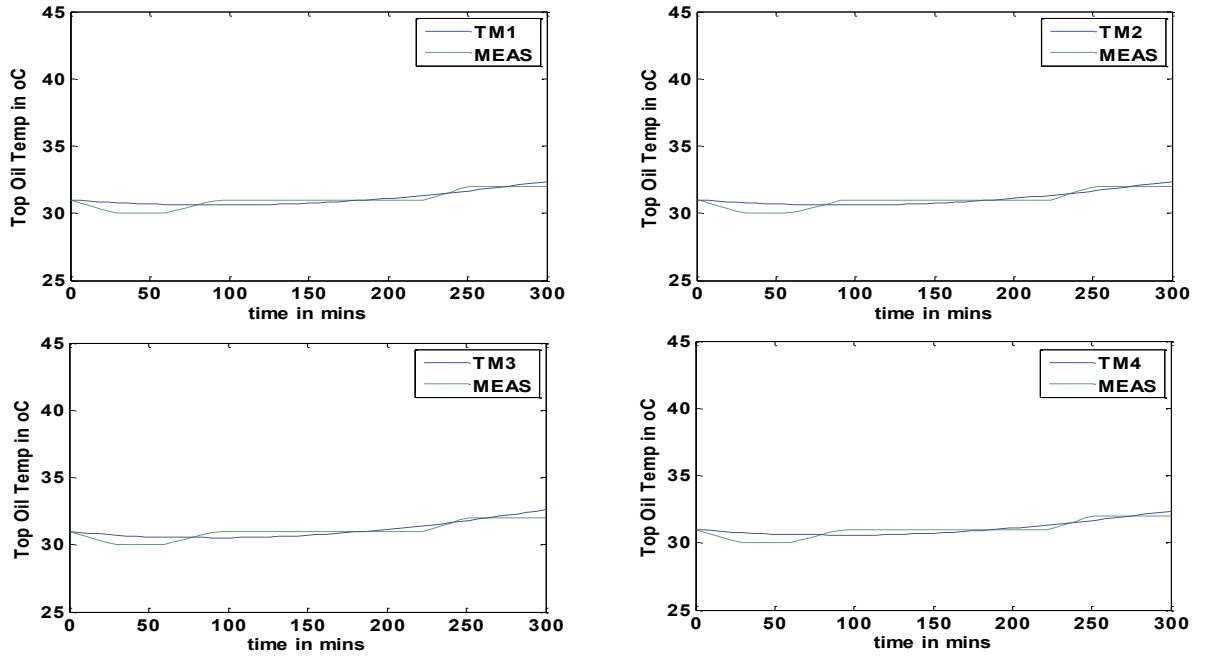
Figure 5.6   TR43 Top Oil Temperature Simulation Results in OFAF mode 1 using genetic algorithm optimization
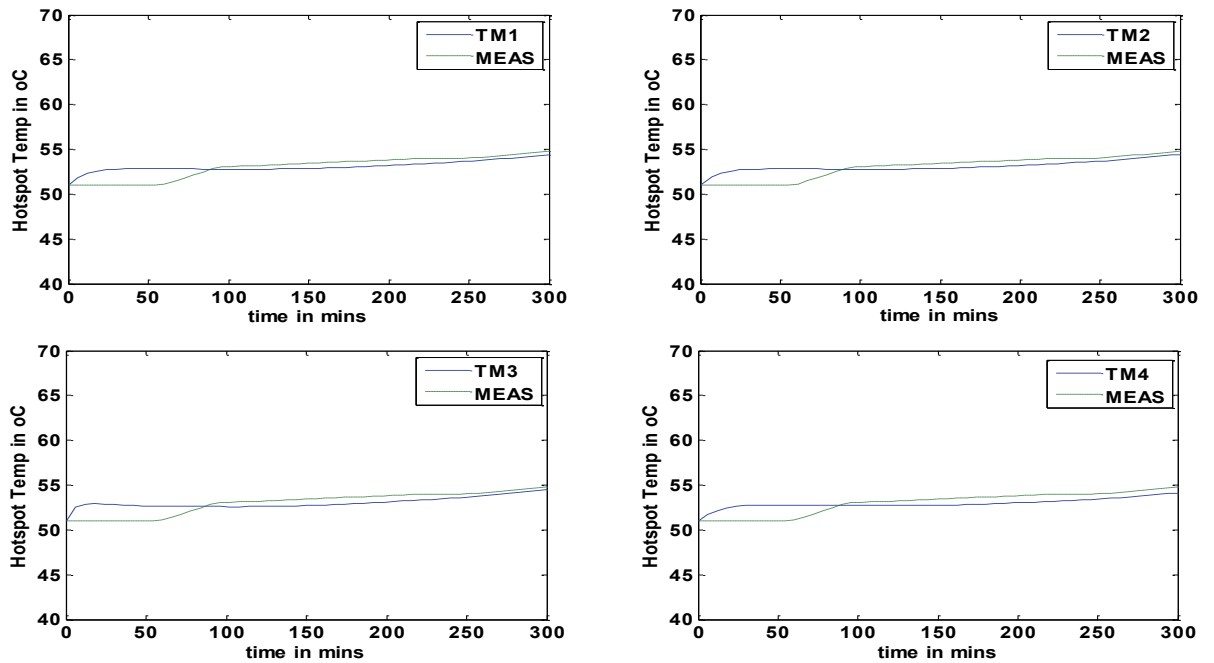
Figure 5.7   TR43 Hotspot Temperature Simulation Results in OFAF mode 1 using genetic algorithm optimization
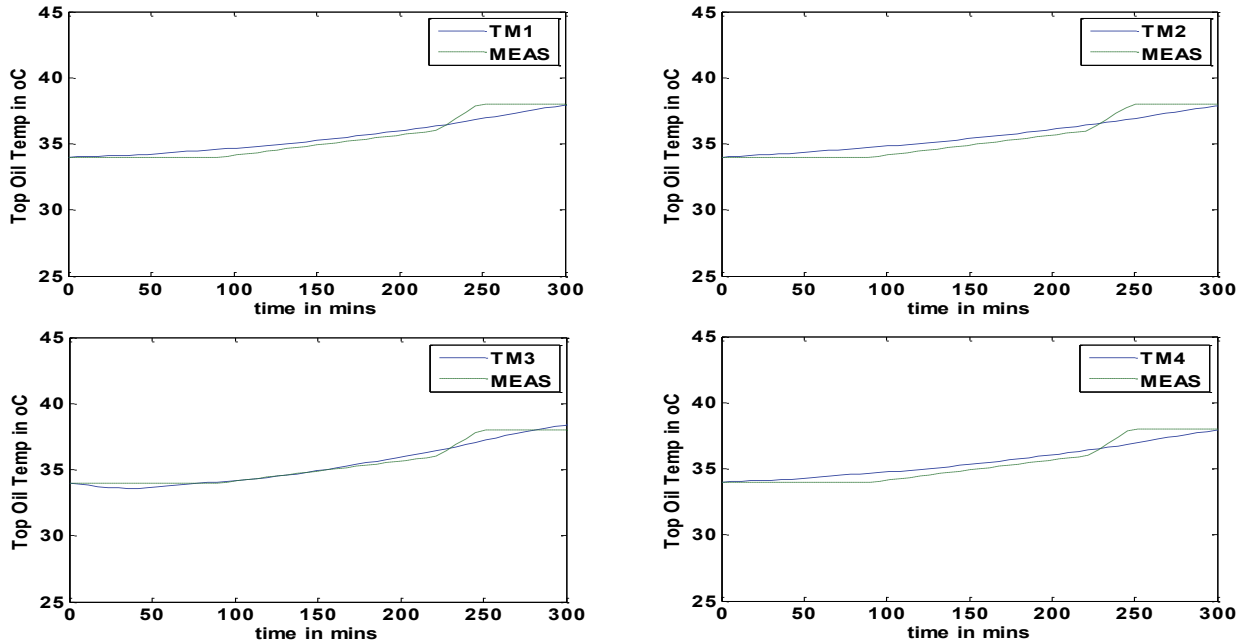
Figure 5.8   TR44 Top Oil Temperature Simulation Results in OFAF mode 1 using
               genetic algorithm optimization
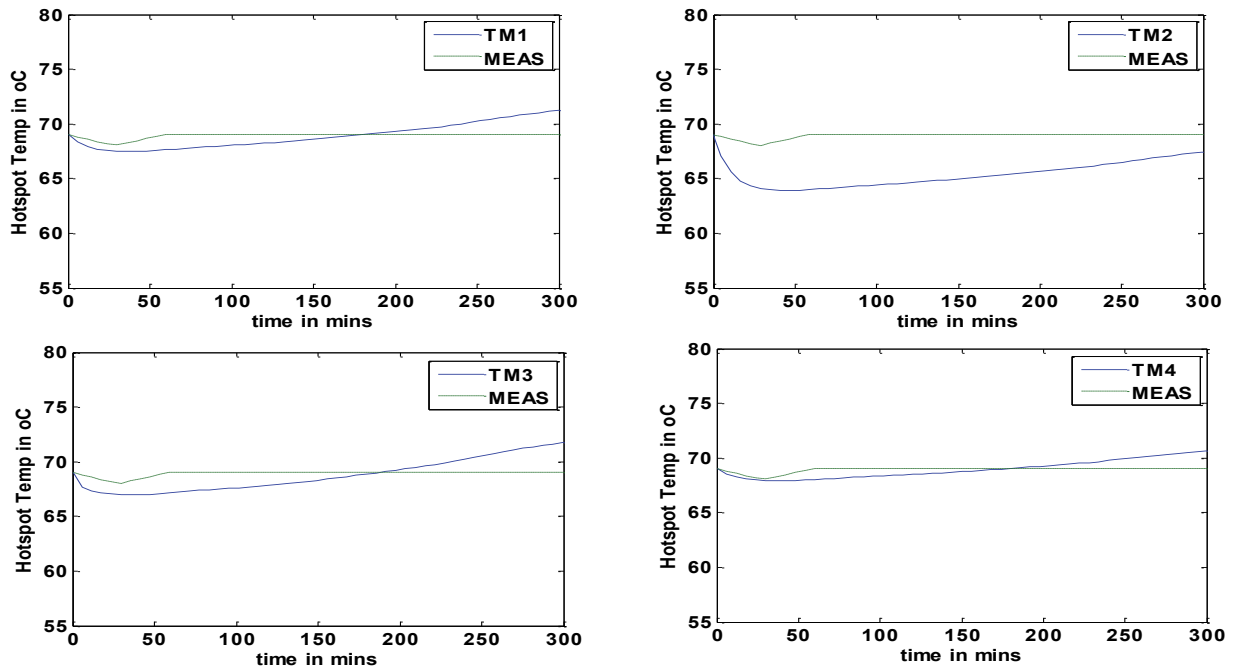
Figure 5.9   TR44 Hotspot Temperature Simulation Results in OFAF mode 1 using
               genetic algorithm optimization

96
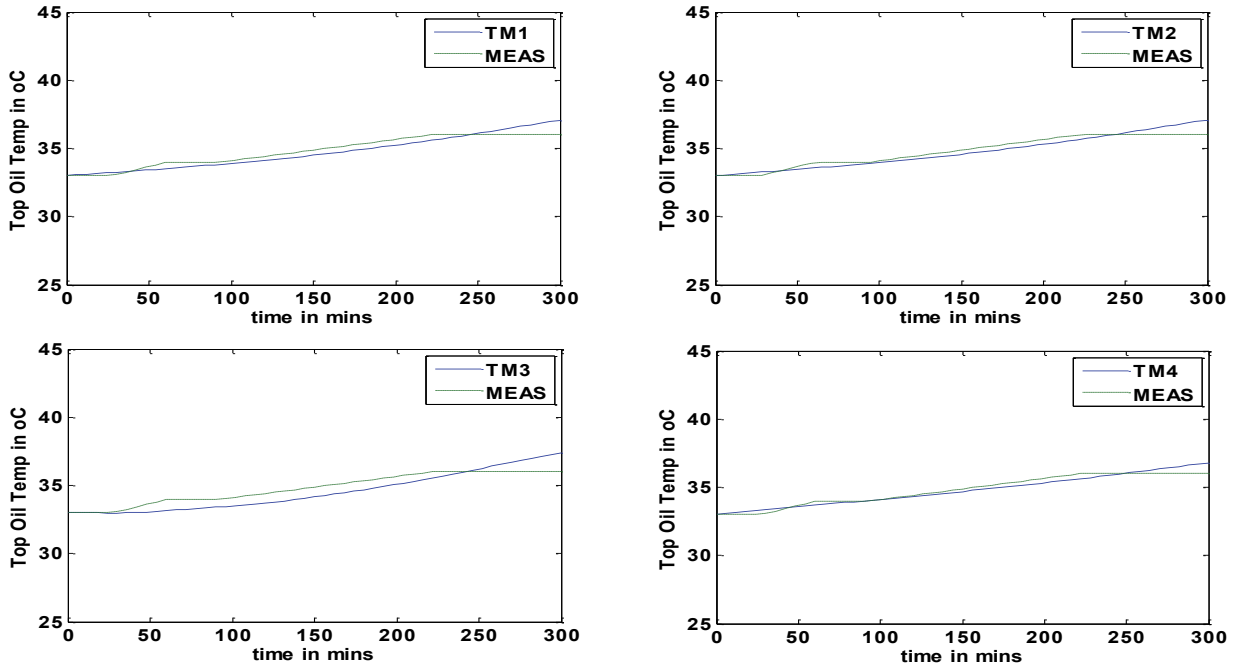
Figure 5.10   TR45 Top Oil Temperature Simulation Results in OFAF mode 1 using genetic algorithm optimization
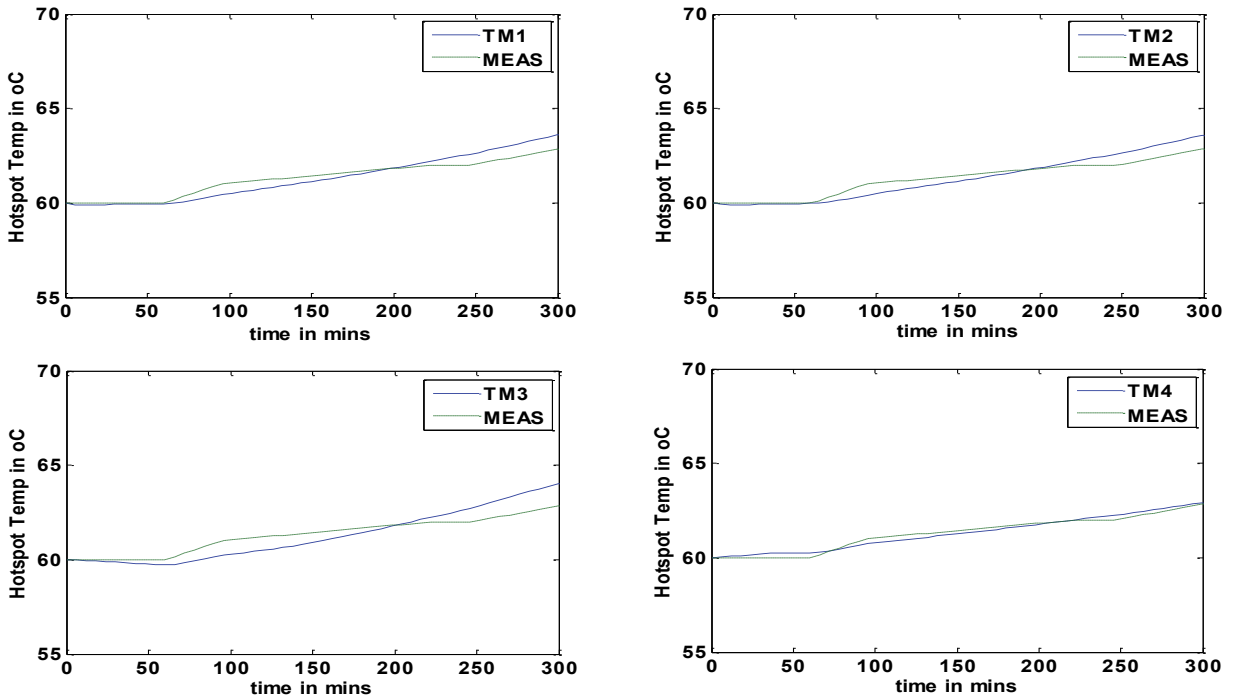
Figure 5.11   TR45 Hotspot Temperature Simulation Results in OFAF mode 1 using genetic algorithm optimization
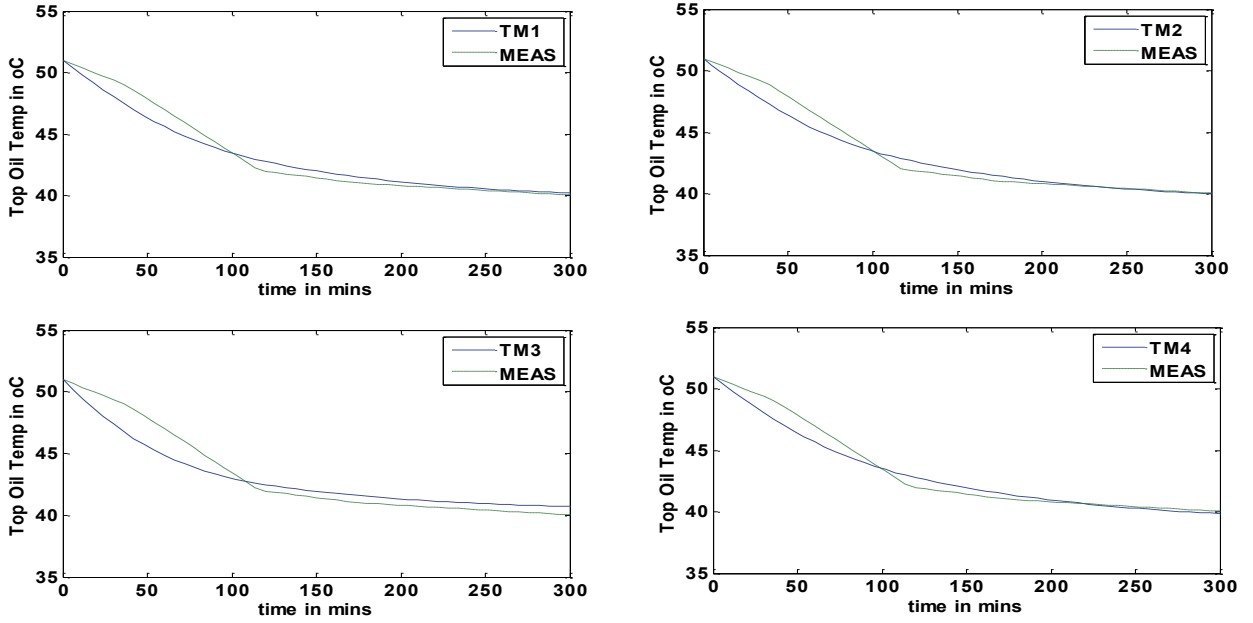
Figure 5.12   TR41 Top Oil Temperature Simulation Results in OFAF mode 2 using genetic algorithm optimization
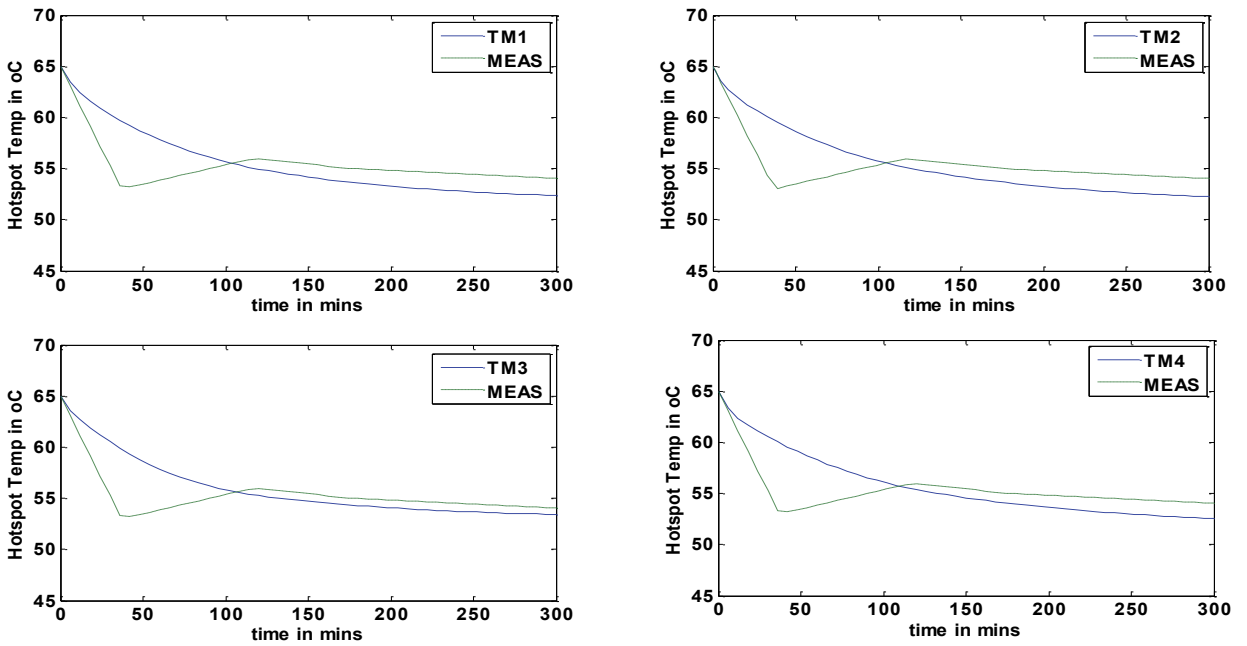
Figure 5.13   TR41 Hotspot Temperature Simulation Results in OFAF mode 2 using genetic algorithm optimization
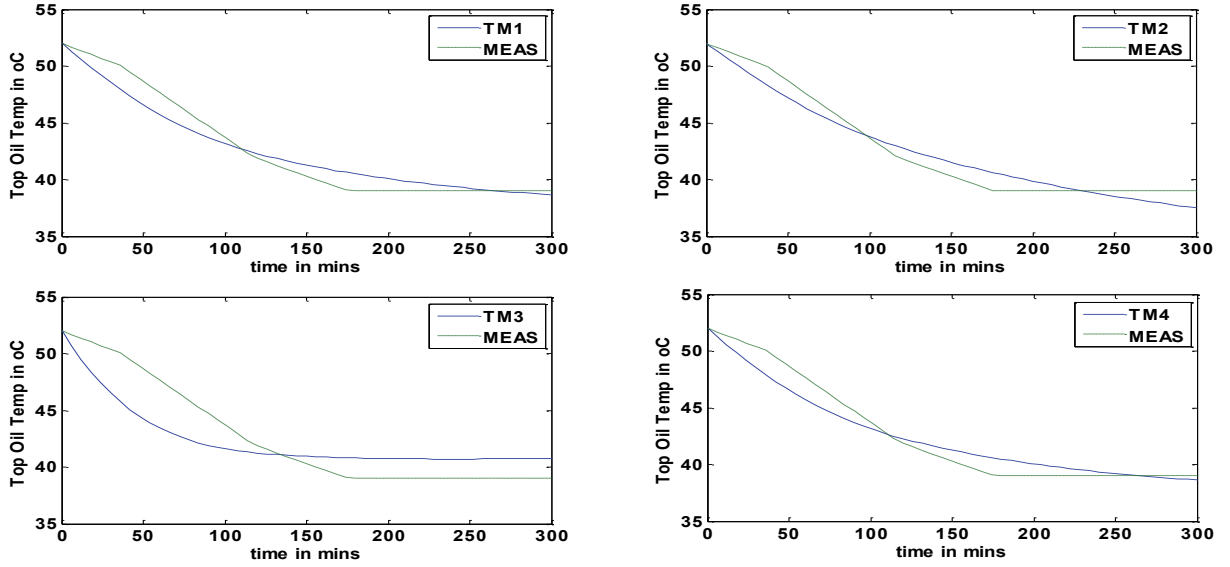
Figure 5.14   TR42 Top Oil Temperature Simulation Results in OFAF mode 2 using genetic algorithm optimization
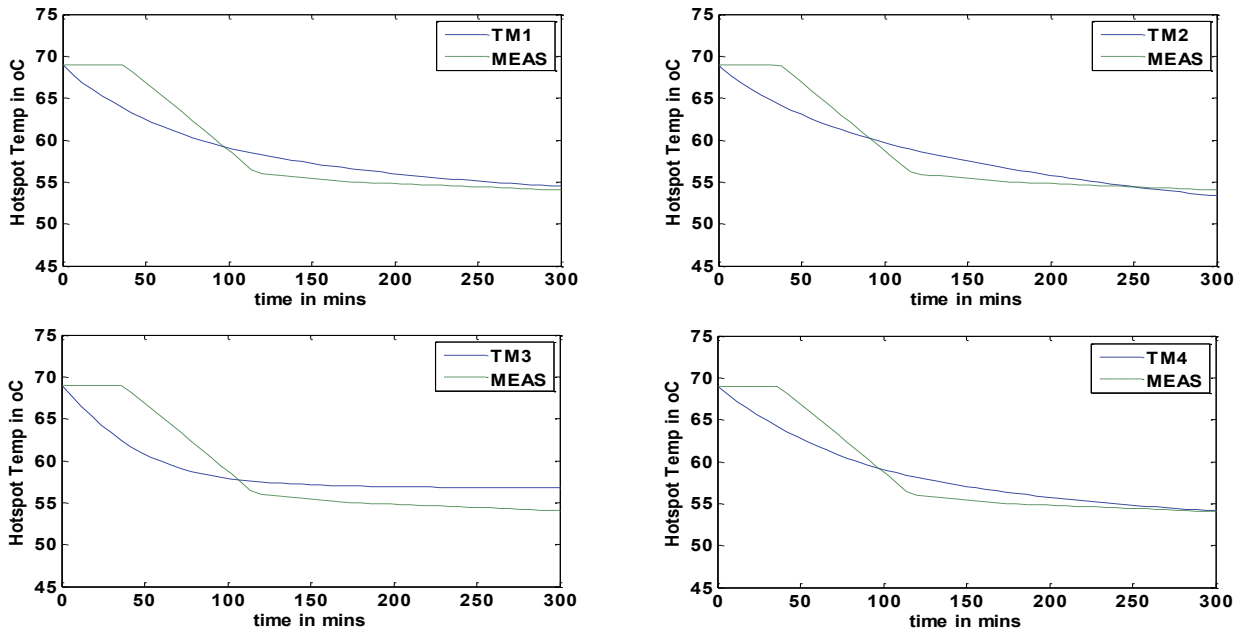
Figure 5.15   TR42 Hotspot Temperature Simulation Results in OFAF mode 2 using genetic algorithm optimization
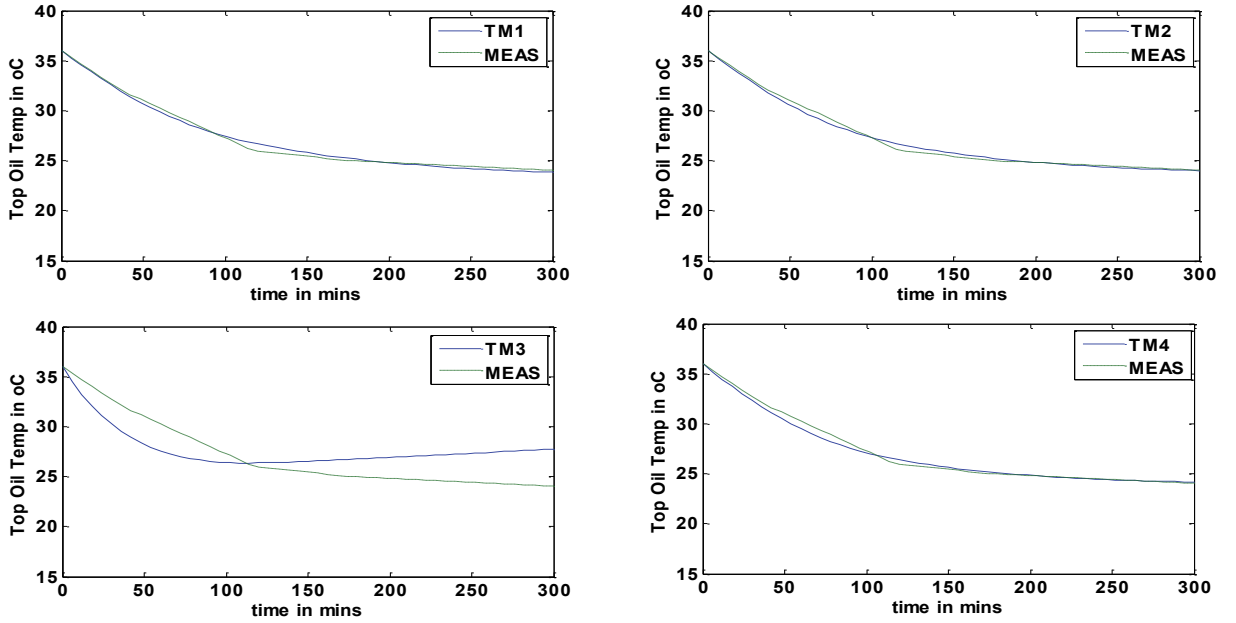
Figure 5.16   TR43 Top Oil Temperature Simulation Results in OFAF mode 2 using genetic algorithm optimization
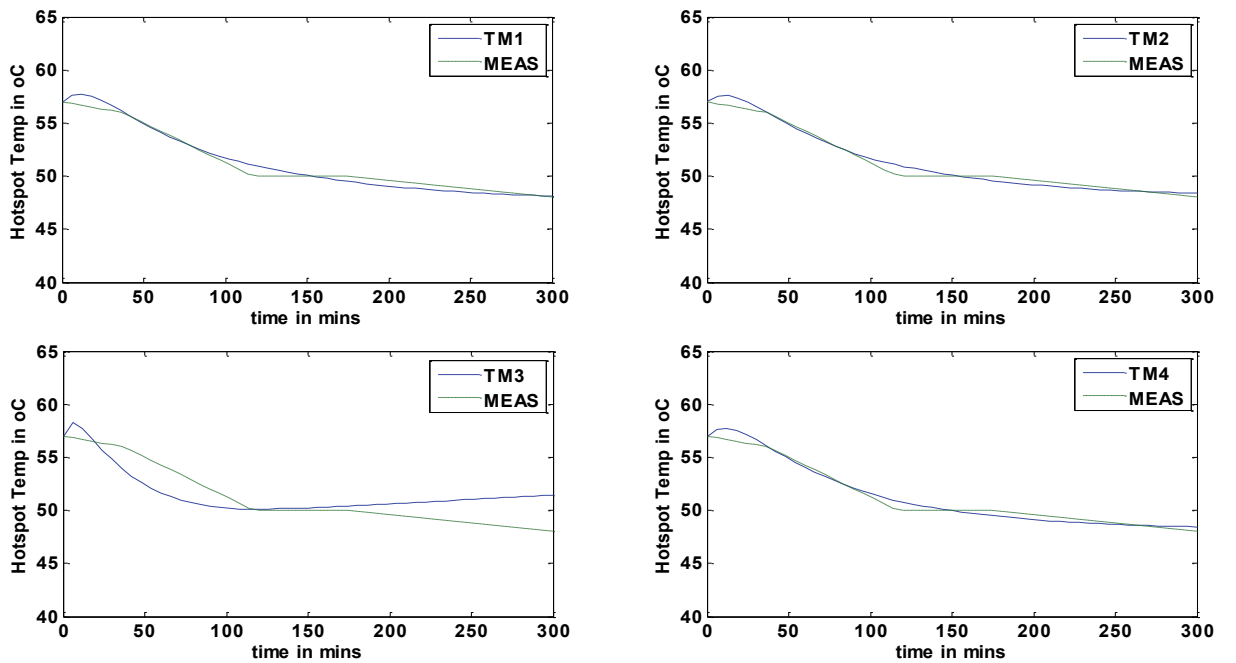
Figure 5.17   TR43 Hotspot Temperature Simulation Results in OFAF mode 2 using genetic algorithm optimization
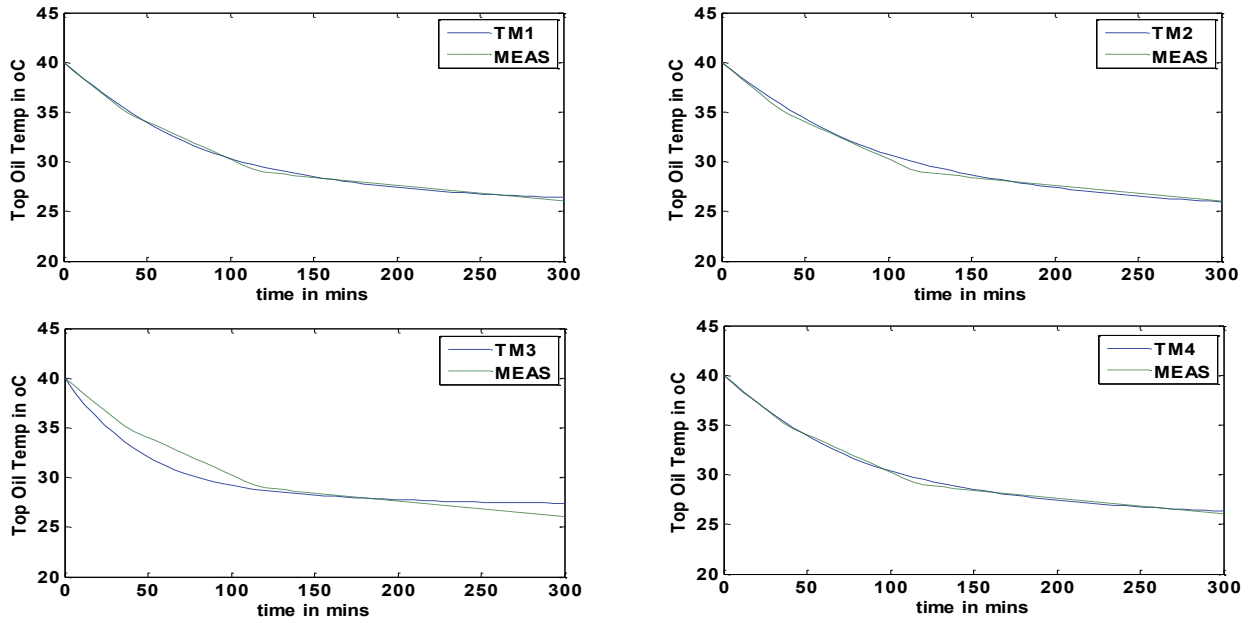
Figure 5.18   TR44 Top Oil Temperature Simulation Results in OFAF mode 2 using genetic algorithm optimization
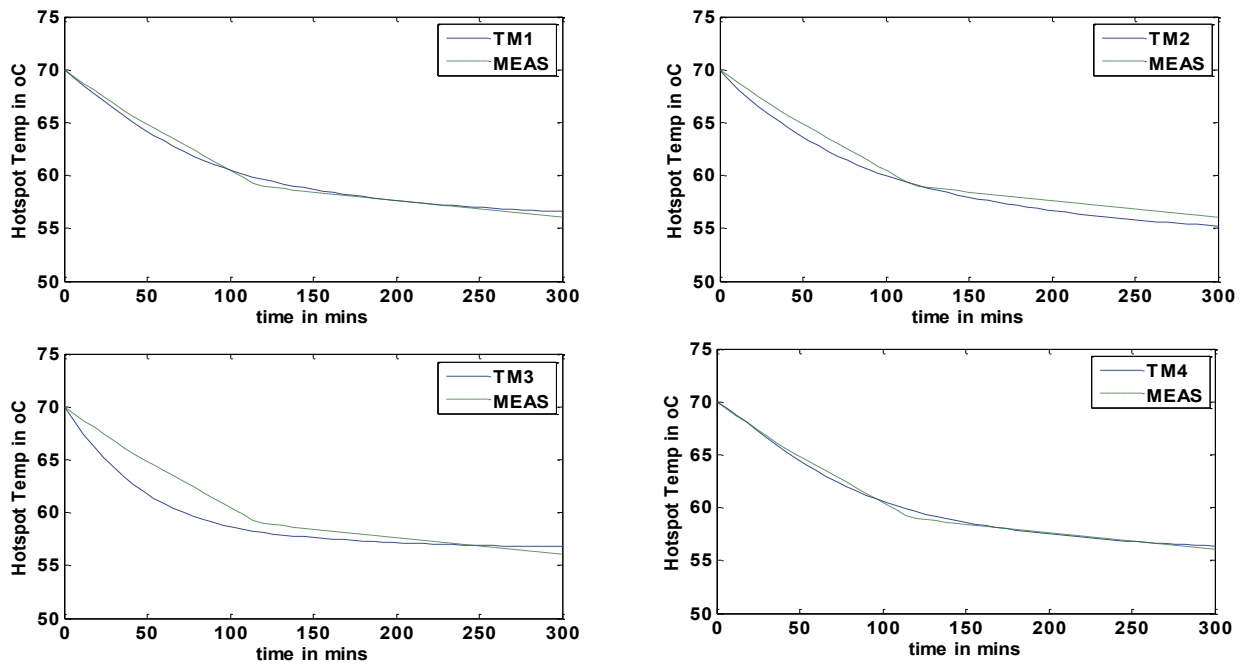
Figure 5.19   TR44 Hotspot Temperature Simulation Results in OFAF mode 2 using genetic algorithm optimization
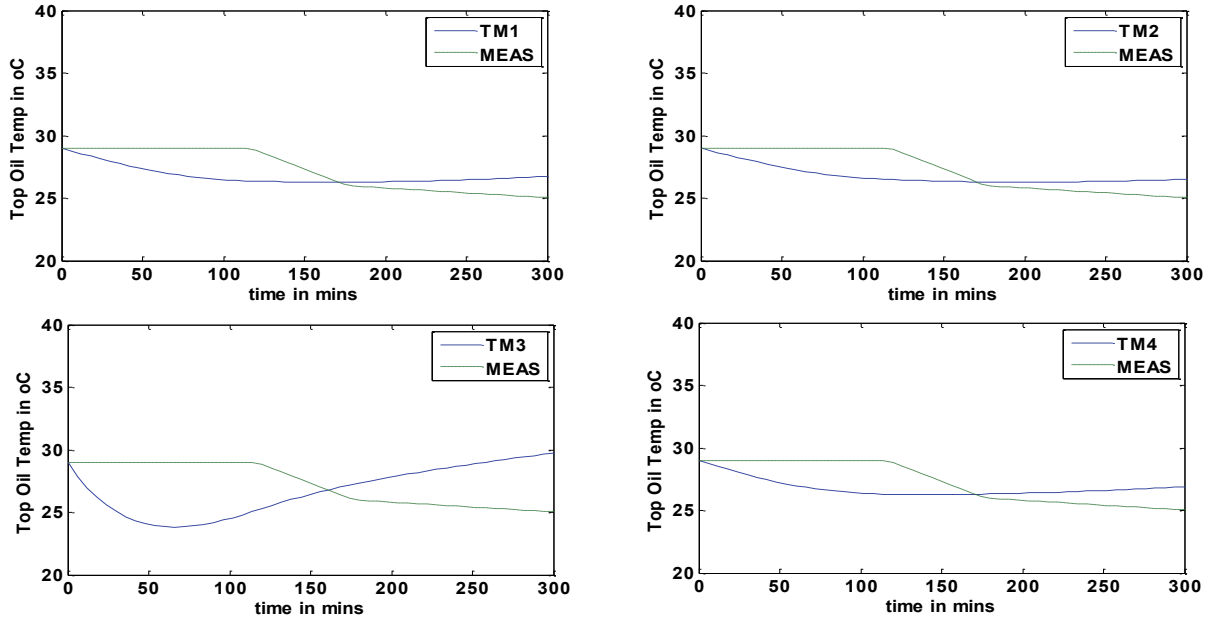
Figure 5.20   TR45 Top Oil Temperature Simulation Results in OFAF mode 2 using
genetic algorithm optimization
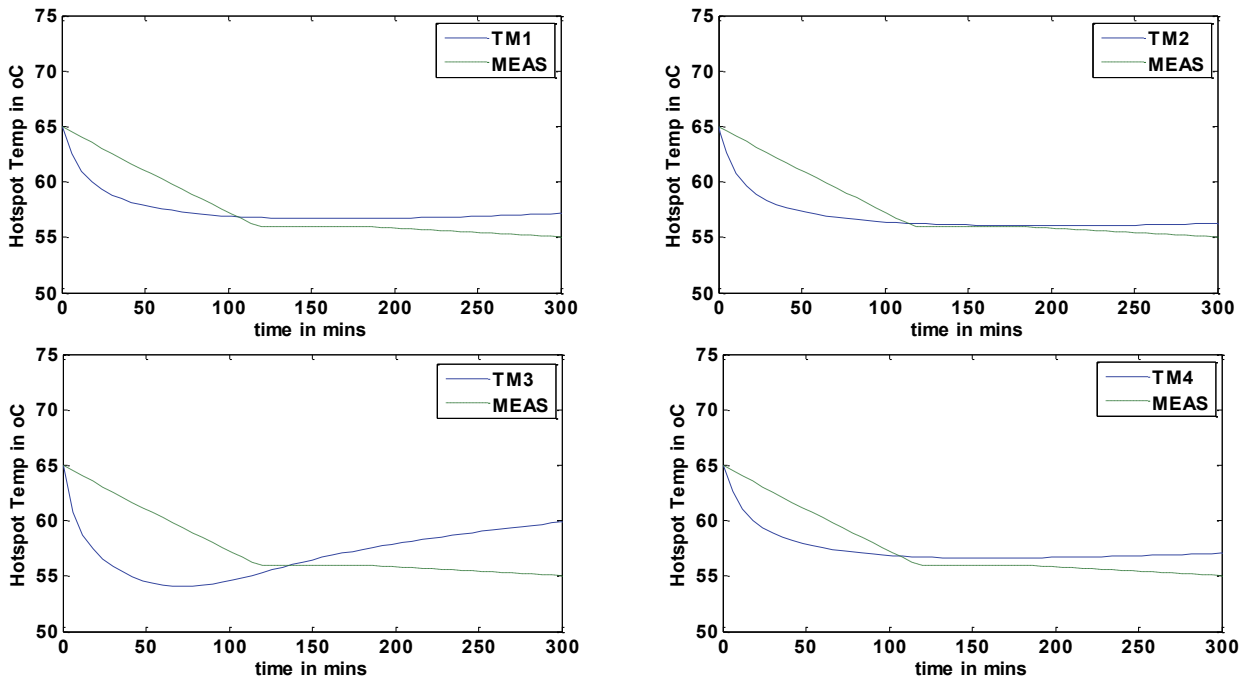
Figure 5.21   TR45 Hotspot Temperature Simulation Results in OFAF mode 2 using
genetic algorithm optimization

A summary of the mean square error (cost) in estimated values of the thermal models and measured temperature values of the results obtained from the simulation is shown in Tables 5.5 and 5.6 below.

Table 5.5   Deviation of Results using Genetic Algorithms in OFAF Mode 1

Mean Squared Error with Measured Values					
		TM1	TM2	TM3	TM4
TR41	O_{TO} (ºC)	0.3564	0.3718	0.2076	0.4796
	O_H (ºC)	0.3823	0.3652	0.2243	0.5126
TR42	O_{TO} (ºC)	0.2668	0.2665	0.3295	0.2627
	O_H (ºC)	0.5882	0.5515	0.5546	0.6404
TR43	O_{TO} (ºC)	0.3479	0.3479	0.3558	0.3432
	O_H (ºC)	0.8786	0.8265	0.9338	0.9252
TR44	O_{TO} (ºC)	0.4427	0.5185	0.2862	0.4736
	O_H (ºC)	1.0420	3.4529	1.3592	0.7461
TR45	O_{TO} (ºC)	0.3985	0.3771	0.6319	0.2793
	O_H (ºC)	0.3964	0.3611	0.5854	0.1671

Table 5.6   Deviation of Results using Genetic Algorithms in OFAF Mode 2

Mean Squared Error with Measured Values					
		TM1	TM2	TM3	TM4
TR41	O_{TO} (ºC)	0.7081	0.7071	1.0582	0.6703
	O_H (ºC)	2.3432	2.2760	2.0589	2.2540
TR42	O_{TO} (ºC)	1.0834	1.0082	2.3311	1.1102
	O_H (ºC)	1.9721	1.8202	2.8092	1.9465
TR43	O_{TO} (ºC)	0.2953	0.2849	2.2411	0.3388
	O_H (ºC)	0.4694	0.3572	1.5234	0.4183
TR44	O_{TO} (ºC)	0.2008	0.2849	1.0416	1.5522
	O_H (ºC)	0.3665	0.7619	1.5348	0.2617
TR45	O_{TO} (ºC)	1.4725	1.3863	3.4861	0.3388
	O_H (ºC)	1.8342	1.7756	3.8616	1.5482

The results obtained show that the improved IEEE thermal model temperature estimation has the least errors when compared to the other 3 models; the IEC model, the G. Swift model and the D. Susa model. The results of the improved IEEE model have mean square errors ranging from $0.27^{o}C$ to $0.44^{o}C$ for the top oil temperature and $0.38^{o}C$ to $1.04^{o}C$ for the hotspot temperature in the OFAF mode 1 condition and mean square errors between $0.20^{o}C$ to $1.47^{o}C$ for the top oil temperature and $0.37^{o}C$ to $2.34^{o}C$ for the hotspot temperature in the OFAF mode 2 conditions.

The errors obtained with the improved IEEE model are within satisfactory ranges as with other estimations in [14, 20, 21, 22, 23, 24] and also are within acceptable ranges for Alcoa. Therefore the developed IEEE model is recommended as the thermal model for the purpose of online monitoring and future estimation of Alcoa rectifier transformer top oil and hotspot temperatures.

5.4.2 Validation of Rectifier Thermal Model for Rectifier Transformer TR41

A validation of the developed IEEE rectifier thermal model was done for rectifier transformer TR41. On the 9th of July 2014, the oil and winding temperatures were recorded at 1pm with an ambient temperature of $25^{o}C$. The transformer was operating at 36 KA which is equivalent to 0.9 p.u and was running in the OFAF mode 2. The recorded top oil temperature and hotspot temperature were $60^{o}C$ and $73^{o}C$ respectively.

In order to validate the model with this measured data, the ambient weather profile for the day was retrieved from the weather channel, accuweather.com [33] from 12 am to 10 pm and a constant load at 0.9 p.u for the transformer was assumed for the same time period.

The simulated results for the ambient temperature, top oil temperature and hotspot temperature are presented in figure 5.22
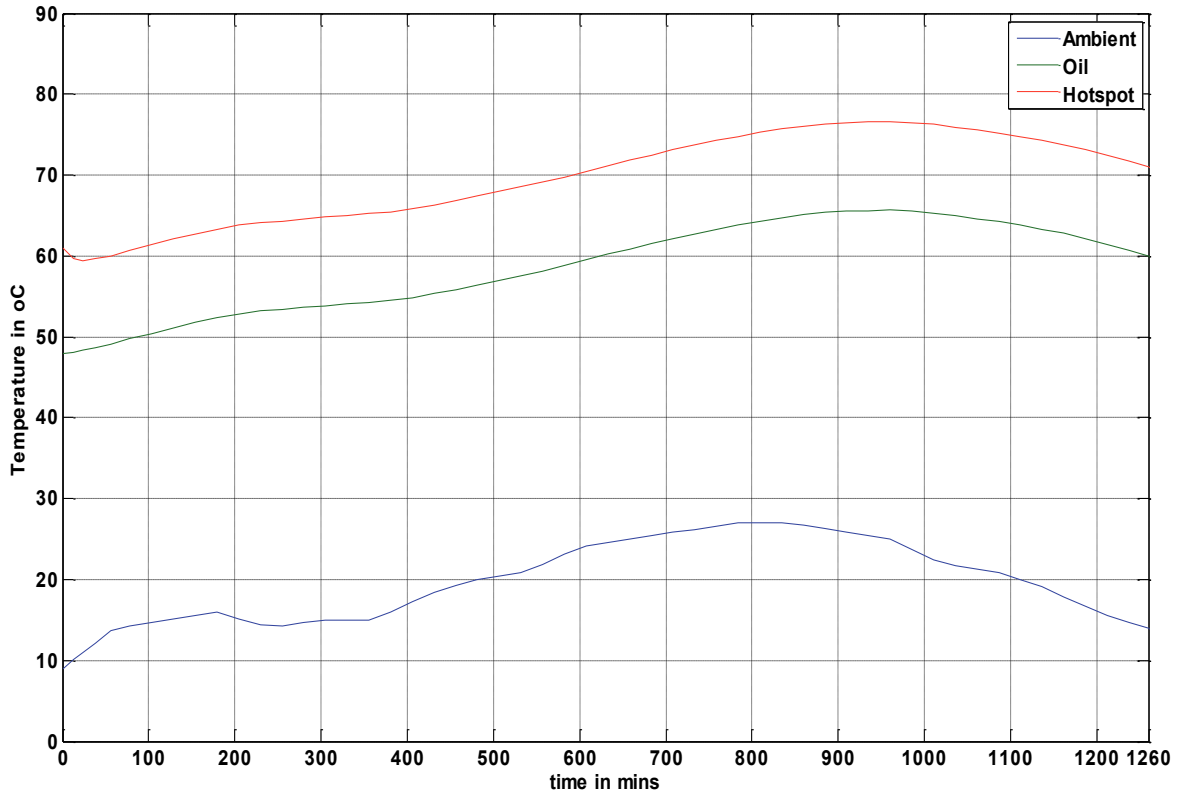
Figure 5.22   Ambient Temperature, Estimated Top Oil and Hotspot Temperature for TR41 on July 9th 2014

The results show that at the 660th minute which is equivalent to 1pm, the ambient temperature was at $25^{o}C$. The simulated top oil temperature and hotspot temperatures at the 660th minutes are $60.9^{o}C$ and $72^{o}C$ respectively. The results obtained are within good range of the measured values with a deviation of $0.9^{o}C$ in the top oil and $1^{o}C$ in the hotspot temperature.

CHAPTER 6 APPLICATION OF RECTIFIER TRANSFORMER THERMAL MODELING

6.1 Introduction

The monitoring of the hotspot temperature of rectifier transformer has become a major area of interest in estimating the useful life of this critical equipment for aluminum smelting industries. In this chapter, the developed IEEE rectifier transformer thermal models is used to effectively optimize the rectifier transformers life cycle to suit the needs of Alcoa as well as to optimize production output and power utilization all year round.

6.2 Alcoa Baie Comeau Objectives for the Rectifier Transformers

The Alcoa Baie Comeau smelter is presently researching ways of estimating the useful life of their rectifier transformers in the pot line D as to effectively plan for a replacement of the transformers. The smelter in the pot line D has 6 rectifier transformers which have been in use for 30 years. Over the years, it has been a company replacement policy to change the transformers after every 50 years; therefore it will be desired to keep the present transformers for another 20 years.

Based on the records of hotspot temperatures of the rectifier transformer, the average yearly mean temperature is 73°C. Using the lifetime equation as stated in equation (2.1) in chapter 2 as well as integrating the oxidation and hydrolysis ageing factors which are obtained from the dissolved gas analysis (DGA) and oil tests records and indicate low levels of water and oxygen concentrations, the remaining useful life of the rectifier transformers is determined to be 15 years. In order to use the rectifier transformers for an estimated period of 20 years,

the hotspot temperature should be kept at an average of 68°C yearly based on equation (2.1). The records of hotspot temperature of the transformer show a variance of temperatures between 60°C and 80°C. Therefore, to make sure that the average yearly temperature is within the set average, a maximum hotspot temperature of 70°C is recommended for the rectifier transformers.

6.3   Predictive Maintenance Application for Alcoa Rectifier Transformers

The final aim of this research is to come up with a predictive maintenance solution to effectively utilize the rectifier transformers as well as to draw maximum current with this equipment to obtain maximum output production and optimize power consumption with auxiliary equipment (fans) connected to the transformers. By the use of future estimated hotspot temperatures of the rectifier transformers, a control scheme for optimizing the useful life of these assets can be achieved by preventing the hotspot temperatures from reaching set maximum temperatures and at the same time obtaining maximum possible loading as well as efficient utilization of the auxiliary cooling fans. The method employed for preventing the overshooting of the hotspot temperatures is by an increment of the cooling with the auxiliary cooling fans on the transformers or by a reduction of the loading on the transformers in the event of full utilization of cooling fans possible.

Using the developed IEEE thermal model, a chart with the variation of the hotspot temperature with reference to varying loading factor of the transformer and varying ambient temperature in the steady state for both OFAF cooling modes is proposed to be adopted for the control of the hotspot temperature within the set limits.

The steady state hotspot temperature for the developed IEEE thermal model in equation (6.1) is given as a summation of the steady state top oil temperature and steady state hotspot rise above top oil temperature.

$$\theta_H = \theta_{TO} + \Delta\theta_H \qquad (6.1)$$

where

$$\theta_{TO} = \left[\frac{1 + R_{\mathrm{Re}c} K_{\mathrm{Re}c}^2}{1 + R_{\mathrm{Re}c}}\right]^n \times \left(\Delta\theta_{To-R}\right) + \theta_A \qquad (6.2)$$

$$\Delta\theta_H = \Delta\theta_{H,R} \times K_{\mathrm{Re}c}^{2m}. \qquad (6.3)$$

The charts for transformer TR41 to TR45 is shown below in Figures 6.1 to 6.10.
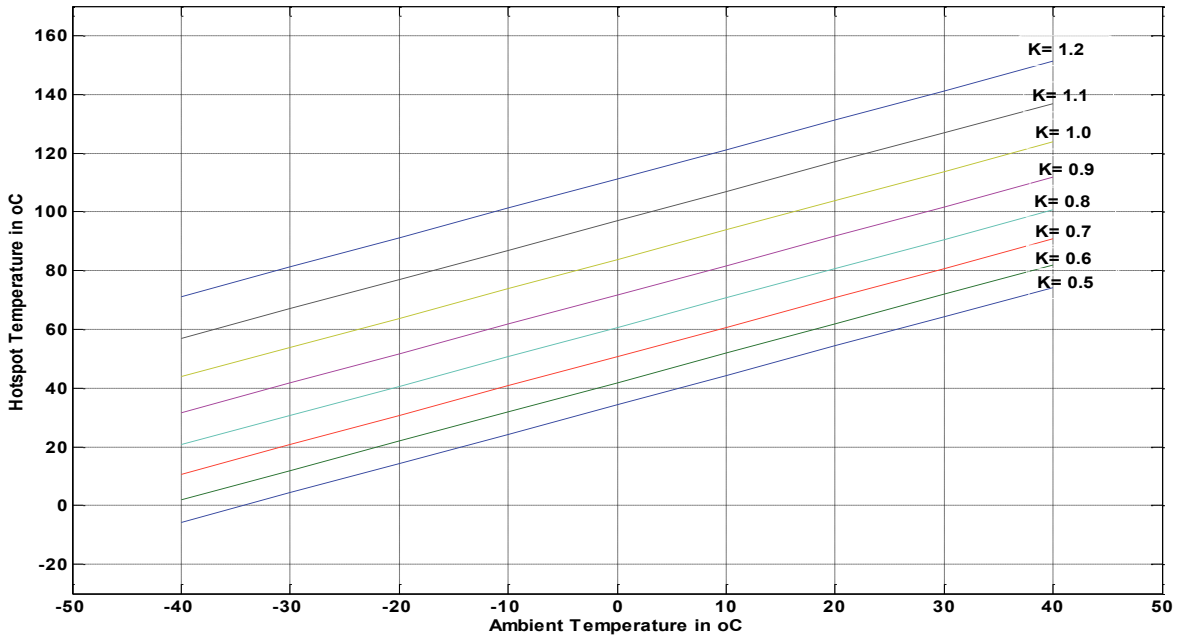
Figure 6.1   Steady State Chart for TR41 Hotspot Temperature under Different Ambient and Load Factor in OFAF Model 1 Conditions.
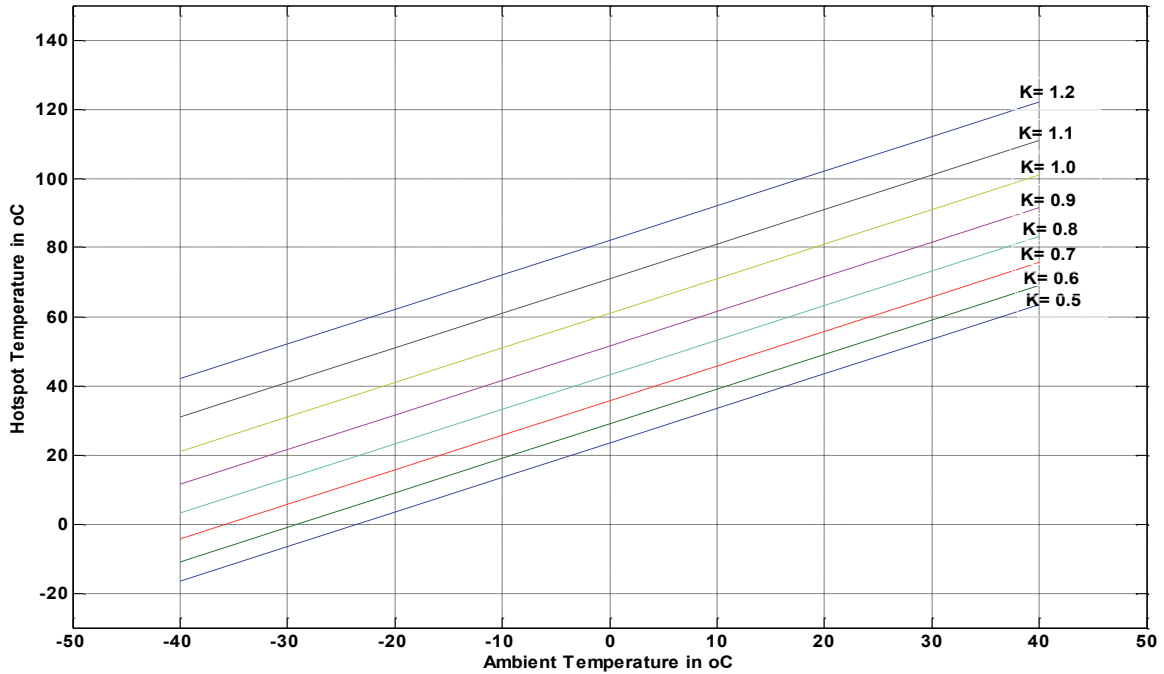
Figure 6.2   Steady State Chart for TR41 Hotspot Temperature under Different Ambient and Load Factor in OFAF Model 2 Conditions.
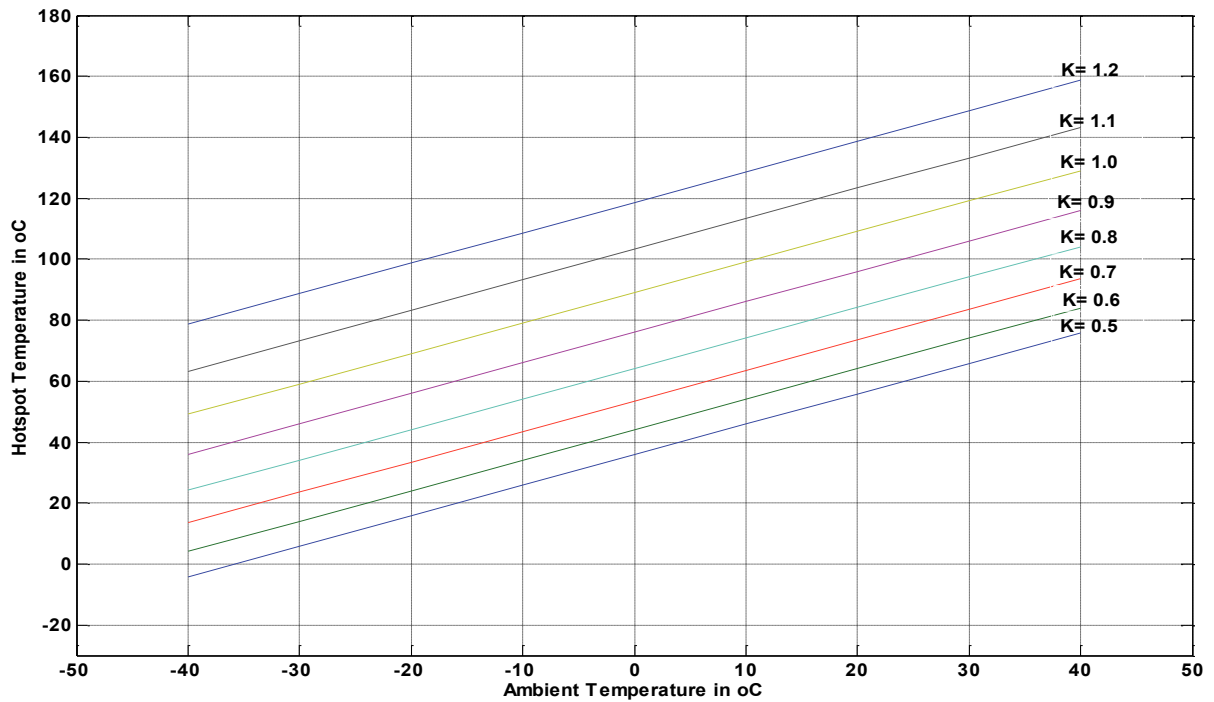
Figure 6.3   Steady State Chart for TR42 Hotspot Temperature under Different Ambient and Load Factor in OFAF Model 1 Conditions.
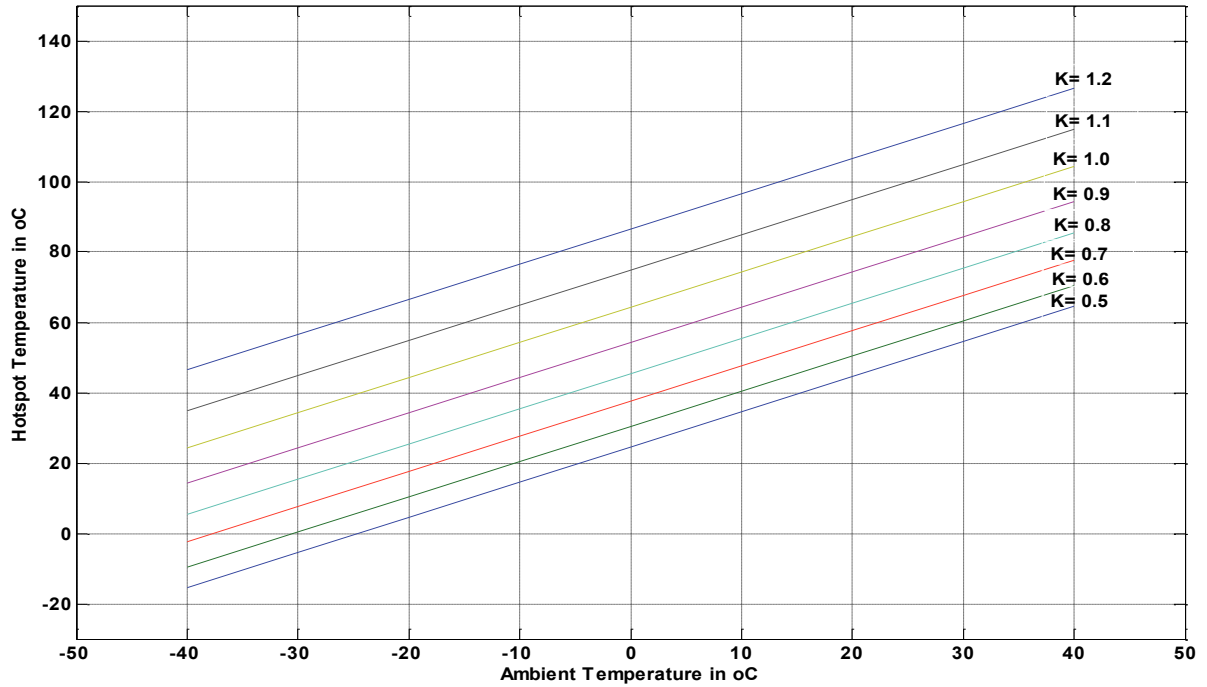
Figure 6.4   Steady State Chart for TR42 Hotspot Temperature under Different Ambient and Load Factor in OFAF Model 2 Conditions.
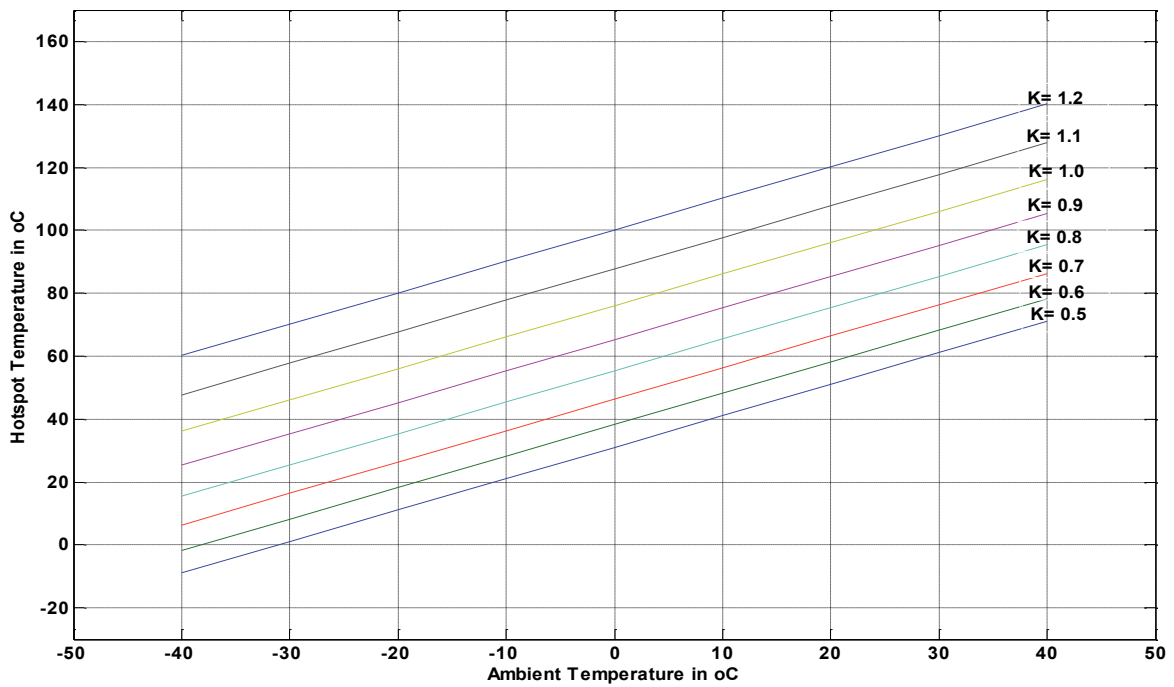
Figure 6.5   Steady State Chart for TR43 Hotspot Temperature under Different Ambient and Load Factor in OFAF Model 1 Conditions.
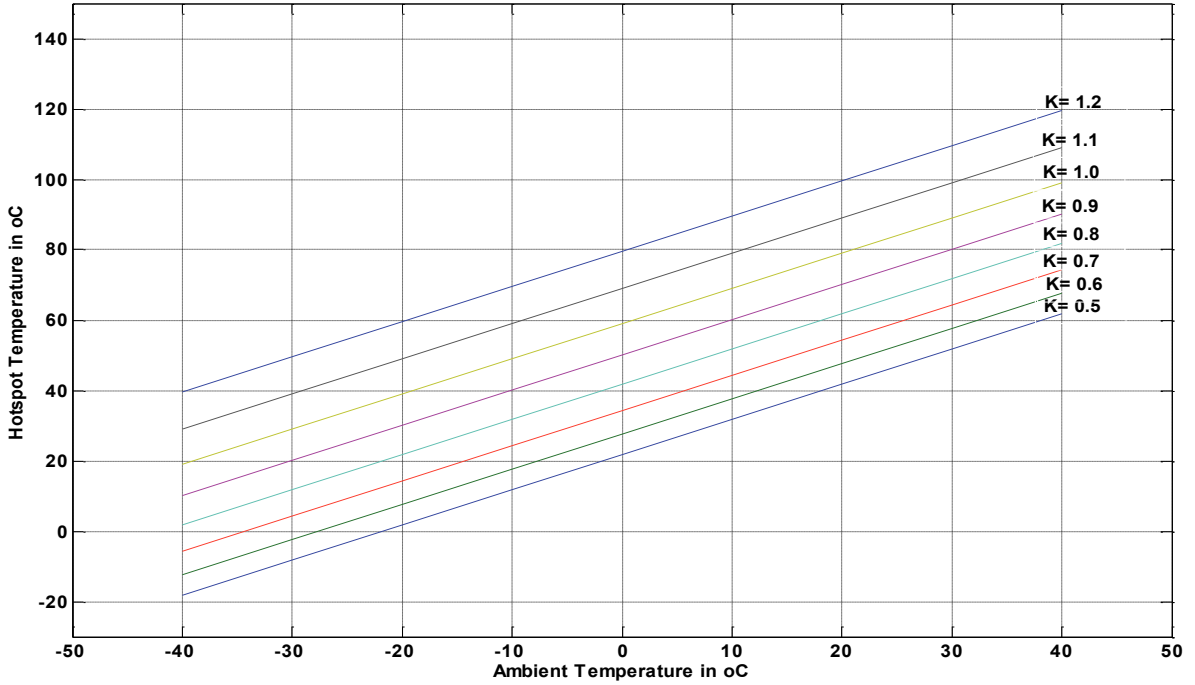
Figure 6.6   Steady State Chart for TR43 Hotspot Temperature under Different Ambient and Load Factor in OFAF Model 2 Conditions.
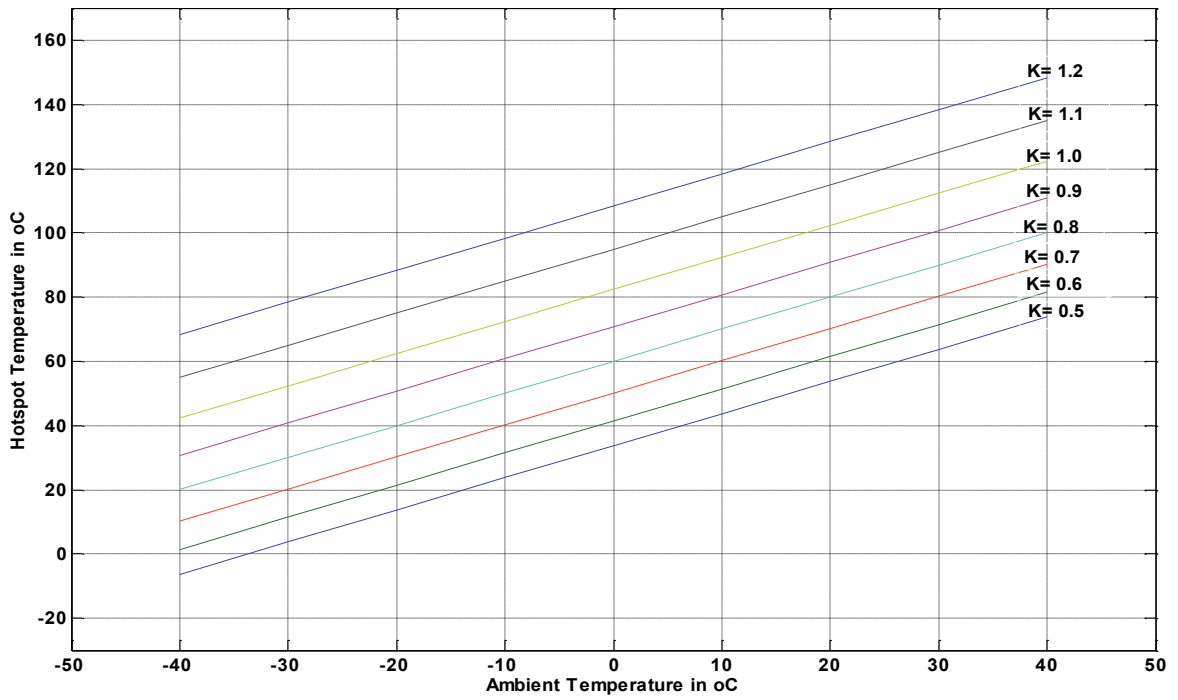
Figure 6.7   Steady State Chart for TR44 Hotspot Temperature under Different Ambient and Load Factor in OFAF Model 1 Conditions.
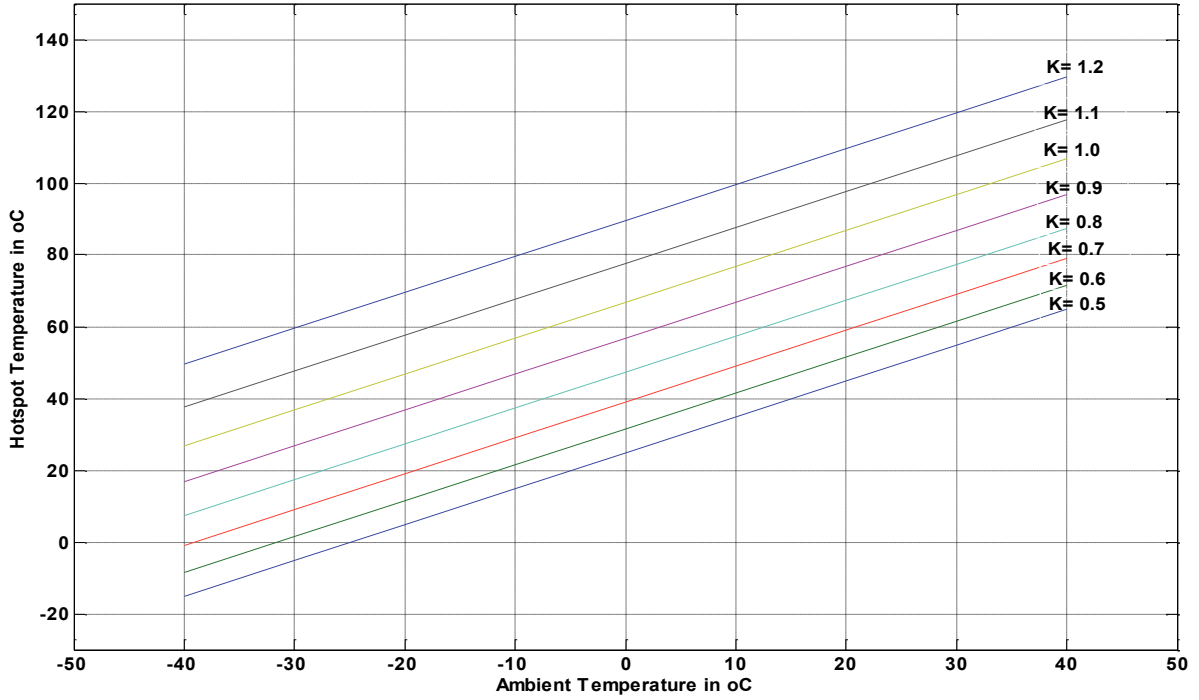
Figure 6.8   Steady State Chart for TR44 Hotspot Temperature under Different Ambient and Load Factor in OFAF Model 2 Conditions.
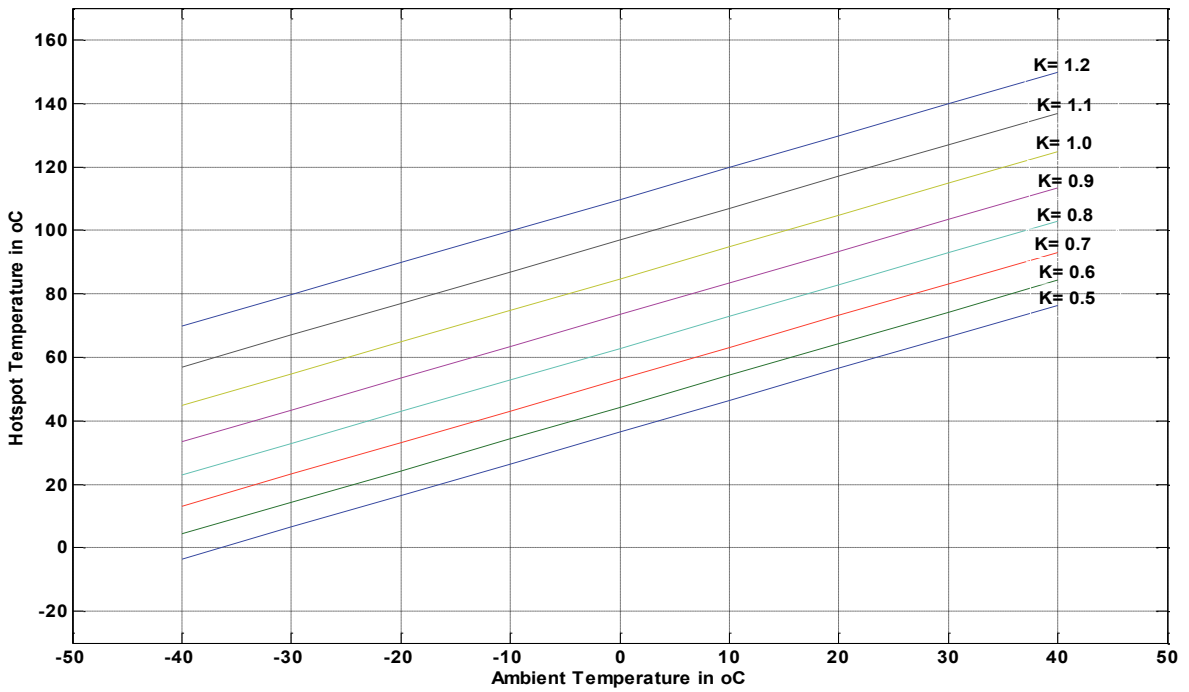
Figure 6.9   Steady State Chart for TR45 Hotspot Temperature under Different Ambient and Load Factor in OFAF Model 1 Conditions.
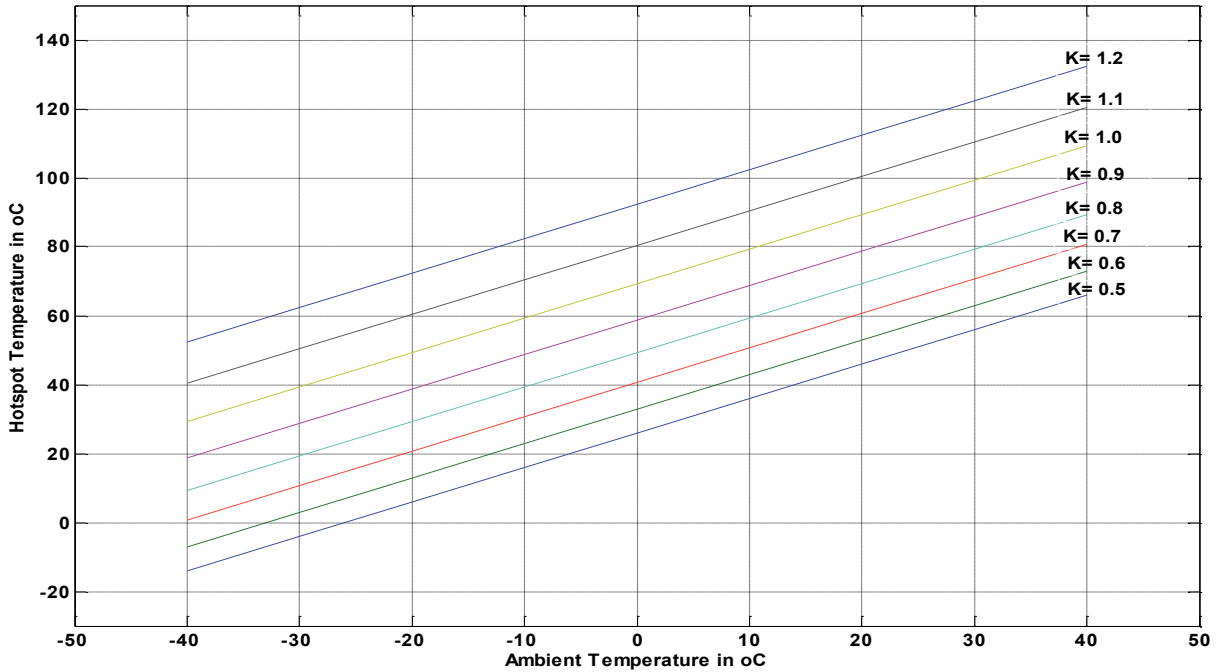
Figure 6.10   Steady State Chart for TR45 Hotspot Temperature under Different Ambient
and Load Factor in OFAF Model 2 Conditions.

The charts show a linear increase in the hotspot temperature with an increase in the ambient

temperature and an increasing temperature rise with every per unit increase in the loading

factor for all transformers and cooling modes. Also, it can be seen that the steady state

hotspot temperatures present lower values in the OFAF mode 2 condition than in the OFAF

mode 1 condition. The temperature range for ambient temperature is varied from -40°C to

40°C as this is the typical variation of temperature in Baie Comeau. The loading factor is

varied from 0.5 p.u to 1.2 p.u as the smelter operates the rectifier transformers at a

minimum of 0.5 p.u and a maximum of 1 p.u. In this project a maximum loading factor of

1.2 p.u is used to allow for overloading of the transformers to prevent reduction in pot line

production in situations when a transformers is out of service for maintenance purpose.

6.3.1   Summer Period Application

An application of the hotspot temperature estimation is demonstrated in this section using forecasted load profile and ambient temperature to regulate the hotspot temperature of the rectifier transformers. Assuming a load profile of 1 per unit for the transformer TR41 with an ambient temperature profile as shown in figure 6.11 during the summer period and operating with three fans (OFAF mode 2), the resultant hotspot temperature for the period is as shown in figure 6.12
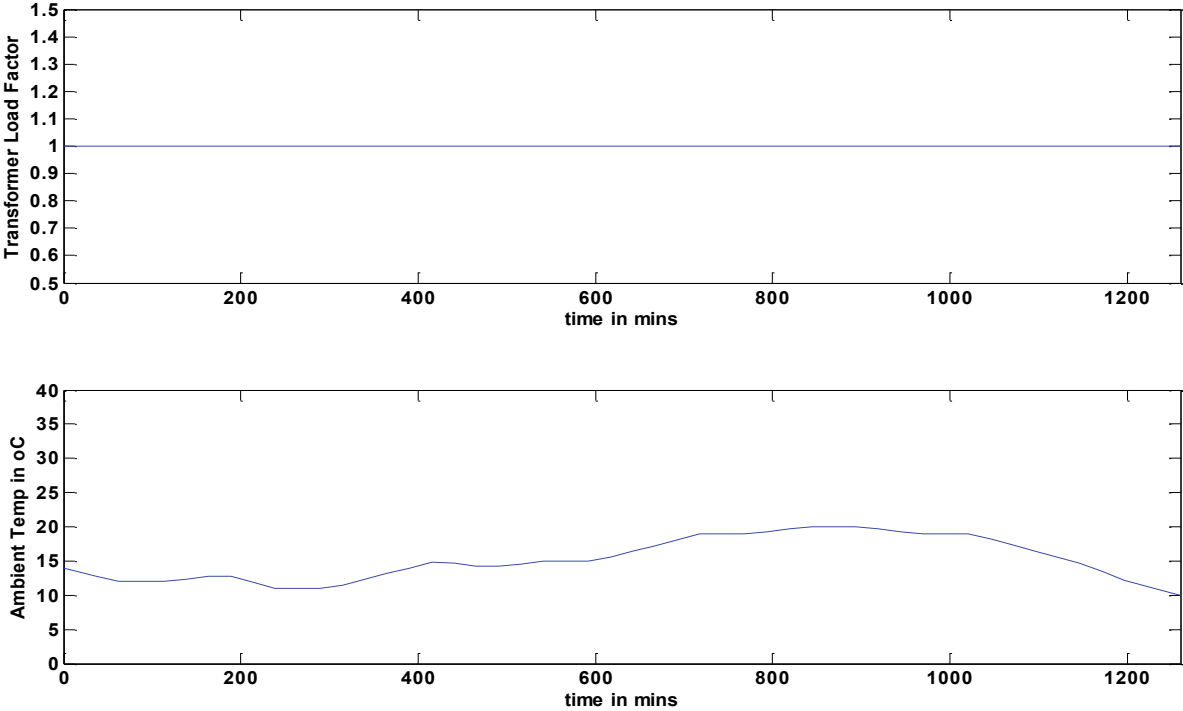
Figure 6.11   Estimated Load Profile and Ambient Temperature during Summer Season in OFAF mode 2
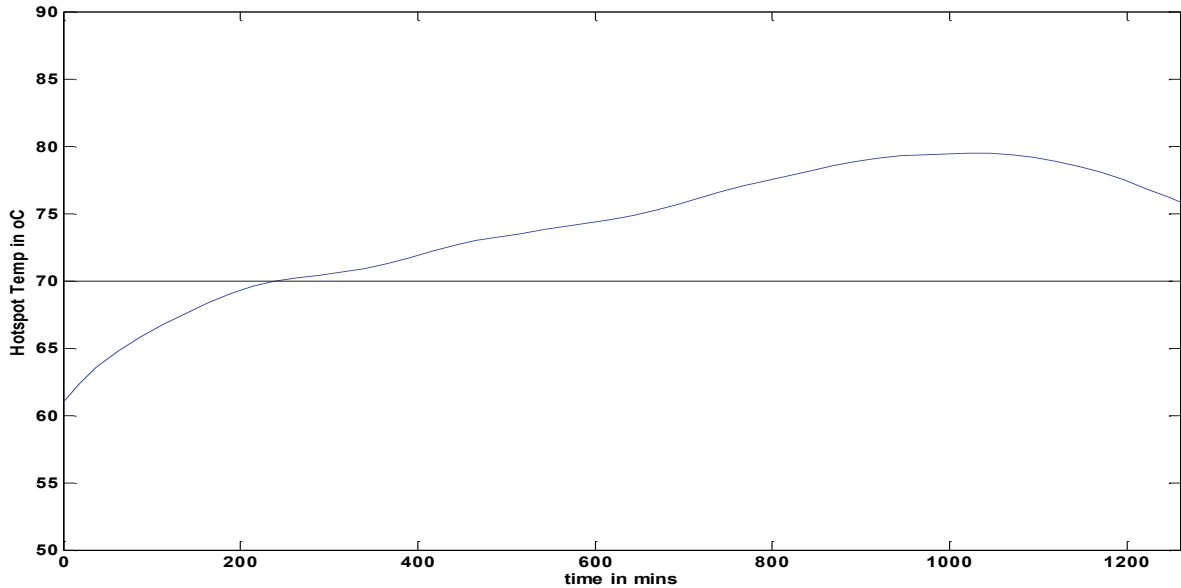
Figure 6.12   Estimated Hotspot Temperature during Summer Season in OFAF mode 2

It can be seen that the estimated temperature for the forecasted period exceeds the maximum threshold temperature of 70°C at the 250th minute. Therefore, to prevent this scenario from occurring, an action of load reduction or increased cooling has to be performed. The transformer is forecasted to be operating with the maximum allowed cooling and therefore the only action to take is to reduce the load. Using figure 6.2 for TR41 in OFAF mode 2 we can see that the transformer operating at 1 p.u with temperatures ranging from 10°C to 20°C will result to hotspot temperatures between 70°C to 80°C in steady state. In order to maintain the hotspot temperature below the maximum threshold temperature of 70°C, a forecasted load of 0.9 p.u for TR41 should be used as the steady state hotspot temperature within the range of 10°C to 20°C is between 60°C to 70°C. Furthermore, the time at which to reduce the load is of great importance to avoid late reduction of the load which could result in temperatures passing the threshold temperature as well as to avoid a very early reduction to reduce the production output before it is

necessary. It will be important to note that the load reduction is not an instantaneous event and usually takes some time. In this thesis, we assume that it takes 60 minutes to reduce the load by 0.1 p.u. With the knowledge that the oil takes a period of time to reach 63% of the maximum hotspot temperature at a certain load and ambient temperature, a suggested time to execute the load reduction will be a time equivalent to the oil time constant before the hotspot temperature exceeds the threshold value. Applying this control strategy to the forecasted load profile, the resultant hotspot temperature is within the threshold temperature range as shown in Figure 6.13.
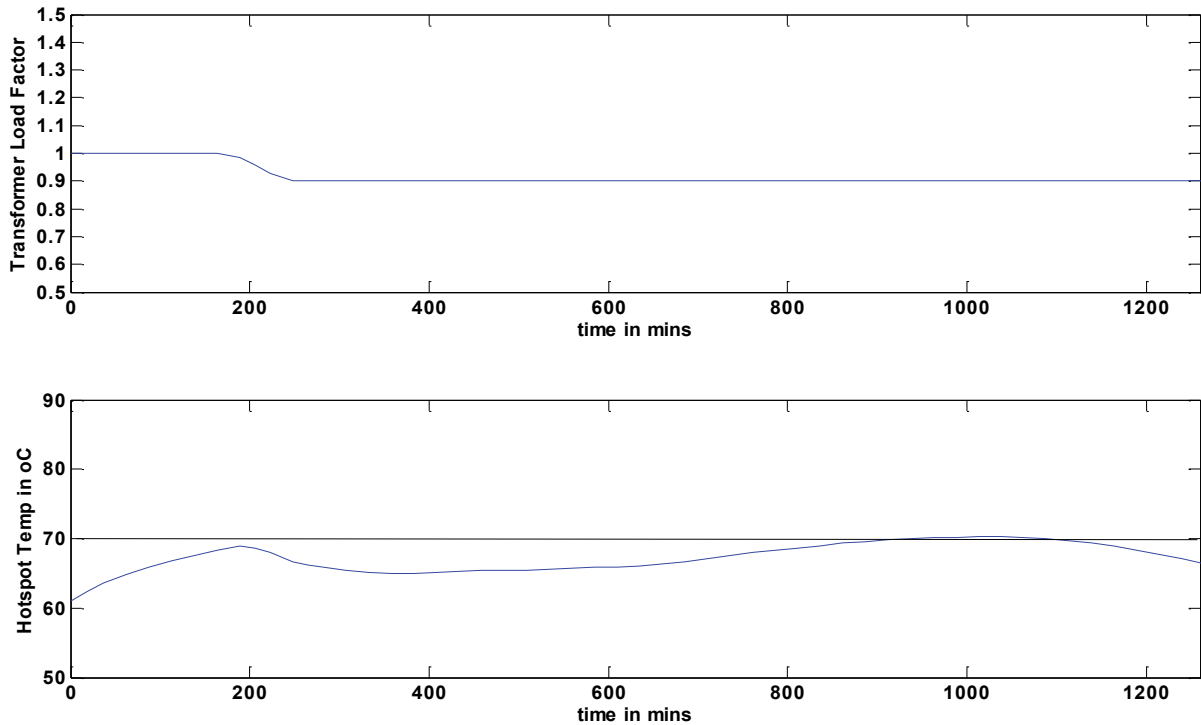
Figure 6.13   Regulated Load Profile and Hotspot Temperature Estimation during Summer Season in OFAF mode 2

116

6.3.2 Winter Period Application

Assuming we have a forecasted load profile of 1 p.u and an ambient temperature profile as shown in figure 6.14 with the transformer operating with one fan on (OFAF mode 1), the resultant estimated hotspot temperature based on the developed IEEE thermal model is as shown in Figure 6.15.
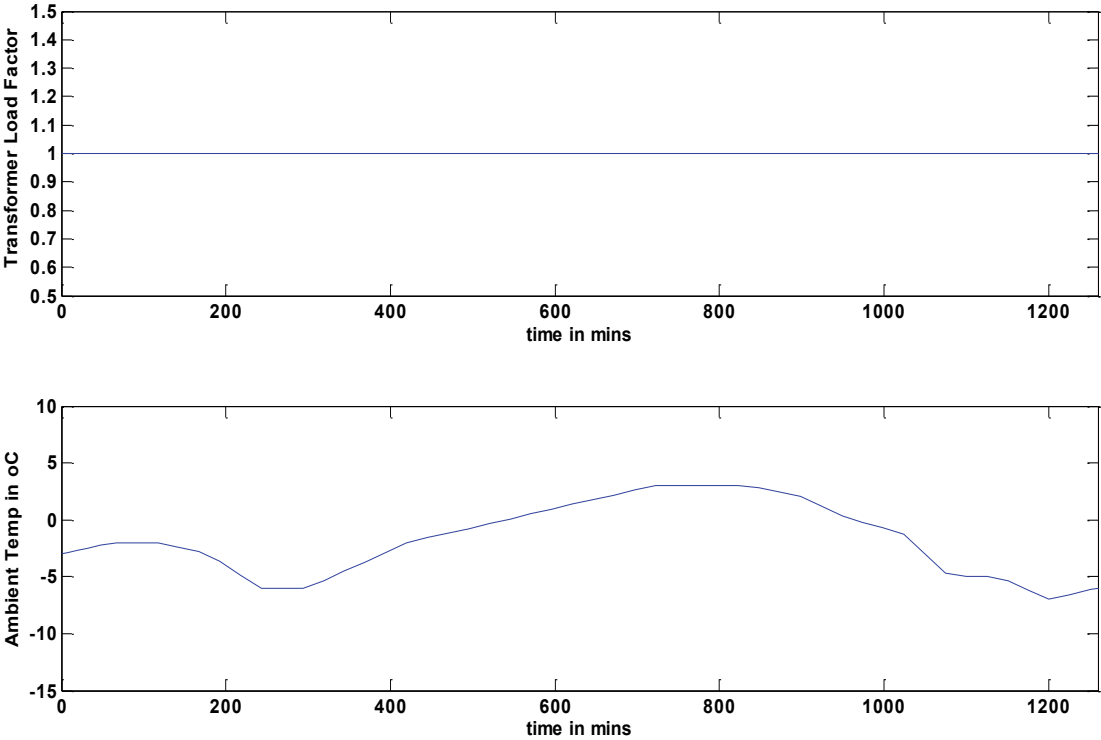
Figure 6.14   Estimated Load Profile and Ambient Temperature during Winter Season in OFAF mode 1
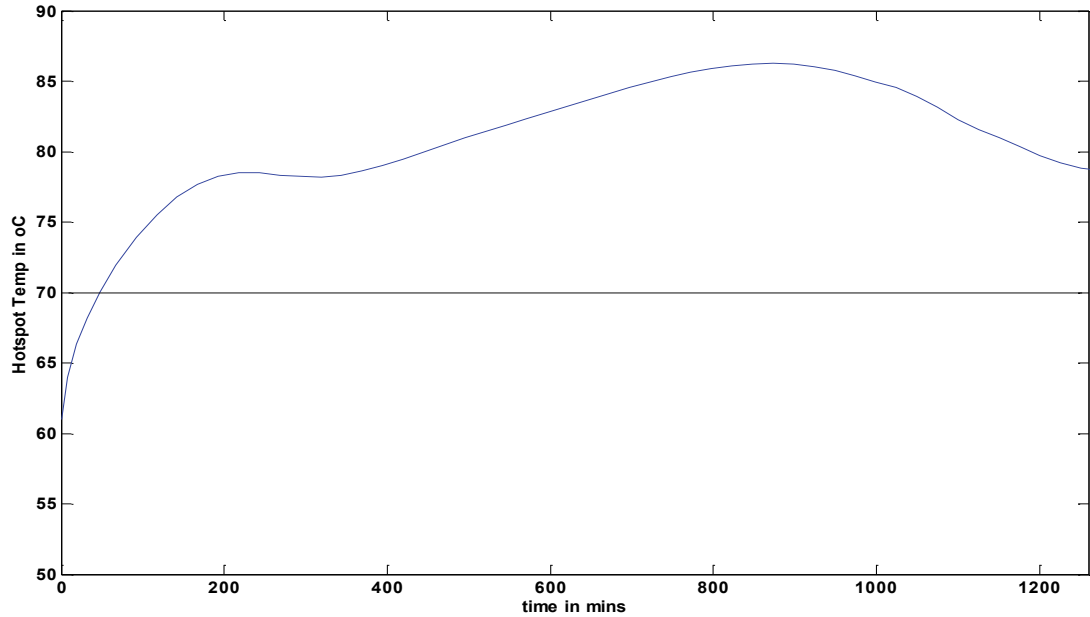
Figure 6.15   Estimated Hotspot Temperature during Winter Season in OFAF mode 1

It can be seen that the hotspot temperature of the rectifier transformer exceeds the threshold temperature at about the 80th minute. In this scenario, two options are possible, a reduction of the transformer loading or an increment in the transformer cooling. The latter is a more favorable option as the cost of electricity with increased cooling is much smaller than the cost of revenue loss with a reduced amount of aluminum production. Using the chart for TR41 in figure 6.2, we can see that the transformer operating with 1 p.u in the ambient temperature range of -10°C to 10°C will result to steady state hotspot temperatures between 50°C to 70°C. This hotspot temperature range is within the limits of the maximum threshold temperature. Also, the time of the change in the cooling mode should approximately equal to the oil time to avoid the hotspot temperature exceeding the limits. In this example the time at which the temperature exceeds the threshold temperature is less than the oil time constant but the change of cooling mode is applied at time 0 minute. The result of the estimated hotspot temperature in the OFAF mode 2 at 1 p.u is shown in figure 6.16.

118
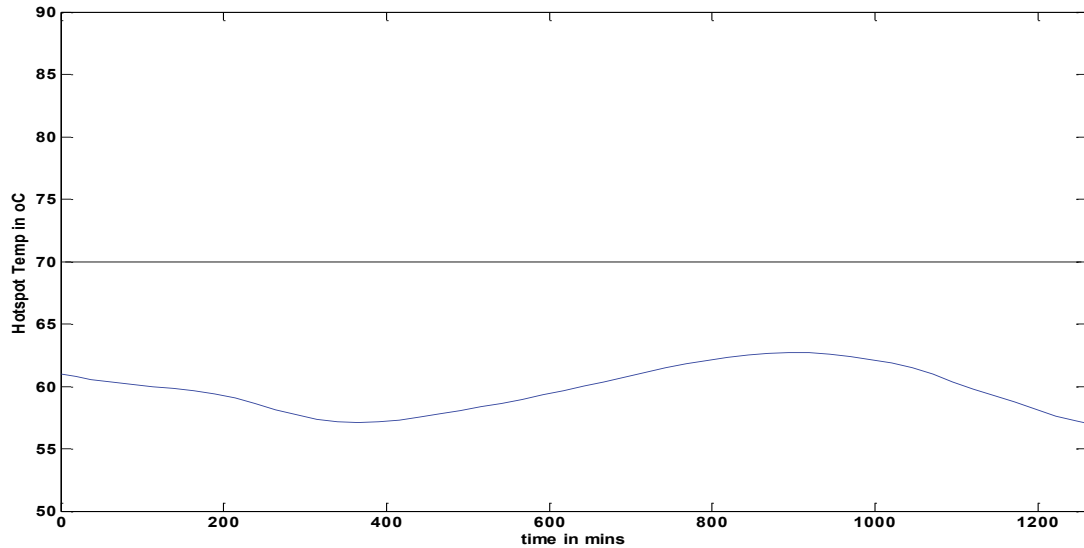
Figure 6.16   Regulated Hotspot Temperature Estimation during Winter Season in OFAF

mode 2

Therefore at the forecasted period, the transformer can be utilized at its rated load capacity to yield maximum production but has to be operated in the OFAF mode 2 to avoid exceeding the set threshold temperature limits.

6.3.3   Cooling System Fault Application

The control scheme used for regulation of the hotspot temperature can be adopted in the event of faults with the cooling fans of the transformer. Using the same load profile and ambient temperature in figure 6.14 with the transformer running in the OFAF mode 2 condition and assuming a fault with two fans resulting to an OFAF mode 1 operation at the 390th minute, the resultant estimated hotspot temperature is as shown in Figure 6.17.
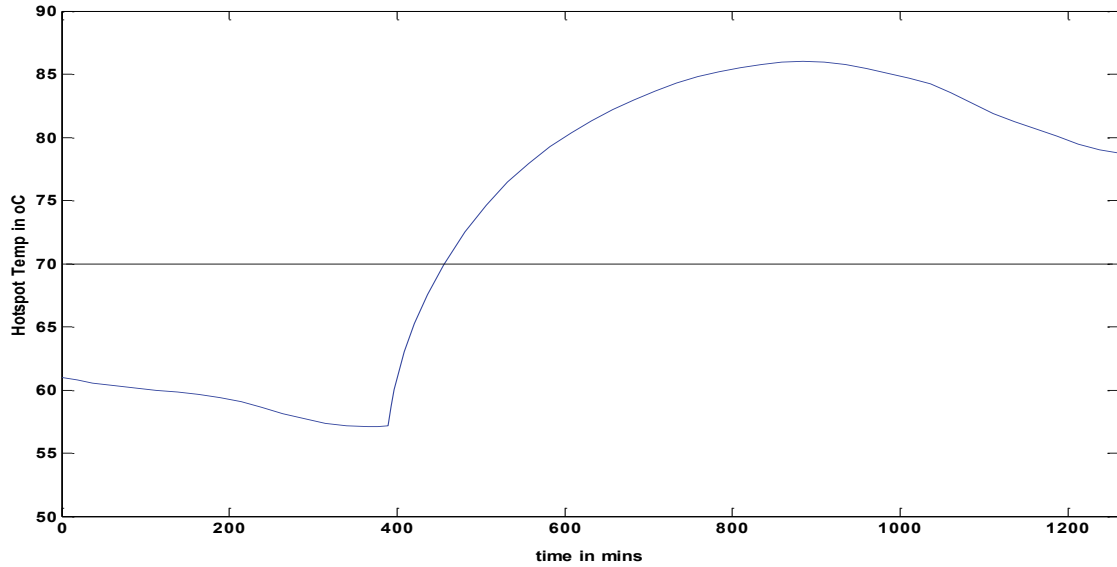
Figure 6.17   Estimated Hotspot Temperature during Faulty Operation in the Winter

Season in OFAF mode 1

From the figure 6.17, it can be seen that the hotspot temperature passes the threshold

temperature. To regulate the temperature within the threshold limits, a load reduction on

the transformer must be done. Using the figure 6.1 for the TR41 in OFAF mode 1, it can

be seen that within the range of temperatures from -10°C to -3°C, a load factor below 0.9

will result to a maximum temperature of 70°C. In order to be within a safe range a load

factor of 0.85 to be the reduced loading factor in this fault scenario. It should be noted that

it is assumed that the transformer takes 60 minutes to reduce by a load factor of 0.1 p.u,

therefore it will take 90 minutes to reduce the transformer load from 1 p.u to 0.85 p.u. The

result of the implemented control strategy is shown in figure 6.18 with the reduced load

and it can be seen that the hotspot temperature is fixed below the 70°C mark.
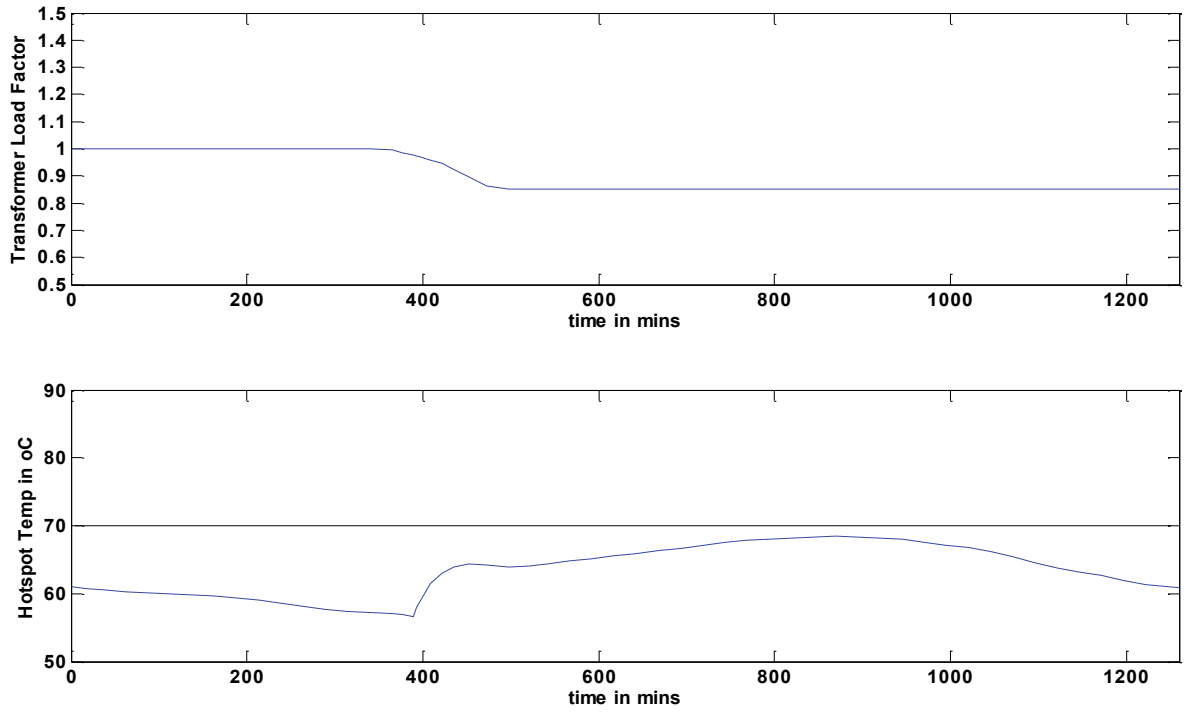
Figure 6.18   Regulated Load Profile and Hotspot Temperature Estimation during Faulty

Operation in the Winter Season in OFAF mode 1

CHAPTER 7   CONCLUSION

7.1   Summary

With the need for an uninterrupted line of production in the aluminum smelting industry due to failure of rectifier transformers, a major component in the production line, predictive maintenance solutions is becoming an area of focus as to keep these assets running until planned replacement periods. The failure of this equipment has been tied to depreciation in the strength of the paper insulation of the winding which is mainly due to excessive heating cause by harmonic currents flowing through the transformer. Therefore, the monitoring and regulation of this heating will be necessary to prevent the rapid deterioration of the paper insulation thus regulating its life span.

In this research work, four existing thermal modes, the improved IEEE model, the IEC model, G. Swift model and D. Susa model are chosen and are adapted to rectifier transformers to account for increased heating due to harmonic currents which are produced during the rectification process. The thermal models are all implemented using Matlab Simulink.

A comparison of techniques to extract the parameters that characterize the thermal model from online measurements is done to avoid the shutting down of the rectifier transformers under case study as they were all in operation during the time of the study. The nonlinear least square method and genetic algorithm optimization are the techniques that are explored. As well the rectifier transformers are considered under different cooling fan operations OFAF mode 1 (one fan on) and OFAF mode 2 (all 3 fans on). The results show that the genetic algorithm optimization is a better candidate for the parameter extrapolation

as the estimated top oil and hotspot temperatures of the adapted models yielded lesser errors between the estimated and measured temperatures in both cooling fan modes. Furthermore, all the adapted thermal models yielded good estimations with the improved IEEE thermal model standing out as the best with a maximum mean square error of 1.47°C between estimated and measured top oil temperatures and maximum mean square error of 2.34°C between estimated and measured hotspot temperatures.

A predictive maintenance technique is implemented for the Alcoa rectifier transformers using steady state hotspot temperature charts to regulate future estimated hotspot temperatures within safe temperature limits of 70°C as derived using an industry accepted end of life equation. Future loading profiles of the transformers as well as forecasted temperatures from the accuweather channel are utilized as inputs to the rectifier thermal models to estimate the future estimated hotspot temperatures. Furthermore, the predictive maintenance technique presented is used for optimizing the rectifier transformer loading factor as well as effective utilization of the cooling fans during the summer, winter and periods with faulty cooling fan operation.

This thesis therefore concludes that by the estimating and regulation of the hotspot temperatures of the Alcoa rectifier transformers with the set thermal limits as a predictive maintenance technique, the transformers can be used safely before the planned replacement time.

7.2   Future Work

1.   The Rectifier transformers under case study are located in Baie Comeau in the subarctic climate which experience very cold winter periods with wind chill

effects and humid summer periods. This wind chill phenomenon causes the atmospheric temperature to feel cooler than the normal ambient temperature and acts as an additional source of cooling to the rectifier transformers. In this thesis, the loading factor and the ambient temperature were solely taken as the attributes that affect the hotspot temperature of the rectifier transformers. It will be important to include the effect of wind chill as to create a more accurate hotspot temperature prediction for both winter and summer periods.

2.   Investigate the use of other global minimum seeking optimization algorithms such as particle swarm optimization and memetic algorithms to obtain the rectifier thermal model parameters and compare results with those as obtained using the genetic algorithm.

3.   Create a closed loop control for effectively optimizing the maximum power of the rectifier transformers and switching effectively between cooling states to optimize power usage.

4.   Investigate the effect of other cooling system faults such as oil pump failure on the hotspot temperature of the rectifier transformer. Furthermore, a possible development of a control strategy will be made to keep the transformer in continuous operation before a maintenance action on the pump is taken.

REFERENCES

[1] T.K. Saha, "Review of Modern Diagnostic Techniques for Assessing Insulation Condition in Aged Transformers", IEEE Transactions on Dielectrics and Electrical Insulation, vol.10, no. 5, pp. 903-917, Oct 2003.

[2] A.M. Emsley, and G.C. Stevens, "Review of Chemical Indicators of Degradation of Cellulosic Electrical Paper Insulation In Oil-filled Transformers", IEEE Proc-Sci. Meas. Technol, Vol 141, no. 5, September 1994.

[3] M.K. Pradhan, "Assessment of the Status of Insulation during Thermal Stress Accelerated Experiments on Transformer Prototypes", IEEE Transactions on Dielectrics and Electrical Insulation, vol.13, no. 1, pp. 227-237, Feb 2006.

[4] "IEEE Guide for Loading of Oil-Immersed Power Transformers", IEEE std C57.91 – 1995.

[5] "IEC Guide for Loading of Oil-immersed Power Transformers", IEC 60076-7-2005.

[6] N. Lelekakis, D. Martin, and J. Wijaya, "Ageing Rate of Paper Insulation Used in Power Transformers Part 1: Oil/Paper System in Low Oxygen Concentration", IEEE Trans., vol.19, no. 6, pp. 1998-2008, Dec 2012.

[7] N. Lelekakis, D. Martin, and J. Wijaya, "Ageing Rate of Paper Insulation Used in Power Transformers Part 2: Oil/Paper System With Medium and High Oxygen Concentration", IEEE Trans., vol.19, no. 6, pp. 2009-2018, Dec 2012.

[8] S.P. Kennedy, "Design and Application of Semiconductor Rectifier Transformers", IEEE Trans. on Industrial App., vol. 38, no. 4, pp. 927-933, July 2002

[9] "IEC Guide On Semiconductor Converters- General Requirements and Line Commutated Converters", IEC 600146- 2009.

[10] "IEEE Standard Practices and Requirement for Semiconductor Power Rectifier Transformers", IEEE std C57.18.10-1998

[11] S. Crepaz, "Eddy Current Losses in Rectifier Transformers", IEEE Trans., vol. 89, no. 7, pp. 1651-1656, Oct 1970

[12] S.P. Kennedy, and C.L. Ivey, "Application, Design and Rating of Transformers Containing Harmonic Currents", IEEE Paper and Pulp Industry Technical Conference, pp. 19-31, June 1990.

[13] A. Elmoudi, "Evaluation of Power Systems Harmonic Effects on Transformers: Hotspot Calculation and Loss of Life Estimation", PhD Dissertation, Helsinki University of Technology, April 2006.

[14] B.C. Lesieutre, W.H. Hagman, and J.L. Kirtley Jr., "An Improved Transformer Top Oil Temperature Model For Use in An On-Line Monitoring and Diagnostic System", IEEE Trans on Power Del., vol. 12, no. 1, pp. 249-254, Jan 1997.

[15] G. Swift, T.S. Molinski, and W. Lehn, "A Fundamental Approach to Transformer Thermal Modeling-Part 1:Theory and Equivalent Circuit", IEEE Trans., vol. 16, pp. 171-175, Apr 2001.

[16] G. Swift, T.S. Molinski, and W. Lehn, "A Fundamental Approach to Transformer Thermal Modeling - Part 2: Field Verification", IEEE Trans., vol. 16, pp. 176-180, Apr 2001.

[17] A. Elmoudi, M. Lehtonen, and H. Nordman, "Thermal Model for Power Transformers Dynamic Loading", IEEE Trans on Electrical Insulation, pp. 214-217, June 2006.

[18] D. Susa, M. Lehtonen, and H. Nordman, "Dynamic Thermal Modeling of Power Transformers", IEEE Trans on Power Delivery, vol. 20, pp. 197-204, Jan 2005.

[19] D. Susa, M. Lehtonen, and H. Nordman, "Dynamic Thermal Modelling of Power Transformers: Further Development-Part 1", IEEE Transaction on Power Delivery, vol. 21, pp. 1961-1969, Oct 2006.

[20] A. Elmoudi, "Thermal Modeling and Simulation of Transformers", IEEE Power and Energy Society General Meeting, pp. 1-4, July 2009.

[21] A. Elmoudi, J. Palola, and M. Lehtonen, "A Transformer Thermal Model for Use in an Online Monitoring and Diagnostic System", IEEE Power Systems Conference and Exposition, pp. 1092-1096, Oct 2006.

[22] A. Elmoudi, "Thermal Modeling and Simulation of Distribution Transformers", IEEE Conference on Systems, Signal and Devices, pp. 1-4, July 2008.

[23] V. Galdi, L. Ippolito, A. Piccolo, and A. Vaccaro, "Parameter Identification of Power Transformers Thermal Model Via Genetic Algorithm", Electric Power Systems Research, vol. 60, pp. 107-113, Sept 2001.

[24] W.H. Tang, and Q.H. Wu, "A Simplified Transformer Thermal Model Based on Thermal-Electric Analogy", IEEE Transaction on Power Delivery, vol. 19, no. 3, pp. 1112-1119, July 2004.

[25] "IEEE Guide for Application for Monitoring Equipment to Liquid Immersed Transformers and Components", IEEE std C57.143-2012.

[26] Pool Cathode Mercury-Arc Rectifier Transformer, ANSI/IEEE C57.18 – 1964.

[27] "Best Practice Manual for Electric Transformers"- http://www.energymanagertraining.com/CodesandManualsCD-5Dec%2006/BEST%20PRACTICE%20MANUAL-TRANSFORMERS.pdf.

[28] John Wolberg, Data Analysis Using the Method of Least Squares, Springer, 2006, ISBN 3-540-25674-1.

[29] Sanford Weisberg, Applied Linear Regression, 3rd Edition John Wiley and Sons, Inc, 2005, ISBN 0-471-66379-4.

[30] A. Croeze, L. Pittman, W. Reynolds, "Solving Nonlinear Least Squares Problems with the Gauss Newton and Levenberg Marquardt Methods", pp. 1-16,- http://www.math.Isu.edu/system/files/munzogroup1-paper.pdf.

[31] Introduction to Gradient Descent - http://hbfs.wordpress.com/2012/04/24/introduction-to-gradient-descent/

[32] D.W. Marquardt, "An Algorithm for Least Squares Estimation of Nonlinear Parameters", J.Soc. Indust. Applied Math., vol. 11, no. 2, pp. 431-441, June 1963.

[33] The AccuWeather .com Weather Network- http://www.accuweather.com.

[34] Matlab Simulink Nonlinear Least Square Estimator.

[35] R.L. Haupt, and S.E. Haupt, Practical Genetic Algorithms, 2nd Edition John Wiley and Sons Inc, 2004, ISBN 0-471-45565-2.

APPENDIX 1

The Winding Oil constant is defined in [18] as

$$\tau_{TO} = \frac{C_{th-oil} * \Delta\theta_{TO-R}}{P_T}$$

with the oil thermal capacitance defined as

$$C_{th-oil} = 0.48 * M_{oil}$$

where

C_{th-oil} - oil thermal capacitance

τ_{TO} - oil time constant

M_{oil} - Mass of Oil in Kg

$\Delta\theta_{TO-R}$ - top oil rise over ambient temperature which can be determined by actual test as specified in the IEEE std c57.12.90-1993 or can be derived from the manufacturers

P_T - Total Transformer Losses

The winding time constant (τ_W) is the time it takes the transformer winding to reach 62% of its rated winding hotspot rise stated in the IEC guide [5] to be 7 mins approximately for power transformers with forced air and oil cooling (OFAF). This value is utilized in the absent of the constant for a specific transformer.

The winding hotspot temperature is defined as suggested in the IEEE guide [4] as

$$\Delta\theta_{H,R} = \Delta\theta_{H.A,R} - \Delta\theta_{TO-R}$$

where

$\Delta\theta_{H.A,R}$ - hotspot rise over ambient temperature at rated load which has a value of 65oC for 55oC average winding rise above ambient transformer and 80oC for a 65oC average winding rise above ambient transformer.

$\Delta\theta_{H,R}$ - rated hottest spot temperature rise over top oil temperature

$\Delta\theta_{TO-R}$ - top oil rise over ambient temperature which can be determined by actual test as specified in the IEEE std c57.12.90-1993 or can be derived from the manufacturers.

From the transformer specification documents, the top oil rise over ambient temperature obtained during the heat run test with the transformers operating at full load with two fans in operation is 42.1. Using this value and applying it with the above equations the parameters for the initial parameters for the nonlinear least square method is shown in the table A.1 below.

Table A.1   Initial Parameters for Transformers TR41 to TR45 using Nonlinear Least Squares Method

	TR41	TR42	TR43	TR44	TR45
$\Delta\theta_{TO-R}$ (K)	42.1	42.1	42.1	42.1	42.1
τ_{TO}(mins)	122.47	116.80	120.43	118.94	118.30
$\Delta\theta_{(H,R)}$ (K)	22.9	22.9	22.9	22.9	22.9
τ_w(mins)	7.0	7.0	7.0	7.0	7.0

As well, the values of the exponent n and m initial values s as shown in the table A.2 below which is based on values specified for OFAF transformers in the various models.

Table A.2   Initial Exponent Values for Thermal Models Using Nonlinear Least Squares

Method

	n	m
TM1	0.9	0.8
TM2	1.0	0.8
TM3	1.0	0.8
TM4	0.25	0.25

where

TM1 – Improved IEEE model

TM2 – IEC Model

TM3 – G. Swift Model

TM4 – D. Susa Model

APPENDIX 2

Genetic Algorithm Matlab Code

```matlab
%PARAMETERS
Varhi1=1; %highest posible value for nonlinear constant n
Varlo1=0; %lowest posible value for nonlinear constant n
Varhi2=200; %highest posible value for oil time constant
Varlo2=100; %lowest posible value for oil time constant
Varhi3=80; %highest posible value for rated top oil rise
Varlo3=10; %lowest posible value for rated top oil rise
npar=3;
ff='test_function1'; %objective function

%Stopping Criteria
maxit=100; %max number of iterations
mincost=0; %mininum cost

% GA Parameter Setup
popsize=20; %set population size
mutrate=0.2; %set mutation rate
selection =0.5; %fraction of population to be kept
Nt=npar; %number of parameters
keep=floor(selection*popsize); %Number of Population memebers to survive
nmut=ceil((popsize-1)*Nt*mutrate); %total number of mutations
M= ceil((popsize-keep)/2); %number of matings

%INITIAL POPULATION
iga=0; %generation counter
par1=(Varhi1-Varlo1)*rand(popsize,1)+Varlo1;
par2=(Varhi2-Varlo2)*rand(popsize,1)+Varlo2;
```

```
par3=(Varhi3-Varlo3)*rand(popsize,1)+Varlo3;
par=[par1,par2,par3];

%Finding Cost for each chromosones
cost=feval(ff,par); %calculate population cost using ff
[cost,ind]=sort(cost); %min cost in element
par=par(ind,:); %sort continuous
minc(1)=min(cost);
meanc(1)=mean(cost);

%Iteration
while iga<maxit
    iga=iga+1; %increment of generation counter

    %Pair and Mate
    M= ceil((popsize-keep)/2); %number of matings
    prob=flipud([1:keep]'/sum([1:keep])); %weight chromosomes
    odds=[0 cumsum(prob(1:keep))']; %probability distribution function
    pick1=rand(1,M); %mate #1
    pick2=rand(1,M); %mate #2

    %ma and pa contains the indices of the chromosomes that will mates
    ic=1;
    while ic<=M
        for id=2:keep+1
            if pick1(ic)<=odds(id) & pick1(ic)>odds(id-1)
                ma(ic)=id-1;
            end
            if pick2(ic)<=odds(id) & pick2(ic)>odds(id-1)
                pa(ic)=id-1;
            end
```

```
        end
    ic=ic+1;
end


%Performing Mating using single point crossover
ix=1:2:keep; %index of mate 1
xp=ceil(rand(1,M)*Nt); %crossover point
r=rand(1,M); %mixing parameters
for ic=1:M
    xy=par(ma(ic),xp(ic))-par(pa(ic),xp(ic)); %ma and pa mate
    par(keep+ix(ic),:)=par(ma(ic),:); %1st offspring
    par(keep+ix(ic)+1,:)=par(pa(ic),:); %2nd offspring
    par(keep+ix(ic),xp(ic))=par(ma(ic),xp(ic))-r(ic).*xy; %1st
    par(keep+ix(ic)+1,xp(ic))=par(pa(ic),xp(ic))-r(ic).*xy; %2nd
    if xp(ic)<npar %crossover whenever last variable not selected
        par(keep+ix(ic),:)=[par(keep+ix(ic),1:xp(ic)) par(keep+ix(ic)+1,xp(ic)+1:npar)];
        par(keep+ix(ic)+1,:)=[par(keep+ix(ic)+1,1:xp(ic)) par(keep+ix(ic),xp(ic)+1:npar)];
    end
end


%Mutate the population
mrow=sort(ceil(rand(1,nmut)*(popsize-1))+1);
mcol=ceil(rand(1,nmut)*Nt);
for ii=1:nmut
    if mcol==1
        par(mrow(ii),mcol(ii))=(Varhi1-Varlo1)*rand+Varlo1;
    elseif mcol==2
        par(mrow(ii),mcol(ii))=(Varhi2-Varlo2)*rand+Varlo2;
    elseif mcol==3
        par(mrow(ii),mcol(ii))=(Varhi3-Varlo3)*rand+Varlo3;
    end
```

```matlab
end

%The new offspring and mutated chromosomes are evaluated
cost=feval(ff,par);

%Sort the costs and associated parameters
[cost,ind]=sort(cost);
par=par(ind,:);

%Do statistics for a single nonaverging run
minc(iga+1)=min(cost);
meanc(iga+1)=mean(cost);

%Stopping criteria
if iga>maxit | cost(1)<mincost
    break
end

[iga cost(1)]
end
```

Test_function1 Code

```matlab
function [ y ] = test_function1( par )
n=par(:,1);
TTO=par(:,2);
DOTOR=par(:,3);
assignin('base','n1',par(:,1));
assignin('base','TTO',par(:,2));
assignin('base','DOTOR',par(:,3));
```

```matlab
for i=1:(length(par))
    n1=par(i,1);
    TTO=par(i,2);
    DOTOR=par(i,3);
    assignin('base','n1',n1);
    assignin('base','TTO',TTO);
    assignin('base','DOTOR',DOTOR);
    sim('experiment_GA');
    y(i)=sqrt(sum((yout(:,2)-yout(:,1)).^2)/length(yout));
    assignin('base','yout',yout)
end
```

APPENDIX 3
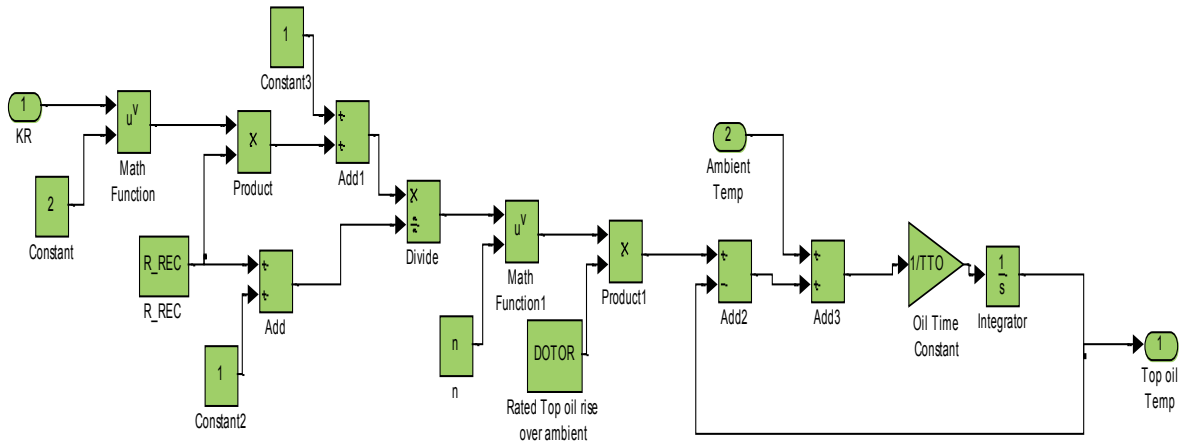
Figure A.1   Improved IEEE Matlab Simulink Top Oil Model
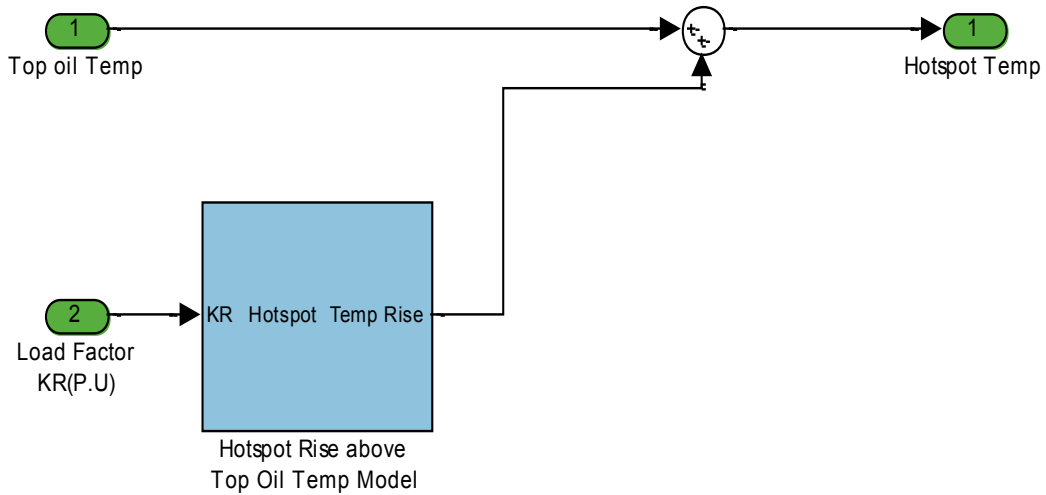
Figure A.2   Improved IEEE Matlab Simulink Hotspot Model
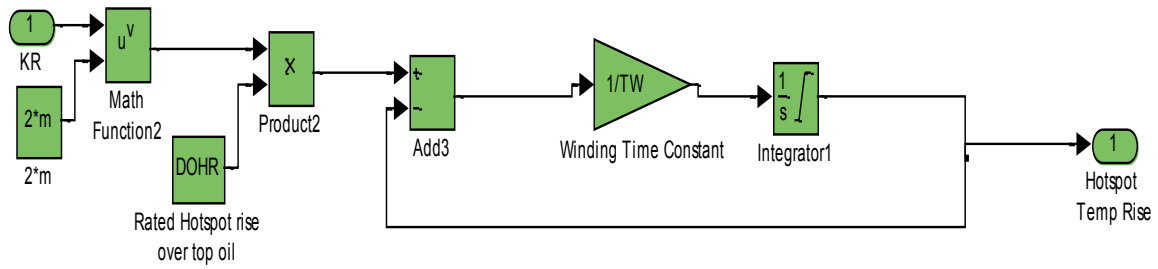
Figure A.3   Improved IEEE Matlab Simulink Hotspot Rise Model
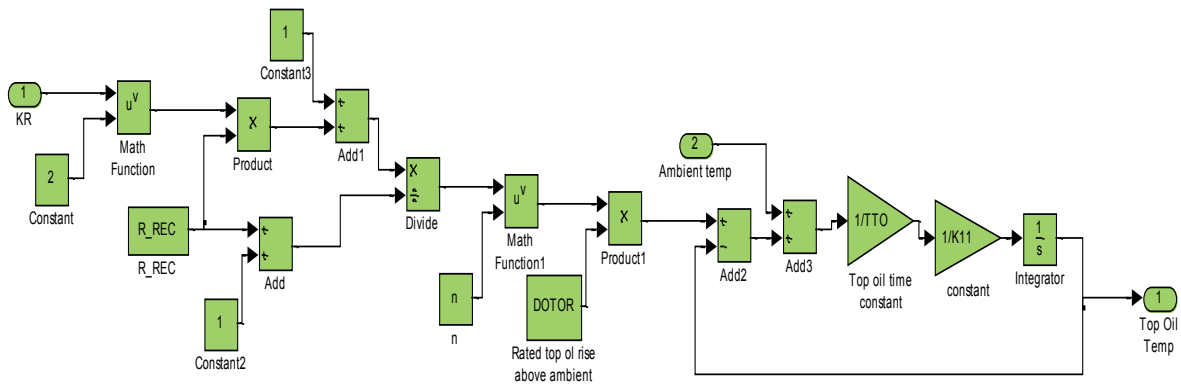
Figure A.4   IEC Matlab Simulink Top Oil Model
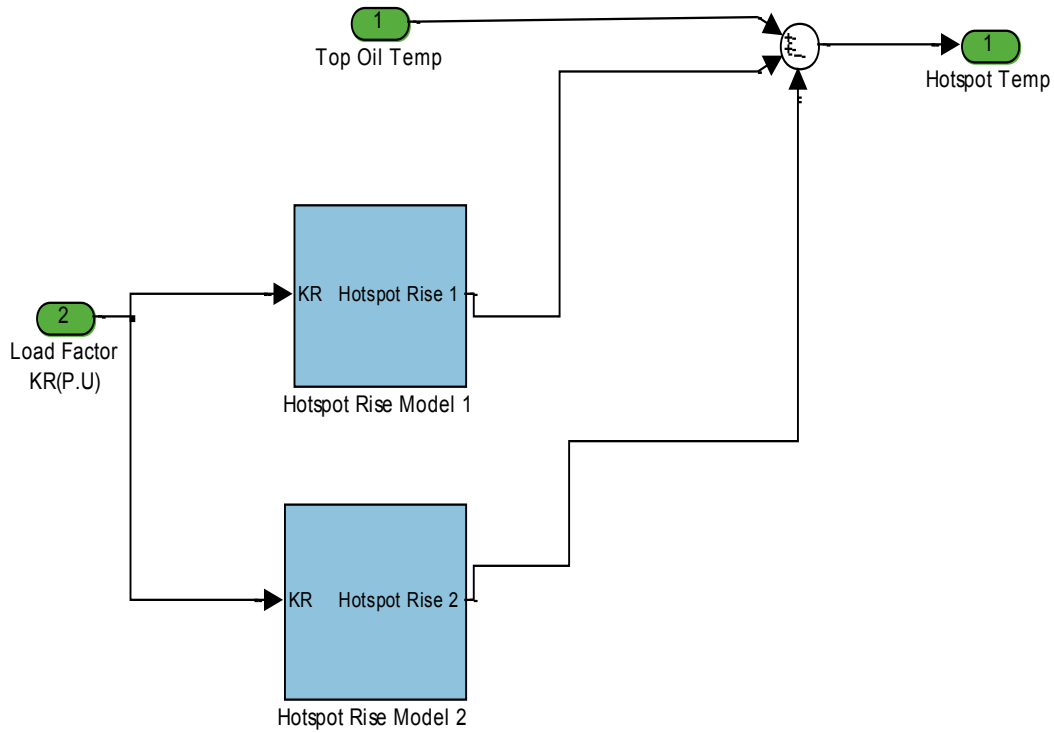
Figure A.5   IEC Matlab Simulink Hotspot Model
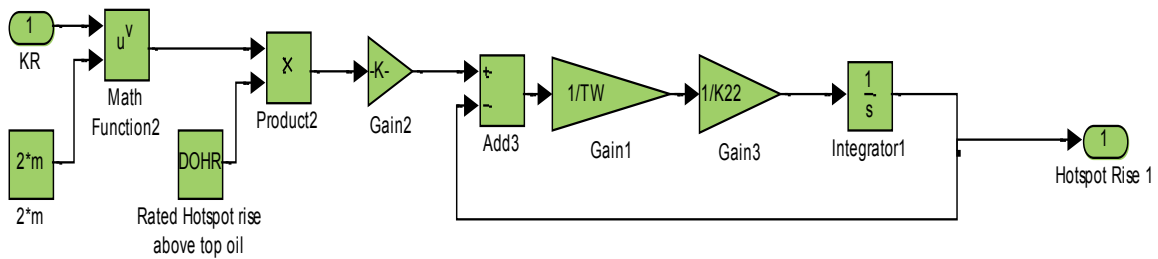
Figure A.6   IEC Matlab Simulink Hotspot Rise Model 1

139
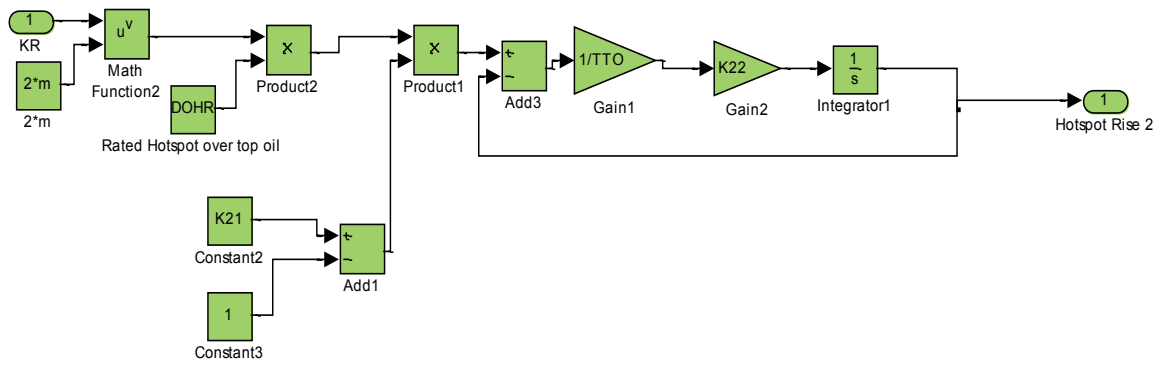
Figure A.7   IEC Matlab Simulink Hotspot Rise Model 2
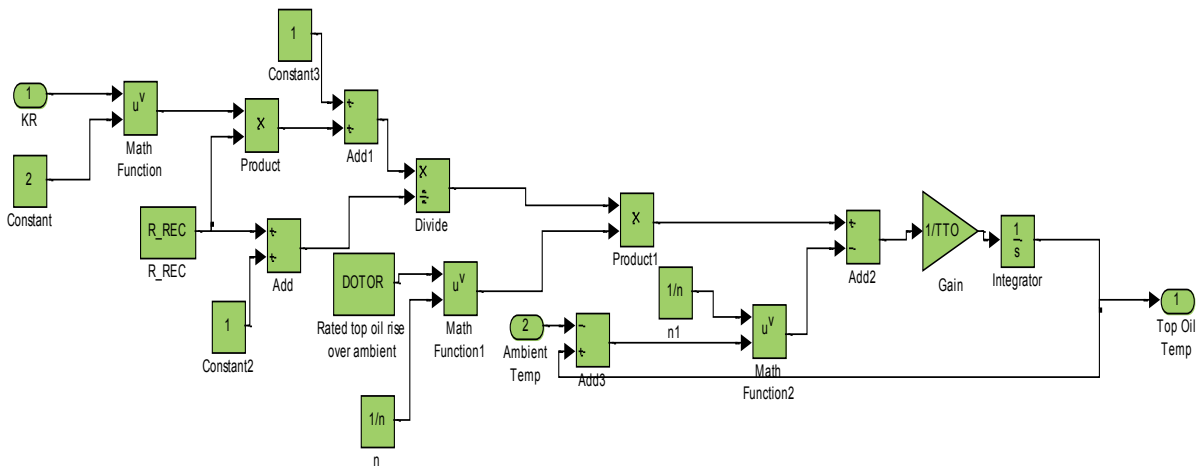
Figure A.8   G. Swift Matlab Simulink Top Oil Model
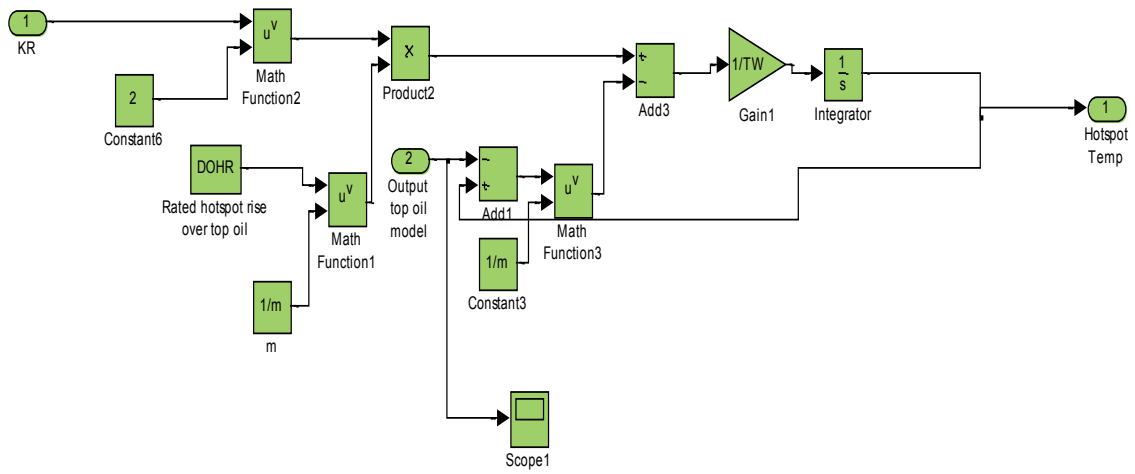
Figure A.9   G. Swift Matlab Simulink Hotspot Model
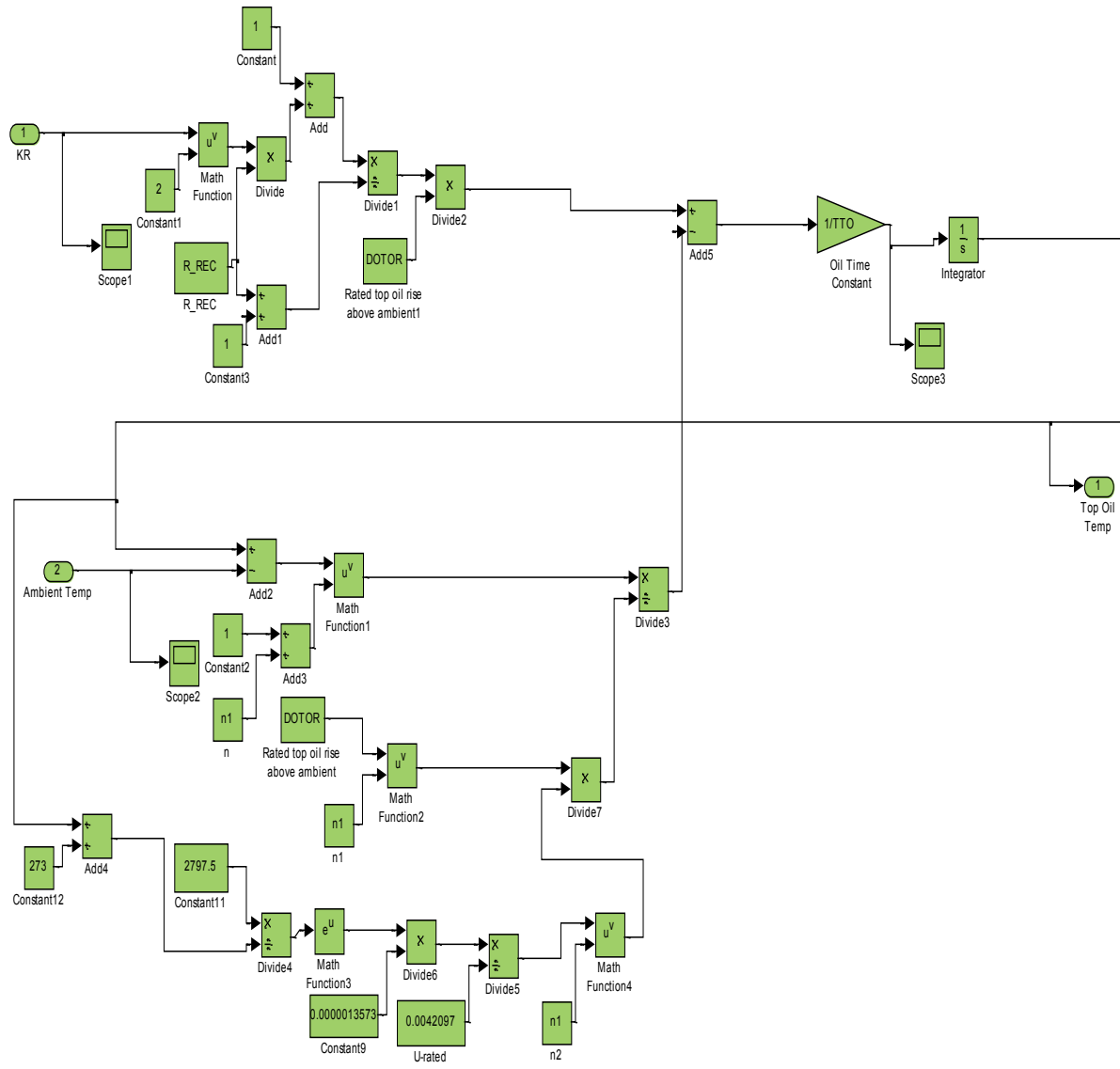
Figure A.10   D. Susa Matlab Simulink Top Oil Model
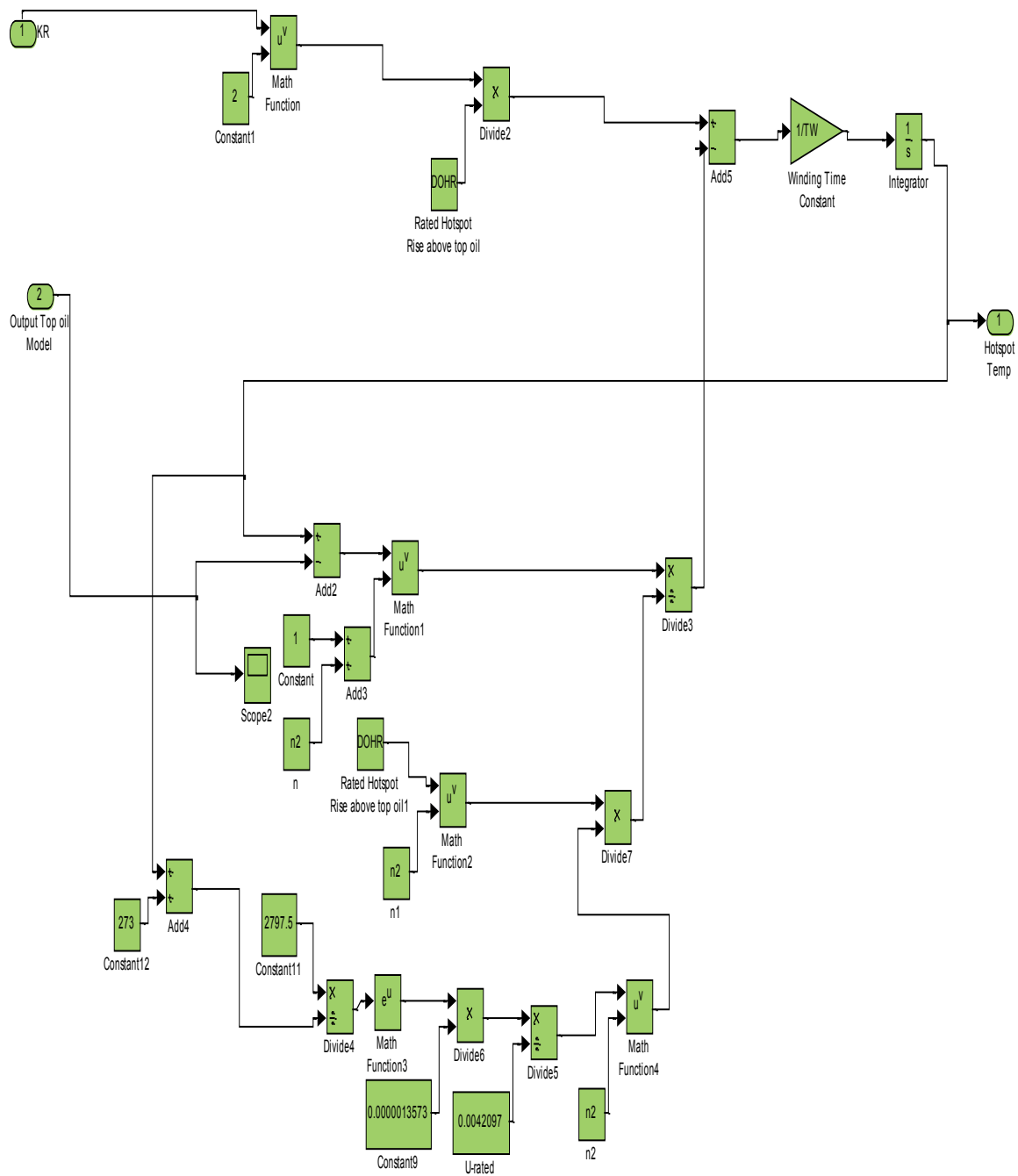
Figure A.11   D. Susa Matlab Simulink Hotspot Model

APPENDIX 4

Figure A.12   Alcoa Rectifier Transformer TR43

Figure A.13   Alcoa Rectifier Transformer TR43 Output DC Current Panel

Figure A.14   Alcoa Rectifier Transformer TR43 Top Oil and Hotspot Temperature Guages